



Holtec Center, 555 Lincoln Drive West, Marlton, NJ 08053

Telephone (856) 797-0900

Fax (856) 797-0909

Mr. John Goshen
c/o Document Control Desk
U. S. Nuclear Regulatory Commission
Washington, DC 20555-0001

November 4, 2010

Subject: Response to NRC Request for Additional Information on License Amendment Request No. 8 to Holtec International HI-STORM 100 Certificate of Compliance No. 1014

References:

- [1] NRC Letter (Goshen) to Holtec (Morin), dated May 28, 2010
- [2] Holtec Letter 5014692, dated November 24, 2010
- [3] USNRC Docket No. 72-1014, TAC No. L24398

Dear Mr. Goshen:

By letter dated May 28, 2010 [1] NRC provided a first request for additional information (RAI) on License Amendment Request (LAR) #8 to Certificate of Compliance (CoC) 1014 [2]. This letter transmits the responses to the RAI, along with supporting documentation, in Attachments 1 through 4, as listed below.

Please note that in the original transmittal of the LAR [2], the proposed Technical Specifications Appendix B Table 2.1-3, contained three editorial errors. The water rod thickness for the 10x10F and 10x10G fuel assembly array/classes and the channel thickness for the 10x10G were incorrect by a factor of 10. The proposed corrections to the table are provided in Attachment 5.

The revised proposed FSAR Supplements labeled "N.III", where N is the chapter, are provided in Attachment 7.

- Attachment 1: Responses to RAI (39 pages)
- Attachment 2: Supplements 54 and 55 from Holtec Report HI-2012787, Revision 14 (Proprietary - 22 Pages)
- Attachment 3: Appendix K from Holtec Report HI-2043317, Revision 11 (Proprietary- 25 pages)
- Attachment 4: Appendix X from Holtec Report HI-2012771, Revision 16 (Proprietary - 14 pages)
- Attachment 5: Technical Specifications, Appendix B Table 2.1-3, page 4 of 5 (1 page)
- Attachment 6: Non-Proprietary Affidavit Pursuant to 10CFR2.390 (5 pages)
- Attachment 7: Revised Proposed FSAR Supplements (81 pages)

NM5501



Holtec Center, 555 Lincoln Drive West, Marlton, NJ 08053

Telephone (856) 797-0900

Fax (856) 797-0909

If you have any questions regarding this transmittal, please contact me at 856-797-0900 x687.

Sincerely,

Tammy S. Morin
Licensing Manager
Holtec Technical Services, Holtec International

cc: Mr. Robert Johnson, USNRC
Mr. Douglas Weaver, USNRC
Holtec Group 1

Holtec's Response to
Request for Additional Information
on LAR 1014-8

3.0 Structural Evaluation

- 3-1 Clarify the use of Metamic Classic and Metamic-HT for Multi Purpose Canister (MPC). Section 3.0 "Design Features" lists ¹⁰B loadings for several baskets; several of them include "METAMIC". The definition of METAMIC encompasses both Metamic Classic and Metamic-HT. Does Holtec intend to use Metamic-HT solely as a neutron absorber in previously approved MPC's?

This information is required to determine compliance with 10 CFR 72.24(c)(3).

Holtec Response:

The reviewer is correct in concluding that Holtec is planning to eventually convert all fuel baskets in the HI-STORM 100 System from stainless steel baskets with panels of Metamic classic affixed to it to Metamic-HT. The present submittal documents the significant improvements in all aspects of the system's safety performance that occur when the Metamic-HT basket replaces the stainless steel basket in the MPC-68. In particular, it is shown that:

1. The significantly greater thermal conductivity of Metamic-HT compared to the stainless steel increases the heat dissipation capacity of the system resulting in lower cladding temperatures.
2. The thicker wall of the Metamic-HT basket in comparison to the stainless steel leads to much smaller basket wall stresses. In the non-mechanistic tip-over event, the flexural stress in the Metamic-HT basket does not reach the yield point; in the stainless steel baskets the stress limit is well in the plastic range (as set forth for the Level D service condition of the ASME Code). Greater margins to the stress limits will mean a greater level of structural safety.
3. The reduced weight of the Metamic-HT basket means reduced weight on the site's overhead crane. At sites with limited crane capacity the water jacket of the HI-TRAC is left empty until the HI-TRAC is removed from the pool. The reduced weight of the basket may allow the water jacket to be filled during the lift and will result in lower occupational dose.
4. The neutron absorber in the Metamic-HT basket completely surrounds the fuel as opposed to the stainless steel basket. This means the margin to the allowable reactivity limit is increased.
5. The Metamic-HT basket has a smaller wetted surface area than the stainless steel basket which has Metamic classic panels affixed under the stainless steel sheathing. This will result in reduced drying times and the associated occupational dose.

We believe that the above comparison provides a significant incentive in terms of improved safety margins to replace the stainless steel basket with a Metamic-HT basket in all MPC designs.

3-2 Provide the following analyses and clarifications.

a) Provide analyses for different basket orientations for side drop analysis.

Holtec Report HI-2012787, page 1, states:

“For the side drop event, only the 0° fuel basket circumferential orientation is analyzed and the 45° fuel basket circumferential orientation is disregarded. The 0° orientation is considered to be bounding because the basket panels are more vulnerable when each fuel assembly is directly supported only by one basket panel instead of being equally supported by two adjacent basket panels in the 45° orientation.”

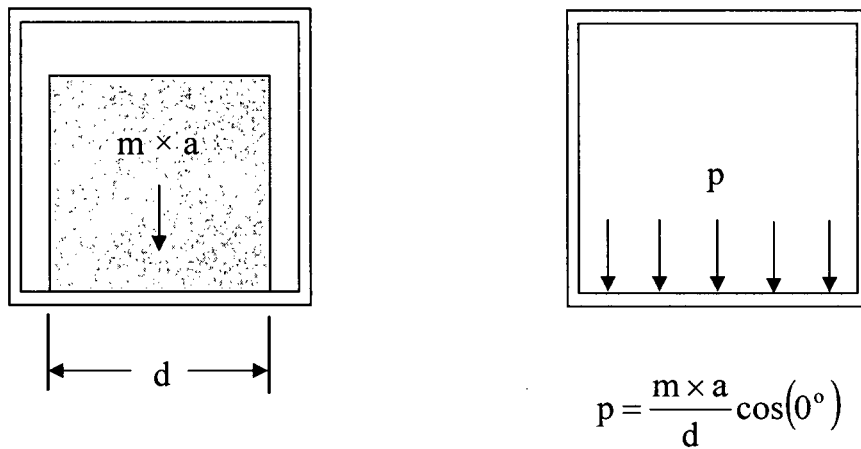
The applicant is applying what should be a conclusion of the analysis as an assumption. The loading in the 45° orientation is potentially a worse load condition than the one analyzed.

Holtec Response: Per Section 2.III.0.1 of the LAR, the structural acceptance criterion for the MPC-68M basket is defined in terms of the maximum lateral deflection of a basket panel under accident loading conditions. Thus, the limiting accident event is the one which causes the maximum lateral deflection of a basket panel relative to its end supports. Since the lateral deflection is proportional to the lateral load on a basket panel, the limiting accident event can also be viewed as the one which maximizes the lateral load on a single basket panel. For the MPC-68M fuel basket inside a HI-STORM overpack, the lateral load on a single basket panel is maximized during the non-mechanistic tip-over event with the fuel basket in the 0° circumferential orientation.

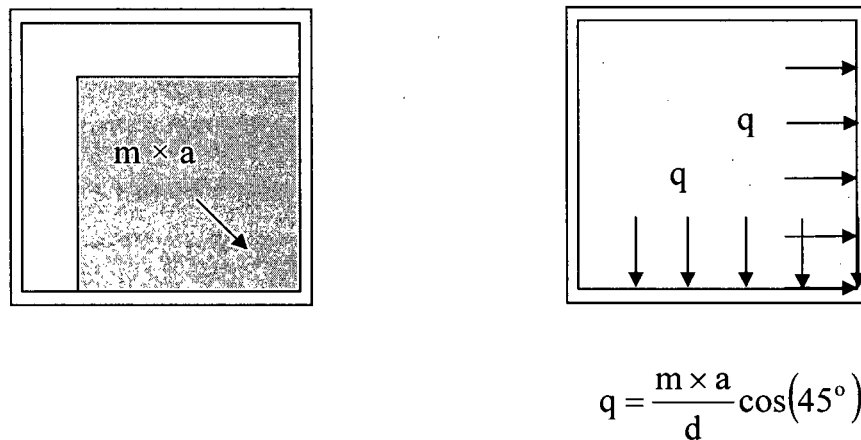
In the 0° orientation, the amplified weight of each stored fuel assembly (during the 70g impact event) bears entirely on one basket panel. Conversely, in the 45° orientation, the amplified weight of each stored fuel assembly is equally supported by two basket panels. The difference in loading between the two basket orientations is pictorially shown in Figure 3-2.1 below, where “m” denotes the fuel assembly mass, “a” denotes the maximum lateral deceleration, and “d” denotes the enveloping size of the fuel assembly. For comparison purposes, the pressure loads on the basket panels are denoted as “p” and “q”, respectively, for the 0° and 45° orientations. From the figure, the pressure load p that develops in the 0° orientation is 41% greater than the pressure load q that develops in the 45° orientation. Hence, the lateral deflection of a basket panel is much greater for the 0° orientation, which is why the 0° orientation is chosen for analysis in Section 3.III.4.4.3.1. It is also noted that the 90° corners where the basket panels intersect do not provide any additional moment resistance because of the slotted joint construction (see Figure 1.III.1 in LAR); therefore, the 45° orientation does not give rise to any prying loads at the cell corners. Finally, to ensure that the analysis performed in Section 3.III.4.4.3.1 for the 0° orientation is conservative and bounds all other basket orientations, the analysis is performed based on a lateral impact deceleration of 70g even though, according to the results presented in Section 3.III.4.10 of LAR, the maximum impact deceleration due to the non-mechanistic tip over event (measured at the top of the overpack lid) is less than 45g.

In summary, the 0° orientation is the most limiting orientation for the design and analysis of the MPC-68M fuel basket since it maximizes the load transmitted to a single basket panel. Therefore, the 0° orientation is the focus of the analysis presented in Section 3.III.4.4.3.1 of the LAR. Nevertheless, to further ensure that the finite element results for the 0° orientation bound all other basket orientations, the analysis is carried out using a bounding deceleration load of 70g.

Section 3.III.4.4.3.1 of the LAR has been revised to include this information.



(a) 0° Orientation



(b) 45° Orientation

Figure 3-2.1: Fuel Loading for 0° and 45° Basket Orientations

b) Clarify the provenance of bounding deceleration. Holtec Report HI-2012787, page 1, states: "A 70 g's bounding deceleration in the lateral direction is specified in the HI-STORM FSAR...." The staff cannot find that number in the reference.

Holtec Response:

The applied load of 70 g's is stated as bounding because it exceeds the design basis deceleration limit of 45 g's for the non-mechanistic tip over of the HI-STORM storage overpack, as well as the design basis lateral deceleration limit of 60 g's for the HI-STAR transport cask. With regard to the statement in Holtec Report HI-2012787, the reference (i.e., [1]) was identified incorrectly as HI-STORM FSAR Rev. 8. The correct reference is Proposed Rev. 8 of the HI-STORM FSAR (i.e., LAR 1014-8), which discusses the bounding deceleration of 70 g's. Holtec Report HI-2012787 has been revised to correct reference [1]. In addition, Section 3.III.4.4.3.1 of the FSAR has been revised to further explain the basis for the 70 g lateral deceleration.

c) Justify use of elastic model for basket shims. Holtec Report HI-2012787, page 2, states: "Elastic model is defined for the basket shims since no plastic deformation is expected." There is no mentioned basis for the "expected" behavior, and the elastic model does not allow for plastic strain to develop.

This information is required to determine compliance with 10 CFR 72.236(l).

Holtec response:

The use of a linear elastic material model for the basket shims is validated by the results of the non-mechanistic tip-over analysis, since the maximum computed stress at any point in the basket shims under the 70-g applied load is less than 40% of the material yield strength. The basket shims are made from aluminum alloy (B221 2219-T8511), which has a yield strength of 26 ksi at 500°F per Table 3.III.3 of the LAR (Note: 500°F is the maximum basket shim temperature per Table 4.III.3). Figure 3-2.2 below plots the Von Mises stress distribution in the basket shims due to the 70-g lateral deceleration, as determined by ANSYS. The maximum stress value is 9,532 psi, which is equal to 37% of the material yield strength at 500°F. Therefore, since the stress level in the basket shims does not exceed the yield point (i.e., no plastic strain), the use on a linear elastic material model is justified. Holtec Report HI-2012787 has been revised to include this justification.

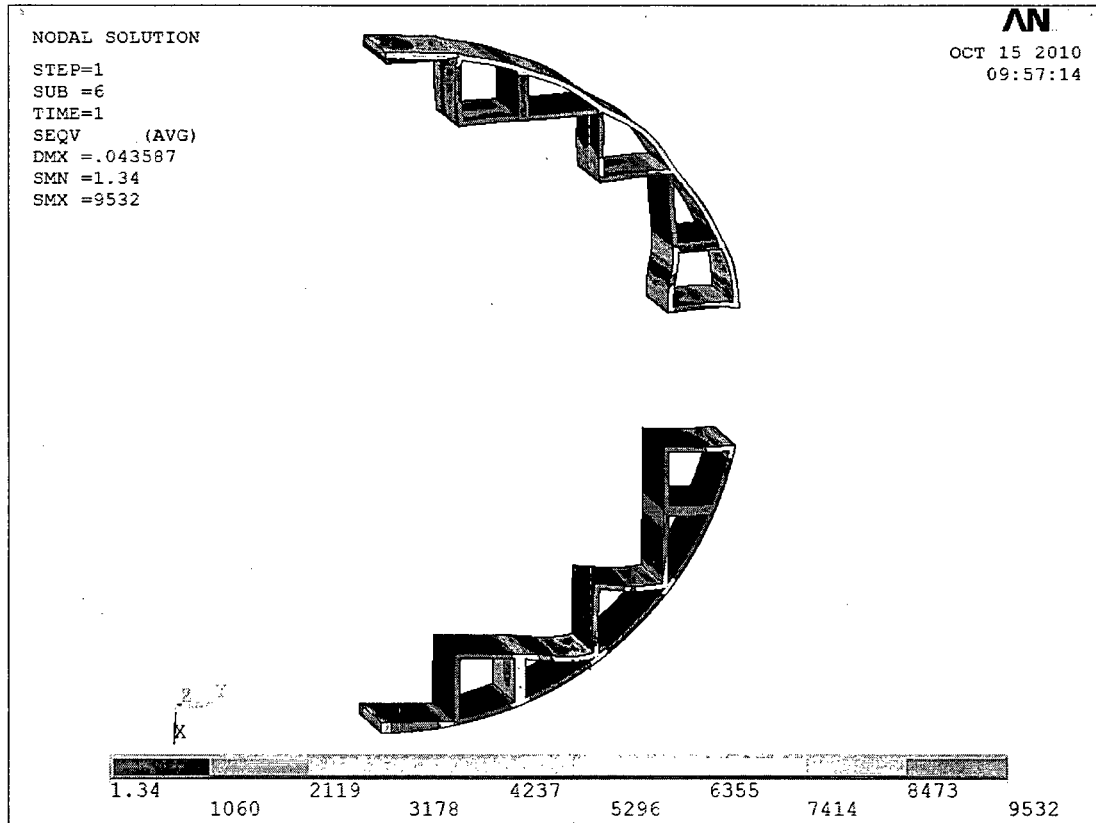


Figure 3-2.2 – Von Mises Stress Distribution in Basket Shims Under 70-g Load

- 3-3 Evaluate the potential for crack propagation and growth for the MPC baskets under tipover conditions. Attachment D of the Metamic HT Sourcebook is based on results for conditions applicable only to the HI-STAR 180 and not the HI-STORM MPC-68M multiple-purpose canister system.

This information is required to determine compliance with 10 CFR 72.236(l).

Holtec response:

The table below provides a comparison of the parameters significant to crack propagation and crack growth for the Metamic-HT panels in the HI-STAR 180 F-37 fuel basket, qualified in Attachment D of the Metamic-HT Sourcebook, and the MPC-68M fuel basket.

	HI-STAR 180 F-37 (Attachment D of Sourcebook)	MPC-68M
Storage cell width, w (in)	8.11	6.05
Panel thickness, t (in)	0.59	0.40
Reference metal temperature (°C)	275	307
Design basis g-load under lateral loading event, acc (g)	95	70
Fuel dead load per unit length, f (lbf/in)	8.04	4.42
Panel stress*, σ (ksi)	13.35	8.77
<p>* To facilitate comparison, panel stress is computed according to the following formula (parameters are defined in first column of table):</p> $\sigma = \frac{3 \cdot acc \cdot f \cdot w}{4 \cdot t^2}$ <p>which assumes that the storage cell wall acts as a simply supported beam strip under a uniformly distributed load equal to the amplified fuel weight.</p>		

The above tabular comparison shows that the demand load (i.e., panel stress) on the HI-STAR 180 F-37 fuel basket due to the 9-meter drop accident bounds the demand load on the MPC-68M fuel basket due to the design basis 70-g lateral impact. The reference metal temperature, however, is higher for the MPC-68M fuel basket. Thus, the crack propagation analysis in Attachment D of the Metamic-HT Sourcebook does not uniformly bound the MPC-68M fuel basket. Therefore, explicit calculations for the MPC-68M fuel basket are carried out in the manner of the analysis in the Metamic-HT Sourcebook and included in Subsection 3.III.4.4.3.1 of the HI-STORM FSAR to quantify the margins of safety under the non-mechanistic tip-over scenario.

4.0 Thermal Evaluation

- 4-1 Provide a hypothetical fire accident analysis of the MPC-68M under the credible fire transient duration.

The applicant stated that as the MPC-68M temperatures during storage or under on-site transfer are bounded by the MPC-68 temperatures, the MPC-68M temperatures are likely bounded by the MPC-68 temperatures in the fire test. The applicant neither performed the thermal analysis nor provided the resulting temperatures of the pool fire test to support this statement.

The staff finds that with better heat transfer capability due to using the Metamic-HT as the fuel basket material in the MPC-68M, it is likely that more heat will be transferred from the fire to the stored fuels within the MPC-68M, and the MPC-68M should not be bounded by the MPC-68. The applicant is required to perform a fire analysis and provide the base to justify the credible fire duration (4~5 minutes, 10~15 minutes or even longer) by using the bounding regionalized storage scenario (the maximum decay heat of 36.9 kW and the fuel storage configuration of $X=0.5$), removing the uniform gap of 0.4 mm on each side (from bottom to top) of the intersection basket panel in the fire-transient analysis, including the combined forced convection and thermal radiation (with a conservative radiation emissivity of at least 0.9 and an ambient temperature of 1475oF in the model) in the fire-transient analytical model, replacing the specific heat of 914 J/kg-°K with 879.2 J/kg-°K (= 0.21 Btu/lb-°F in Supplement III Table 4.III.1) for Metamic-HT fuel basket to make the model analysis consistent with the SAR.

The applicant should list all the test conditions, parameters and data, as well as the resulting maximum component temperatures and MPC pressure during the fire transient and the subsequent post-fire cool-down in the FSAR.

This information is required by the staff to determine compliance with 72.24(d), 72.122(c), 72.122(h)(1), 72.128(a)(4), and 72.236(f).

Holtec response:

The staff is correct in their observation that an explicit fire transient analysis for the HI-STORM 100 system containing an MPC-68M had not been performed. This was due to the fact that the steady state fuel cladding temperature field in the case of the MPC-68M is substantially lower than that for MPC-68 models employing the stainless steel baskets (the peak temperature under identical heat load is approximately 100 deg. F lower). As can be seen from the results in the FSAR (please see Section 4.6 in Chapter 4) short thermal transient characteristic of the fire event is known to have a minor effect on the peak cladding temperature and huge margins to the allowable temperature limit remain. The main consequence of the fire event, as observed in Section 4.6 of the FSAR is to scorch the external surface of the overpack due to the radiated heat incident on it. The effect on the fuel, protected by the massive overpack from a direct thermal radiation of the fire, is far from being governing.

Nevertheless, to comply with the staff's request, an upper bound effect of fire on the fuel cladding has been obtained by applying previously approved NRC methodology in this

HI-STORM docket. The fire event simulated in the analysis is the Licensing Basis fire event for the HI-STORM 100 system (Please see Section 4.6 in chapter 4). (All design basis loading events for HI-STORM 100 system are established in the FSAR through previous certifications; a new fire event definition for this amendment would be inconsistent.) A safety evaluation pursuant to 10CFR72.212 is required if the fire event for a particular ISFI is more severe than the event considered in the FSAR.) Details of the analysis and results are documented in Supplement 4.III, Section 4.III.6.2 in the revised FSAR. As expected, the results show large margins of safety with respect to the fuel cladding temperature.

4.2 Perform the transient analysis for vacuum drying (VD) process for the proposed change of "Vacuum drying of the MPC-68M is not subject to time limit."

The applicant proposed to modify Appendix A, LCO 3.1.1 in LAR 1014-8 with "Vacuum drying of the MPC-68M is not subject to time limit," and supported the proposed change with two steady-state analyses: (1) Scenario A with the moderate burnup fuel assemblies and the decay heat of 36.9 kW, and (2) Scenario B with one or more high burnup fuel assemblies and the decay heat of 29 kW. The applicant modeled the analyses with the moisture in the MPC and conservatively assumed that the water in the HI-TRAC annulus is boiling under the hydrostatic head of water at the annulus bottom (232°F) and the bottom surface of the MPC is insulated.

However, it's likely that the fuel cladding temperature will continuously rise up during the VD process until a balance of heat transfer is reached and a maximum, stable temperature exists. Therefore, the applicant is required to perform the transient analysis, display the fuel cladding temperature history, and verify a maximum, stable fuel cladding temperature is available and is below the allowable temperature limit during the VD process.

This information is required by the staff to determine compliance with 72.24(d), 72.122(c), 72.122(h)(1), 72.128(a)(4), and 72.236(f).

Holtec response:

The MPC-68M vacuum drying calculations follow the methodology defined in the generic HI-STORM FSAR 4.5.3.1 for evaluating vacuum drying operations. In accordance with the methodology upper bound 232°F annulus water temperature is applied to the MPC shell with vacuum inside the canister and steady state maximum fuel temperatures computed. As justified below steady state conditions provide an upper bound to the time-temperature history during vacuum drying operations.

Staff's concern that the steady state solutions reported in the SAR may not bound the transient solutions, while relevant to a general transient event, can be established to be inapplicable to this problem, as explained below.

The output variable in this analysis is the temperature of the fuel cladding. For the output variable to overshoot the steady state solution, at least one of the input variables must behave non-monotonically during the transient event. In the fuel drying transient this

condition cannot be obtained. This is because all three contributing heat transfer mechanisms, namely conduction (in the fuel, water vapor, and the metal), convection, and radiation which is the dominant variable as the system temperature rises, either rise or decline uniformly throughout the transient event. Absent an inflection point which would cause a reversal in the value of a contributory mechanism, the transient temperature of the fuel is assured to rise monotonically and asymptotically reach the steady state value.

4.3 Provide more information of the fuel debris and justify its impacts on the adjacent intact fuel assemblies or the cask.

The MPC-68M is designed to accommodate to sixty eight intact BWR fuel assemblies. However, up to sixteen damaged fuel containers (DFCs) containing BWR damaged fuel assemblies and/or up to eight DFCs containing fuel debris may be stored in the MPC- 68M, with the remaining fuel storage locations filled with intact BWR fuel assemblies. Since the fuel debris can be in a type of rubble fuel assembly which may be concentrated in a smaller area and create hot spots in the cask and increase the cladding temperatures of the adjacent intact assemblies. The applicant is required to provide more information of the fuel debris, and perform the thermal analysis, if the fuel debris exists as a type of rubble fuel assembly, to ensure the pressure and the fuel cladding temperature will be below the limits.

This information is required by the staff to determine compliance with 72.24(d), 72.122(c), 72.122(h)(1), 72.128(a)(4), and 72.236(f).

Holtec response:

Fuel debris is permitted for storage in up to eight peripheral cells under the uniform loading heat load limits specified in Section 2.4 of the Technical Specifications. To comply with the Staff's request, a thermal analysis of the canister assuming a most conservative debris canister geometry and design heat load has been performed and documented in the revised FSAR. The following assumptions are adopted to maximize the computed fuel cladding temperatures:

1. The fuel debris is assumed to be completely pulverized and compacted into a square prismatic bar enclosed by the damaged fuel canister (DFC). Thus the height of the prismatic bar emitting heat is minimized resulting in the maximization of lineal thermal loading (kw/ft) of the DFC and co-incident local heating of the fuel basket and neighboring storage cells.
2. All 16 peripheral storage locations (not just the 8 permitted by CoC) are assumed to contain fuel debris emitting maximum heat permitted by Technical Specifications (CoC Appendix B, Section 2.4, Table 2.4-1) and all interior cells are emitting design heat under the uniform loading storage scenario. The analysis documented in the revised FSAR Section 4.III.4.4 shows that the peak cladding temperature is essentially unchanged and remains well below the ISG-11 Rev 3 limit.

5.0 Shielding Evaluation

- 5-1 Provide additional details on the differences between the design-basis Babcock & Wilcox 15x15 and the 15x15I fuel assemblies.

Using the upper limits given in section 2 and the initial bounding analysis from the FSAR, identify how the proposed fuel assembly differs in any significant way from the design basis assembly.

This information is necessary to determine compliance with 10 CFR 72.236

Holtec response: The 15x15I assembly array/class does not differ significantly from the shielding analysis design basis (DB) Babcock & Wilcox 15x15 fuel assembly and in fact the 15x15I array/class is bounded by the DB Babcock & Wilcox 15x15 fuel assembly. The 15x15I array class was created to bound the ANF 15x15 CE PWR assembly which is not bounded by any of the previously approved array/classes in the HI-STORM 100 System criticality analysis.

Below is a table comparing the specific values that affect the shielding analysis of the 15x15I array/class against the DB 15x15 B&W fuel assembly. The information for the DB fuel assembly is taken from FSAR Table 5.2.1. The 15x15I assembly data is taken from the HI-STORM FSAR Table 2.1.9 for design initial U and reference [5.2.5] for the non-fuel components of the assembly.

As can be seen from the table below the DB B&W 15x15 fuel assembly bounds the 15x15I in Inconel and stainless steel content as well as initial U content.

Fuel assembly characteristic	Design Basis B&W 15x15 fuel assembly (from FSAR Table 5.2.1)	15x15I fuel assembly array/class
Maximum Design Initial U (kg/assembly)	495.485	495
Total Stainless Steel Content in non-fuel components (kg)	17.7	9.14
Total Inconel Content in non-fuel components (kg)	7.5	1.2

- 5-2 EDITORIAL: The example given in the zone 1 contribution analysis of the MPC-68M uses the MPC-32 analysis from the FSAR as an example. However, the conclusion drawn for the neutron dose contribution is more in line with that of the MPC-68 (21% versus 27%). Correct or clarify the example.

This information is necessary to determine compliance with 10 CFR 72.236

Holtec response: The text in Supplement 5.III will be changed to reflect the analysis from the main chapter which supports MPC-68 as a comparison to the MPC-68M.

6.0 Criticality Evaluation

6-1 Justify the fuel specification of the 9x9E and 9x9F fuel assemblies.

For the 9x9E and 9x9F Note 13 in Table 2.1.4 of the FSAR says: For the SPC 9x9-5 fuel assembly, each fuel rod must meet either the 9x9E or the 9x9F set of limits or clad O.D., clad I.D., and pellet diameter. Provide additional information justifying that the criticality analysis for the MPC-68M was performed considering the most conservative set of fuel specifications.

This information is needed to determine compliance with 10 CFR 72.236(a) and (c).

Holtec response:

A schematic diagram has been added in Supplement 6.III, Section 6.III.4, that identifies the location of the different rod types in the assembly that is used in the analysis. Note that there are two known patterns of water rod locations for this assembly type. A new study in Subsection 6.III.4.2 verifies that the more conservative pattern is used in the design basis calculation (see Table 6.III.4.3).

6-2 Justify the fuel specification of the 8x8B and 8x8D fuel assemblies.

a. In Table 2.1.4, the 8x8B and 8x8D are specified with two separate values for "No. of fuel rod locations." Justify that the most reactive value was used in the criticality analysis in the MPC-68M for these fuel types.

b. In Table 2.1.4, the 8x8B can have either 1 or 0 water rods. Justify that the most reactive value was used in the criticality analysis for the MPC-68M for this fuel type.

This information is needed determine compliance with 10 CFR 72.236(a) and (c).

Holtec response:

Studies have been added to Supplement 6.III, Section 6.III.4 to demonstrate that versions of the 8x8B and 8x8D assembly with different number of fuel or water rod locations are bounded by the analyses that are currently presented for those assembly types (see Table 6.III.4.3).

6-3 Demonstrate that the fuel dimensional variations (such as minimum fuel clad OD versus maximum and maximum channel thickness versus minimum, etc.) listed in Table 2.III.3 and 2.1.4 give the maximum reactivity for all fuel assembly types that are to be stored in the MPC-68M.

The staff finds that the FSAR does not provide enough information to show that the dimensional characteristics would be bounding for the assemblies proposed for storage in the MPC-68M considering the new assembly classifications and increased fuel enrichments. Section 6.2.1 of the FSAR (Rev. 7, 8-08) states that "For each assembly class, calculations have been performed for all of the dimensional variations for which data is available." The FSAR then states that these calculations were used to determine the fuel parameters that determine the

maximum reactivity. Provide information demonstrating that the previous analyses are applicable to the new basket and contents including increased enrichments and new fuel classifications (10x10F and 10x10G). The staff needs this information to determine that k-eff has been calculated with the maximum reactivity and to ensure that the applicant has met the requirements in 10 CFR 72.124(a) and 72.236(c).

Holtec response: Discussions and studies have been added to Supplement 6.III, Section 6.III.4 to verify that the fuel dimensional characteristics are appropriate and bounding.

6-4 Justify the use of planar averaged enrichments rather than maximum or discrete radial enrichments.

Appendix 6B of the FSAR (Rev. 7, 8/08) has some analyses showing that this is conservative for certain assemblies within certain MPC geometries. The results shown in Table 6.III.2.1 of the FSAR show that distributed enrichment case 2 has a higher reactivity than the reference case (planar averaged enrichment). Additionally, these results are only applicable for the 10x10A. Justify the use of the planar averaged enrichments despite this known possible non-conservatism and to quantify the maximum difference in k-eff (Δk) for the most reactive fuel type (10x10G) and justify that this would bound all other fuel types to be stored in the MPC-68M considering the higher enrichments and the specific basket materials and geometry. The subtraction of this value from the upper subcriticality limit should be incorporated into the next FSAR Revision upon amendment approval.

This information is needed to determine compliance with 10 CFR 72.236(a) and (c).

Holtec response:

Additional calculations have been performed and added to Supplement 6.III Section 6.III.2. These new studies include additional fuel assembly classes. Based on the results of the studies, a bias of 0.0021 is applied to k_{eff} results for all 10x10 fuel assembly classes.

6-5 Justify the UO_2 fuel density used in the criticality calculations for the MPC-68M is realistic or conservative.

The staff needs this information to determine that k-eff has been calculated with the maximum reactivity and to ensure that the applicant has met the requirements in 10 CFR 72.124(a) and 72.236(c).

Holtec response:

The fuel stack density is assumed to be at 97.5% of the theoretical density for all criticality analyses. This is a conservative value, since it corresponds to a very high pellet density of 99% or more of the theoretical density. Note that this difference between stack and pellet density is due to the necessary dishing and chamfering of the pellets.

6-6 Provide additional information on the assumptions used about the part length rods (PLR) in the MPC-68M.

For assemblies that will contain PLRs were the PLRs modeled? If so, what length was used, and is this a minimum or maximum length? Provide PLR fuel rod specifications and add them to Table 2.1.3 of the Technical Specifications (TS) to reflect the modeling assumptions. They then need to be incorporated into the next FSAR Revision upon amendment approval.

This information is needed to determine compliance with 10 CFR 72.236(a) and (c).

Holtec response:

A discussion has been added in Section 6.III.4 to address part length rods, explaining that all assemblies with part length rods are modeled either with those rods completely removed or with those rods considered full length rods, whichever results in a higher reactivity. With this approach, there is no need to specify the length of any part length rods in the acceptable content tables.

- 6-7 Provide additional information about the modeling of damaged fuel and fuel debris for the MPC-68M and justify that they are conservative.
- a. Explain the difference between the model for damaged fuel and the model for fuel debris.
 - b. Explain Table 6.III.4.1. Why was 11x11 the only array size calculated for the 10x10F array class?
 - c. What were the modeling assumptions for the DFC and/or fuel debris locations? Include information such as enrichment, array size, pellet size, etc.
 - d. What were the modeling assumptions of the intact fuel? Table 6.III.1.3 shows that several assembly classes were grouped together, what fuel was used to represent the intact fuel for each of these classes?
 - e. What were the moderation assumptions used in the DFC models?

The staff needs this information to determine that k-eff has been calculated with the maximum reactivity and to ensure that the applicant has met the requirements in 10 CFR 72.124(a) and 72.236(c).

Holtec response:

A new subsection 6.III.4.1 has been added to Supplement 6.III that discusses the main aspects of the modeling approach for damaged fuel and fuel debris for the MPC-68M, and the corresponding calculations and results. Note that the damaged fuel and fuel debris analyses for the MPC-68M are performed using the same approach previously used for the MPC-68.

- 6-8 Demonstrate that the manufacturing tolerances used within the criticality model are conservative for all fuel types that are allowed in the MPC-68M.

Table 6.III.3.1 of the FSAR presents the results of calculations performed to demonstrate that the tolerances chosen are more conservative than the nominal dimensions. The SAR states that this analysis uses 4.8% enriched 10x10A fuel for the MPC-89M. Per the results in Table 6.III.1.1, the 10x10G is the most reactive. Additionally Table 6.III.1.3 shows the damaged fuel evaluations are even more reactive. Section 6.III.3 of the FSAR (Page 6.III-6) states that the "reactivity effect

(positive or negative) of the manufacturing tolerances is not assembly dependent.” Provide justification for this position.

This information is needed to determine compliance with 10 CFR 72.236(a) and (c).

Holtec response:

Additional calculations have been added to Table 6.III.3.1 to show that the bounding basket assumptions apply to all fuel types.

6-9 Justify the separation in METAMIC in the basket panels used.

This was analyzed using 10x10A fuel for the MPC-68M. Per Tables 6.III.1.1 and 6.III.3 of the FSAR, this fuel type is not the most reactive fuel type for the MPC-68M, and damaged fuel appears to be more reactive. Justify that the calculation performed is bounding or representative of all fuel types to be stored in the MPC-68M. Provide the conditions used in the analysis and a justification used for the proposed separation.

The staff needs this information to determine that k-eff has been calculated with the maximum reactivity and to ensure that the applicant has met the requirements in 10 CFR 72.124(a) and 72.236(c).

Holtec response:

Additional discussion and calculations have been added to Supplement 6.III Section 6.III.4 (see Table 6.III.4.5). Note that the gap and gap distance are conservatively assumed. The licensing drawing for MPC-68M requires that the panels are placed in direct contact. See Drawing 7195R4, Note 4 sent with original amendment request.

6-10 Provide additional information on how the structural material for the fuel assemblies was modeled.

The staff was unable to locate any information describing how the structural material (spacers, top and bottom nozzle, etc.) was modeled in the criticality analysis for the MPC- 68 M. Justify that the modeling assumptions are conservative.

The staff needs this information to determine that k-eff has been calculated with the maximum reactivity and to ensure that the applicant has met the requirements in 10 CFR 72.124(a) and 72.236(c).

Holtec response:

Neutron absorption in minor structural members is neglected, i.e., spacer grids are replaced by water. This is conservative since studies presented in Supplement 6.III Section 6.III.4 show that all assemblies are under moderated (see Table 6.III.4.2), and that the reduction in the amount of (borated or unborated) water within the fuel assembly always results in a reduction of the reactivity. The presence of any other structural material, which would reduce the amount of water, is therefore bounded by those studies, and neglecting this material is conservative. Additionally, the potential neutron

absorption of those materials is neglected. In the axial direction, the modeling is the same as for the MPC-68 as discussed in Section 6.3.1. Only the active region of the fuel assembly is modeled and areas above and below the active region are replaced by pure water.

- 6-11 Justify the positioning of the assemblies within each basket cell of the MPC-68M. Section 6.III.3 of the SAR states that all evaluations were performed with eccentric fuel positioning where the fuel is placed closest to the center of the basket in each basket cell. The staff did not find any justification that this is the most conservative configuration for this MPC and fuel contents. Additionally Table 6.3.6 of the SAR (Rev. 7, 8/08) does not include results for the MPC-68. Provide additional information justifying the positioning of assemblies and DFCs are conservative.

The staff needs this information to determine that k-eff has been calculated with the maximum reactivity and to ensure that the applicant has met the requirements in 10 CFR 72.124(a) and 72.236(c).

Holtec response:

Supplement 6.III, Section 6.III.4 has been updated with additional discussion and calculations to justify the eccentric positioning of the fuel in the MPC-68M (see Table 6.III.4.6).

- 6-12 Justify that the fully flooded condition is the most conservative for the MPC-68M and its allowable contents.

Section 6.III.4 of the FSAR states that the basket and DFCs are fully flooded and that this assumption is based on the various studies presented in the FSAR for previously approved baskets (the MPC-68) and that these studies are applicable to the MPC-68M due to the strong similarity in basket design. The staff reviewed the studies shown in the FSAR (Rev. 7, 8/08) and found that the studies done to show that the fully flooded condition was bounding was performed for the MPC-68 using 8x8 fuel at 4.2% enrichment. This is for the partial density water (internal and external), partial flooding, pellet-to-clad gap flooding and preferential flooding. Justify that these studies are applicable to the MPC-68M and its fuel types and allowed enrichment limits. Address partial flooding for assembly classes with part-length rods (PLRs) – 8x8 fuel has no PLRs.

The staff needs this information to determine that k-eff has been calculated with the maximum reactivity and to ensure that the applicant has met the requirements in 10 CFR 72.124(a) and 72.236(c).

Holtec response:

Supplement 6.III, Section 6.III.4 has been updated with additional discussion and calculations on the bounding moderation conditions, including calculations with partially flooding.

- 6-13 Justify the use of the 10x10A fuel assembly class and the fuel condition used for the criticality evaluation of the storage cask (overpack).

Table 6.III.1.2 of the FSAR shows the results for a “representative value” of k_{eff} for the storage cask (overpack). This is for the 10x10A fuel. Justify that the use of this fuel assembly class is bounding for all others that are allowed in the MPC-68M. State if this calculation includes DFCs. The staff notes the most reactive condition is for damaged fuel (Table 6.III.1.3).

The staff needs this information to determine that k_{eff} has been calculated with the maximum reactivity and to ensure that the applicant has met the requirements in 10 CFR 72.124(a) and 72.236(c).

Holtec response:

The condition in the HI-STORM 100 overpack under dry condition is bounded by a large margin by the calculation for the flooded condition. Based on the additional discussion presented in Supplement 6.III Section 6.III.4 and the very low reactivity condition of the overpack under dry condition, the choice of the fuel assembly used in the calculation is inconsequential.

6-14 Clarify the criticality justification for the inclusion for the 15x15I in the MPC-32.

The criticality justification on page 6 in the letter to US NRC from T.S Morin, Holtec International, License Amendment Request No. 8 (LAR 1014-8) to HI-STORM 100 Certificate of Compliance, November 24, 2009, (ADAMS Accession No. ML09336046), states “Note that for the 15x15B array/class, the lower values for filled or voided guide tubes are listed below, while the 15x15I array/class has solid guide rods that cannot be filled or voided.” The staff asks the applicant to clarify what is meant by the term “lower values.”

10 CFR 72.11(a) requires that the information provided by the applicant be complete and accurate in all material respects.

Holtec response:

The table from the Summary of Proposed Changes submitted with the LAR is repeated below for convenience. The “lower values for filled or voided guide tubes” for the 15x15B array class are the lower values of k_{eff} with either the guide tubes filled or voided. For MPC-32 @ 4.1% enrichment with soluble boron of 1800 ppm the lower values of k_{eff} presented in the table are for the guide tubes voided (See HI-STORM 100 FSAR Table 6.4.11). For MPC-32 @ 5.0% enrichment with soluble boron of 2500 pmm the lower values for k_{eff} are for the guide tubes filled (See HI-STORM 100 FSAR Table 6.4.10). The values of k_{eff} for the 15x15I assembly array/class, which has solid guide tubes that can neither be filled nor voided, are shown to be bounded by the 15x15B, even when comparing to the condition which results in the lower value of k_{eff} .

Fuel Assembly Array/Class	MAXIMUM keff VALUES (Intact Fuel)			
	MPC-32 @ 4.1 % Minimum Soluble Boron 1800 ppm		MPC-32 @ 5.0 % Minimum Soluble Boron 2500 ppm	
	Water density = 1.0 g/cm ³	Water density = 0.93 g/cm ³	Water density = 1.0 g/cm ³	Water density = 0.93 g/cm ³
15x15I	0.9340	0.9316	0.9402	0.9363
15x15B	0.9385	0.9347	0.9402	0.9420

6-15 Provide proposed revised FSAR pages as part of the supporting documentation for the criticality justification for the inclusion of the 15x15I.

10 CFR 72.11(a) requires that the information provided by the applicant be complete and accurate in all material respects.

Holtec response:

The proposed FSAR pages supporting the inclusion of the 15x15I fuel assembly array/class are provided in marked up format in the following attached pages as "Attachment A to RAI 6-15 Response". These changes will be incorporated into the next revision of the FSAR upon approval of the amendment.

Table 2.1.3 (continued)
PWR FUEL ASSEMBLY CHARACTERISTICS (Note 1)

Fuel Assembly Array and Class	15x15 G	15x15H	16x16 A	17x17A	17x17 B	17x17 C	
Clad Material (Note 2)	SS	ZR	ZR	ZR	ZR	ZR	545Z ZR
Design Initial U (kg/assy.) (Note 3)	≤ 420	≤ 495	≤ 448	≤ 433	≤ 474	≤ 480	≤ 495
Initial Enrichment (MPC-24, 24E, and 24EF without soluble boron credit) (wt % ²³⁵ U) (Note 7)	≤ 4.0 (24) ≤ 4.5 (24E/24EF)	≤ 3.8 (24) ≤ 4.2 (24E/24EF)	≤ 4.6 (24) ≤ 5.0 (24E/24EF)	≤ 4.0 (24) ≤ 4.4 (24E/24EF)	≤ 4.0 (24) ≤ 4.4 (24E/24EF)	≤ 4.0 (24) ≤ 4.4 (24E/24EF)	N/A
Initial Enrichment (MPC-24, 24E, 24EF, 32 or 32F with soluble boron credit – see Note 5) (wt % ²³⁵ U)	≤ 5.0	≤ 5.0	≤ 5.0	≤ 5.0	≤ 5.0	≤ 5.0	≤ 5.0
No. of Fuel Rod Locations	204	208	236	264	264	264	216
Fuel Clad O.D. (in.)	≥ 0.422	≥ 0.414	≥ 0.382	≥ 0.360	≥ 0.372	≥ 0.377	≥ 0.413
Fuel Clad I.D. (in.)	≤ 0.3890	≤ 0.3700	≤ 0.3350	≤ 0.3150	≤ 0.3310	≤ 0.3330	≤ 0.367
Fuel Pellet Dia. (in.) (Note 8)	≤ 0.3825	≤ 0.3622	≤ 0.3255	≤ 0.3088	≤ 0.3232	≤ 0.3252	≤ 0.340
Fuel Rod Pitch (in.)	≤ 0.563	≤ 0.568	≤ 0.506	≤ 0.496	≤ 0.496	≤ 0.502	≤ 0.530
Active Fuel length (in.)	≤ 144	≤ 150	≤ 150	≤ 150	≤ 150	≤ 150	≤ 150
No. of Guide and/or Instrument Tubes	21	17	5 (Note 4)	25	25	25	9
Guide/Instrument Tube Thickness (in.)	≥ 0.0145	≥ 0.0140	≥ 0.0350	≥ 0.016	≥ 0.014	≥ 0.020	≥ 0.0140

HOLTEC INTERNATIONAL COPYRIGHTED MATERIAL		
HI-STORM FSAR		Rev. 9
REPORT HI-2002444	2.1-15	

LAR 1014-8

HI-STORM 100 FSAR
REVISION 9
FEBRUARY 13, 2010

Table 2.1.16

Soluble Boron Requirements for MPC-32 and MPC-32F Wet Loading and Unloading Operations

Fuel Assembly Array/Class	All Intact Fuel Assemblies		One or More Damaged Fuel Assemblies or Fuel Debris	
	Max. Initial Enrichment ≤ 4.1 wt.% ^{235}U (ppmb)	Max. Initial Enrichment 5.0 wt.% ^{235}U (ppmb)	Max. Initial Enrichment ≤ 4.1 wt.% ^{235}U (ppmb)	Max. Initial Enrichment 5.0 wt.% ^{235}U (ppmb)
14x14A/B/C/D/E	1,300	1,900	1,500	2,300
15x15A/B/C/G/I	1,800	2,500	1,900	2,700
15x15D/E/F/H	1,900	2,600	2,100	2,900
16x16A	1,400	2,000	1,500	2,300
17x17A/B/C	1,900	2,600	2,100	2,900

Note:

- For maximum initial enrichments between 4.1 wt% and 5.0 wt% ^{235}U , the minimum soluble boron concentration may be determined by linear interpolation between the minimum soluble boron concentrations at 4.1 wt% and 5.1 wt% ^{235}U .

HOLTEC INTERNATIONAL COPYRIGHTED MATERIAL		
HI-STORM FSAR		Rev. 9
REPORT HI-2002444	2.1-30	

HI-STORM 100 FSAR
 REVISION 9
 FEBRUARY 13, 2010

LAR 1014-8

Table 2.1.28 (cont'd)

PWR FUEL ASSEMBLY COOLING TIME-DEPENDENT COEFFICIENTS
(ZR-CLAD FUEL)

Cooling Time (years)	Array/Class 15x15D/E/F/H / I						
	A	B	C	D	E	F	G
≥ 3	14376.7	102.205	-20.6279	-126.017	1903.36	-210.883	-493.065
≥ 4	24351.4	-2686.57	297.975	-110.819	2233.78	-301.615	-152.713
≥ 5	33518.4	-6711.35	958.544	-122.85	2522.7	-371.286	392.608
≥ 6	40377	-10472.4	1718.53	-144.535	2793.29	-426.436	951.528
≥ 7	46105.8	-13996.2	2515.32	-157.827	2962.46	-445.314	1100.56
≥ 8	50219.7	-16677.7	3198.3	-175.057	3176.74	-492.727	1223.62
≥ 9	54281.2	-19555.6	3983.47	-181.703	3279.03	-499.997	1034.55
≥ 10	56761.6	-21287.3	4525.98	-195.045	3470.41	-559.074	1103.3
≥ 11	59820	-23445.2	5165.43	-194.997	3518.23	-561.422	862.68
≥ 12	62287.2	-25164.6	5709.9	-194.771	3552.69	-561.466	680.488
≥ 13	64799	-27023.7	6335.16	-192.121	3570.41	-561.326	469.583
≥ 14	66938.7	-28593.1	6892.63	-194.226	3632.92	-583.997	319.867
≥ 15	68116.5	-29148.6	7140.09	-192.545	3670.39	-607.278	395.344
≥ 16	70154.9	-30570.1	7662.91	-187.366	3649.14	-597.205	232.318
≥ 17	72042.5	-31867.6	8169.01	-183.453	3646.92	-603.907	96.0388
≥ 18	73719.8	-32926.1	8596.12	-177.896	3614.57	-592.868	46.6774
≥ 19	75183.1	-33727.4	8949.64	-172.386	3581.13	-586.347	3.57256
≥ 20	77306.1	-35449	9690.02	-173.784	3636.87	-626.321	-205.513

HOLTEC INTERNATIONAL COPYRIGHTED MATERIAL		
HI-STORM FSAR		Rev. 9
REPORT HI-2002444	2.1-50	

HI-STORM 100 FSAR
REVISION 9
FEBRUARY 13, 2010

Attachment A to RAI 6-15 Response

LAR 1014-8

Table 5.2.1

DESCRIPTION OF DESIGN BASIS ZIRCALOY CLAD FUEL

	PWR	BWR
Assembly type/class	B&W 15x15	GE 7x7
Active fuel length (in.)	144	144
No. of fuel rods	208	49
Rod pitch (in.)	0.568	0.738
Cladding material	Zircaloy-4	Zircaloy-2
Rod diameter (in.)	0.428	0.570
Cladding thickness (in.)	0.0230	0.0355
Pellet diameter (in.)	0.3742	0.488
Pellet material	UO ₂	UO ₂
Pellet density (gm/cc)	10.412 (95% of theoretical)	10.412 (95% of theoretical)
Enrichment (w/o ²³⁵ U)	3.6	3.2
Specific power (MW/MTU)	40	30
Weight of UO ₂ (kg) ^{††}	562.029	225.177
Weight of U (kg) ^{††}	495.485	198.516

Notes:

1. The B&W 15x15 is the design basis assembly for the following fuel assembly classes listed in Table 2.1.1: B&W 15x15, B&W 17x17, CE 14x14, CE 16x16, WE 14x14, WE 15x15, CE 15x15, WE 17x17, St. Lucie, and Ft. Calhoun.
2. The GE 7x7 is the design basis assembly for the following fuel assembly classes listed in Table 2.1.2: GE BWR/2-3, GE BWR/4-6, Humboldt Bay 7x7, and Dresden 1 8x8.

^{††} Derived from parameters in this table.

HOLTEC INTERNATIONAL COPYRIGHTED MATERIAL

HI-STORM FSAR
REPORT HI-2002444

5.2-18

HI-STORM 100 FSAR
REVISION 9
FEBRUARY 13, 2010

Attachment A to RAI 6-15 Response

Rev. 7

AR 1014-8

Table 5.2.25 (page 2 of 2)

DESCRIPTION OF EVALUATED ZIRCALOY CLAD PWR FUEL

Assembly	CE 14x14	CE 16x16	B&W 15x15	B&W 17x17
Fuel assembly array class	14x14C	16x16A	15x15DEF HI	17x17C
Active fuel length (in.)	144	150	144	144
No. of fuel rods	176	236	208	264
Rod pitch (in.)	0.580	0.5063	0.568	0.502
Cladding material	Zr-4	Zr-4	Zr-4	Zr-4
Rod diameter (in.)	0.440	0.382	0.428	0.377
Cladding thickness (in.)	0.0280	0.0250	0.0230	0.0220
Pellet diameter (in.)	0.3805	0.3255	0.3742	0.3252
Pellet material	UO ₂	UO ₂	UO ₂	UO ₂
Pellet density (gm/cc) (95% of theoretical)	10.522 (96%)	10.522 (96%)	10.412 (95%)	10.522 (96%)
Enrichment (wt.% ²³⁵ U)	3.4	3.4	3.4	3.4
Burnup (MWD/MTU)	40,000	40,000	40,000	40,000
Cooling time (years)	5	5	5	5
Power/assembly (MW)	13.7	17.5	19.819	20.4
Specific power (MW/MTU)	31.275	39.083	40	42.503
Weight of UO ₂ (kg) [†]	496.887	507.9	562.029	544.428
Weight of U (kg) [†]	438.055	447.764	495.485	479.968
No. of Guide Tubes	5	5	17	25
Guide Tube O.D. (in.)	1.115	0.98	0.53	0.564
Guide Tube Thickness (in.)	0.0400	0.0400	0.0160	0.0175

[†] Derived from parameters in this table.

HOLTEC INTERNATIONAL COPYRIGHTED MATERIAL

HI-STORM FSAR
REPORT HI-2002444

5.2-44

Rev. 7
LAR 1014-8

HI-STORM 100 FSAR
REVISION 9
FEBRUARY 13, 2010

Attachment A to RAI 6-15 Response

Table 5.2:27

COMPARISON OF SOURCE TERMS FOR ZIRCALOY CLAD PWR FUEL
3.4 wt.% ²³⁵U - 40,000 MWD/MTU - 5 years cooling

Assembly	WE 14x14	WE 14x14	WE 15x15	WE 17x17	WE 17x17	CE 14x14	CE 16x16	B&W 15x15	B&W 17x17
Array class	14x14A	14x14B	15x15 ABC	17x17A	17x17B	14x14C	16x16A	15x15 DEFH	17x17C
Neutrons/sec	1.76E+8 1.78E+8	2.32E+8 2.35E+8	2.70E+8 2.73E+8	2.18E+8	2.68E+8	2.32E+8	2.38E+8	2.94E+8	2.68E+8
Photons/sec (0.45-3.0 MeV)	2.88E+15 2.93E+15	3.28E+15 3.32E+15	3.80E+15 3.86E+15	3.49E+15	3.85E+15	3.37E+15	3.57E+15	4.01E+15	3.89E+15
Thermal power (watts)	809.5 820.7	923.5933. 7	10731086	985.6	1090	946.6	1005	1137	1098

Note:

The WE 14x14 and WE 15x15 have both zircaloy and stainless steel guide tubes. The first value presented is for the assembly with zircaloy guide tubes and the second value is for the assembly with stainless steel guide tubes.

BOUNDING MAXIMUM k_{eff} VALUES FOR EACH ASSEMBLY CLASS IN THE MPC-32 FOR 4.1% ENRICHMENT

Fuel Assembly Class	Maximum Allowable Enrichment (wt% ^{235}U)	Minimum Soluble Boron Concentration (ppm) [*]	Maximum [†] k_{eff}		
			HI-STORM	HI-TRAC	HI-STAR
14x14A	4.1	1300	---	---	0.9041
14x14B	4.1	1300	---	---	0.9257
14x14C	4.1	1300	---	---	0.9423
14x14D	4.1	1300	---	---	0.8970
14x14E	4.1	1300	---	---	0.7340
15x15A	4.1	1800	---	---	0.9206
15x15B	4.1	1800	---	---	0.9397
15x15C	4.1	1800	---	---	0.9266
15x15D	4.1	1900	---	---	0.9384
15x15E	4.1	1900	---	---	0.9365
15x15F	4.1	1900	0.4691	0.9403	0.9411
15x15G	4.1	1800	---	---	0.9147
15x15H	4.1	1900	---	---	0.9276
16x16A	4.1	1400	---	---	0.9375
17x17A	4.1	1900	---	---	0.9111
17x17B	4.1	1900	---	---	0.9309
17x17C	4.1	1900	---	0.9365	0.9355

Note: The HI-STORM results are for internally dry (no moderator) HI-STORM storage casks with full water reflection on all sides, the HI-TRAC results are for internally fully flooded HI-TRAC transfer casks (which are part of the HI-STORM 100 System) with full water reflection on all sides, and the HI-STAR results are for unreflected, internally fully flooded HI-STAR casks.

↳ 15x15I | 4.1 | 1800 | - | - | 0.9340 |

* For maximum allowable enrichments between 4.1 wt% ^{235}U and 5.0 wt% ^{235}U , the minimum soluble boron concentration may be calculated by linear interpolation between the minimum soluble boron concentrations specified in Table 6.1.5 and Table 6.1.6 for each assembly class.

† The term "maximum k_{eff} " as used here, and elsewhere in this document, means the highest possible k_{eff} , including bias, uncertainties, and calculational statistics, evaluated for the worst case combination of manufacturing tolerances.

HOLTEC INTERNATIONAL COPYRIGHTED MATERIAL

REPORT HI-2002444

6.1-13

Rev. 7

LAR 1014-8

Fuel Assembly Class	Maximum Allowable Enrichment (wt% ^{235}U)	Minimum Soluble Boron Concentration (ppm)*	Maximum† k_{eff}		
			HI-STORM	HI-TRAC	HI-STAR
14x14A	5.0	1900	---	---	0.9000
14x14B	5.0	1900	---	---	0.9214
14x14C	5.0	1900	---	---	0.9480
14x14D	5.0	1900	---	---	0.9050
14x14E	5.0	1900	---	---	0.7415
15x15A	5.0	2500	---	---	0.9230
15x15B	5.0	2500	---	---	0.9429
15x15C	5.0	2500	---	---	0.9307
15x15D	5.0	2600	---	---	0.9466
15x15E	5.0	2600	---	---	0.9434
15x15F	5.0	2600	0.5142	0.9470	0.9483
15x15G	5.0	2500	---	---	0.9251
15x15H	5.0	2600	---	---	0.9333
16x16A	5.0	2000	---	---	0.9429
17x17A	5.0	2600	---	---	0.9161
17x17B	5.0	2600	---	---	0.9371
17x17C	5.0	2600	---	0.9436	0.9437

Note: The HI-STORM results are for internally dry (no moderator) HI-STORM storage casks with full water reflection on all sides, the HI-TRAC results are for internally fully flooded HI-TRAC transfer casks (which are part of the HI-STORM 100 System) with full water reflection on all sides, and the HI-STAR results are for unreflected, internally fully flooded HI-STAR casks.

↳ 15x15I | 5.0 | 2500 | - | - | 0.9402 |

* For maximum allowable enrichments between 4.1 wt% ^{235}U and 5.0 wt% ^{235}U , the minimum soluble boron concentration may be calculated by linear interpolation between the minimum soluble boron concentrations specified in Table 6.1.5 and Table 6.1.6 for each assembly class.

† The term "maximum k_{eff} " as used here, and elsewhere in this document, means the highest possible k_{eff} , including bias, uncertainties, and calculational statistics, evaluated for the worst case combination of manufacturing tolerances.

HOLTEC INTERNATIONAL COPYRIGHTED MATERIAL

REPORT HI-2002444

6.1-14

Rev. 7

LAR 1014-8

BOUNDING MAXIMUM k_{eff} VALUES FOR THE MPC-32
WITH UP TO 8 DFCs

Fuel Assembly Class of Intact Fuel	Maximum Allowable Enrichment for Intact Fuel and Damaged Fuel/Fuel Debris (wt% ^{235}U)	Minimum Soluble Boron Content (ppm) [†]	Maximum k_{eff}	
			HI-TRAC	HI-STAR
14x14A, B, C, D, E	4.1	1500	---	0.9336
	5.0	2300	---	0.9269
15x15A, B, C, G, I	4.1	1900	0.9349	0.9350
	5.0	2700	---	0.9365
15x15D, E, F, H	4.1	2100	---	0.9340
	5.0	2900	0.9382	0.9397
16x16A	4.1	1500	---	0.9348
	5.0	2300	---	0.9299
17x17A, B, C	4.1	2100	---	0.9294
	5.0	2900	---	0.9367

[†] For maximum allowable enrichments between 4.1 wt% ^{235}U and 5.0 wt% ^{235}U , the minimum soluble boron concentration may be calculated by linear interpolation between the minimum soluble boron concentrations specified for each assembly class.

HOLTEC INTERNATIONAL COPYRIGHTED MATERIAL

REPORT HI-2002444

6.1-19

Rev. 7

LAR 1014-8

Table 6.2.2 (page 4 of 4)
PWR FUEL CHARACTERISTICS AND ASSEMBLY CLASS DEFINITIONS
(all dimensions are in inches)

Fuel Assembly Designation	Clad Material	Pitch	Number of Fuel Rods	Cladding OD	Cladding Thickness	Pellet Diameter	Active Fuel Length	Number of Guide Tubes	Guide Tube OD	Guide Tube ID	Guide Tube Thickness
15x15G Assembly Class											
15x15G01	SS	0.563	204	0.422	0.0165	0.3825	144	21	0.543	0.514	0.0145
15x15H Assembly Class											
15x15H01	Zr	0.568	208	0.414	0.0220	0.3622	150	17	0.528	0.500	0.0140
16x16A Assembly Class											
16x16A01	Zr	0.506	236	0.382	0.0250	0.3255	150	5	0.980	0.900	0.0400
16x16A02	Zr	0.506	236	0.382	0.0250	0.3250	150	5	0.980	0.900	0.0400
16x16A03	Zr	0.506	236	0.382	0.0235	0.3255	150	5	0.970	0.900	0.0350
17x17A Assembly Class											
17x17A01	Zr	0.496	264	0.360	0.0225	0.3088	150	25	0.474	0.442	0.0160
17x17A02	Zr	0.496	264	0.360	0.0250	0.3030	150	25	0.480	0.448	0.0160
17x17B Assembly Class											
17x17B01	Zr	0.496	264	0.374	0.0225	0.3225	150	25	0.482	0.450	0.0160
17x17B02	Zr	0.496	264	0.374	0.0225	0.3225	150	25	0.474	0.442	0.0160
17x17B03	Zr	0.496	264	0.376	0.0240	0.3215	150	25	0.480	0.448	0.0160
17x17B04	Zr	0.496	264	0.372	0.0205	0.3232	150	25	0.427	0.399	0.0140
17x17B05	Zr	0.496	264	0.374	0.0240	0.3195	150	25	0.482	0.450	0.0160
17x17B06	Zr	0.496	264	0.372	0.0205	0.3232	150	25	0.480	0.452	0.0140
17x17C Assembly Class											
17x17C01	Zr	0.502	264	0.379	0.0240	0.3232	150	25	0.472	0.432	0.0200
17x17C02	Zr	0.502	264	0.377	0.0220	0.3252	150	25	0.472	0.432	0.0200

→ 15x15I01 | Zr | 0.550 | 216 | 0.413 | 0.023 | 0.360 | 150 | 9 | — | — | 0.014

HOLTEC INTERNATIONAL COPYRIGHTED MATERIAL

difficult to identify the bounding assembly. Therefore, additional calculations were performed for the bounding assembly in each assembly class with a planar average enrichment of 3.7 wt%. The results are summarized in Table 6.4.7 and demonstrate that the assembly classes 9x9E and 9x9F have the highest reactivity. These two classes share the same bounding assembly (see footnotes for Tables 6.2.33 and 6.2.34 for further details). This bounding assembly is used as the intact BWR assembly for all calculations with DFCs.

Intact PWR assemblies stored together with DFCs in the MPC-24E are limited to a maximum enrichment of 4.0 wt% ²³⁵U without credit for soluble boron and to a maximum enrichment of 5.0 wt% with credit for soluble boron, regardless of the fuel class. The results presented in Table 6.1.3 are for different enrichments for each class, ranging between 4.2 and 5.0 wt% ²³⁵U, making it difficult to directly identify the bounding assembly. However, Table 6.1.4 shows results for an enrichment of 5.0 wt% for all fuel classes, with a soluble boron concentration of 300 ppm. The assembly class 15x15H has the highest reactivity. This is consistent with the results in Table 6.1.3, where the assembly class 15x15H is among the classes with the highest reactivity, but has the lowest initial enrichment. Therefore, in the MPC-24E, the 15x15H assembly is used as the intact PWR assembly for all calculations with DFCs.

Intact PWR assemblies stored together with DFCs in the MPC-32 are limited to a maximum enrichment of 5.0 wt%, regardless of the fuel class. Table 6.1.5 and Table 6.1.6 show results for enrichments of 4.1 wt% and 5.0 wt%, respectively, for all fuel classes. Since different minimum soluble boron concentrations are used for different groups of assembly classes, the assembly class with the highest reactivity in each group is used as the intact assembly for the calculations with DFCs in the MPC-32. These assembly classes are

- 14x14C for all 14x14 assembly classes;
- 15x15B for assembly classes 15x15A, B, C, and G; and I; |
- 15x15F for assembly classes 15x15D, E, F and H;
- 16x16A; and
- 17x17C for all 17x17 assembly classes.

6.4.4.2.2 Bare Fuel Rod Arrays

A conservative approach is used to model both damaged fuel and fuel debris in the DFCs, using arrays of bare fuel rods:

- Fuel in the DFCs is arranged in regular, rectangular arrays of bare fuel rods, i.e. all cladding and other structural material in the DFC is replaced by water.
- For cases with soluble boron, additional calculations are performed with reduced water density in the DFC. This is to demonstrate that replacing all cladding and other structural material with borated water is conservative.

HOLTEC INTERNATIONAL COPYRIGHTED MATERIAL

HI-STORM FSAR
REPORT HI-2002444

6.4-10

Rev 8

LAR1014-8

Table 6.4.10

MAXIMUM k_{eff} VALUES WITH FILLED AND VOIDED GUIDE TUBES
FOR THE MPC-32 AT 5.0 wt% ENRICHMENT

Fuel Class	Minimum Soluble Boron Content (ppm)	MPC-32 @ 5.0 %			
		Guide Tubes Filled,		Guide Tubes Voided,	
		1.0 g/cm ³	0.93 g/cm ³	1.0 g/cm ³	0.93 g/cm ³
14x14A	1900	0.8984	0.9000	0.8953	0.8943
14x14B	1900	0.9210	0.9214	0.9164	0.9118
14x14C	1900	0.9371	0.9376	0.9480	0.9421
14x14D	1900	0.9050	0.9027	0.8947	0.8904
14x14E	1900	0.7415	0.7301	n/a	n/a
15x15A	2500	0.9210	0.9223	0.9230	0.9210
15x15B	2500	0.9402	0.9420	0.9429	0.9421
15x15C	2500	0.9258	0.9292	0.9307	0.9293
15x15D	2600	0.9426	0.9419	0.9466	0.9440
15x15E	2600	0.9394	0.9415	0.9434	0.9442
15x15F	2600	0.9445	0.9465	0.9483	0.9460
15x15G	2500	0.9228	0.9244	0.9251	0.9243
15X15H	2600	0.9271	0.9301	0.9317	0.9333
16X16A	2000	0.9377	0.9375	0.9429	0.9389
17x17A	2600	0.9105	0.9145	0.9160	0.9161
17x17B	2600	0.9345	0.9358	0.9371	0.9356
17X17C	2600	0.9417	0.9431	0.9437	0.9430

↳ 15x15I* | 2500 | 0.9402 | 0.9363 | - | - |

* This array/class has solid guide rods that cannot be filled or voided |

HOLTEC INTERNATIONAL COPYRIGHTED MATERIAL

HI-STORM FSAR
REPORT HI-2002444

6.4-28

Rev. 8

LAR 1014-8

Table 6.4.11

MAXIMUM k_{eff} VALUES WITH FILLED AND VOIDED GUIDE TUBES
FOR THE MPC-32 AT 4.1 wt% ENRICHMENT

Fuel Class	Minimum Soluble Boron Content (ppm)	MPC-32 @ 4.1 %			
		Guide Tubes Filled		Guide Tubes Voided	
		1.0 g/cm ³	0.93 g/cm ³	1.0 g/cm ³	0.93 g/cm ³
14x14A	1300	0.9041	0.9029	0.8954	0.8939
14x14B	1300	0.9257	0.9205	0.9128	0.9074
14x14C	1300	0.9402	0.9384	0.9423	0.9365
14x14D	1300	0.8970	0.8943	0.8836	0.8788
14x14E	1300	0.7340	0.7204	n/a	n/a
15x15A	1800	0.9199	0.9206	0.9193	0.9134
15x15B	1800	0.9397	0.9387	0.9385	0.9347
15x15C	1800	0.9266	0.9250	0.9264	0.9236
15x15D	1900	0.9375	0.9384	0.9380	0.9329
15x15E	1900	0.9348	0.9340	0.9365	0.9336
15x15F	1900	0.9411	0.9392	0.9400	0.9352
15x15G	1800	0.9147	0.9128	0.9125	0.9062
15X15H	1900	0.9267	0.9274	0.9276	0.9268
16X16A	1400	0.9367	0.9347	0.9375	0.9308
17x17A	1900	0.9105	0.9111	0.9106	0.9091
17x17B	1900	0.9309	0.9307	0.9297	0.9243
17X17C	1900	0.9355	0.9347	0.9350	0.9308

↳ 15x15I* | 1800 | 0.9340 | 0.9316 | - | - |

* This array/class has solid guide rods that cannot be filled or voided

HOLTEC INTERNATIONAL COPYRIGHTED MATERIAL

HI-STORM FSAR
REPORT HI-2002444

6.4-29

Rev. 8
LAR 1014-8

Table 6.4.14

BOUNDING MAXIMUM k_{eff} VALUES FOR THE MPC-32
WITH UP TO 8 DFCs UNDER VARIOUS MODERATION CONDITIONS.

Fuel Assembly Class of Intact Fuel	Initial Enrichment (wt% ^{235}U)	Minimum Soluble Boron Content (ppm)	Maximum k_{eff}			
			Filled Guide Tubes		Voided Guide Tubes	
			1.0 g/cm ³	0.93 g/cm ³	1.0 g/cm ³	0.93 g/cm ³
14x14A through 14x14E	4.1	1500	0.9277	0.9283	0.9336	0.9298
	5.0	2300	0.9139	0.9180	0.9269	0.9262
15x15A, B, C, G, I	4.1	1900	0.9345	0.9350	0.9350	0.9326
	5.0	2700	0.9307	0.9346	0.9347	0.9365
15x15D, E, F, H	4.1	2100	0.9322	0.9336	0.9340	0.9329
	5.0	2900	0.9342	0.9375	0.9385	0.9397
16x16A	4.1	1500	0.9330	0.9332	0.9348	0.9333
	5.0	2300	0.9212	0.9246	0.9283	0.9299
17x17A, B, C	4.1	2100	0.9284	0.9290	0.9294	0.9285
	5.0	2900	0.9308	0.9338	0.9355	0.9367

HOLTEC INTERNATIONAL COPYRIGHTED MATERIAL

HI-STORM FSAR
REPORT HI-2002444

6.4-32

Rev. 8
LAR 1014-8

Table 6.C.1 (continued)
 CALCULATIONAL SUMMARY FOR ALL CANDIDATE FUEL TYPES
 AND BASKET CONFIGURATIONS

MPC-32, 4.1% Enrichment, Bounding Cases					
Fuel Assembly Designation	Cask	Maximum k_{eff}	Calculated k_{eff}	Std. Dev. (1-sigma)	EALF (eV)
14x14A03	HI-STAR	0.9041	0.9001	0.0006	0.3185
B14x14B01	HI-STAR	0.9257	0.9216	0.0007	0.4049
14x14C01	HI-STAR	0.9423	0.9382	0.0007	0.4862
14x14D01	HI-STAR	0.8970	0.8931	0.0006	0.5474
14x14E02	HI-STAR	0.7340	0.7300	0.0006	0.6817
15x15A01	HI-STAR	0.9206	0.9167	0.0006	0.5072
B15x15B01	HI-STAR	0.9397	0.9358	0.0006	0.4566
B15x15C01	HI-STAR	0.9266	0.9227	0.0006	0.4167
15x15D04	HI-STAR	0.9384	0.9345	0.0006	0.5594
15x15E01	HI-STAR	0.9365	0.9326	0.0006	0.5403
15x15F01	HI-STORM (DRY)	0.4691	0.4658	0.0003	1.207E+04
15x15F01	HI-TRAC	0.9403	0.9364	0.0006	0.4938
15x15F01	HI-STAR	0.9411	0.9371	0.0006	0.4923
15x15G01	HI-STAR	0.9147	0.9108	0.0006	0.5880
15x15H01	HI-STAR	0.9276	0.9237	0.0006	0.4710
16x16A03	HI-STAR	0.9375	0.9333	0.0007	0.4488
17x17A01	HI-STAR	0.9111	0.9072	0.0006	0.4055
17x17B06	HI-STAR	0.9309	0.9269	0.0006	0.4365
17x17C02	HI-TRAC	0.9365	0.9327	0.0006	0.4468
17x17C02	HI-STAR	0.9355	0.9317	0.0006	0.4469

15x15I | HI-STAR | 0.9340 | 0.9301 | 0.0006 | 0.5488

HOLTEC INTERNATIONAL COPYRIGHTED MATERIAL

HI-STORM FSAR
 REPORT HI-2002444

Appendix 6.C-14

Rev. T
 CAR1014-8

Table 6.C.1 (continued)
 CALCULATIONAL SUMMARY FOR ALL CANDIDATE FUEL TYPES
 AND BASKET CONFIGURATIONS

MPC-32, 5.0% Enrichment, Bounding Cases					
Fuel Assembly Designation	Cask	Maximum k_{eff}	Calculated k_{eff}	Std. Dev. (1-sigma)	EALF (eV)
14x14A03	HI-STAR	0.9000	0.8959	0.0007	0.4651
B14x14B01	HI-STAR	0.9214	0.9175	0.0006	0.6009
14x14C01	HI-STAR	0.9480	0.9440	0.0006	0.6431
14x14D01	HI-STAR	0.9050	0.9009	0.0007	0.7276
14x14E02	HI-STAR	0.7415	0.7375	0.0006	0.9226
15x15A01	HI-STAR	0.9230	0.9189	0.0007	0.7143
B15x15B01	HI-STAR	0.9429	0.9390	0.0006	0.7234
B15x15C01	HI-STAR	0.9307	0.9268	0.0006	0.6439
15x15D04	HI-STAR	0.9466	0.9425	0.0007	0.7525
15x15E01	HI-STAR	0.9434	0.9394	0.0007	0.7215
15x15F01	HI-STORM (DRY)	0.5142	0.5108	0.0004	1.228E+04
15x15F01	HI-TRAC	0.9470	0.9431	0.0006	0.7456
15x15F01	HI-STAR	0.9483	0.9443	0.0007	0.7426
15x15G01	HI-STAR	0.9251	0.9212	0.0006	0.9303
15x15H01	HI-STAR	0.9333	0.9292	0.0007	0.7015
16x16A03	HI-STAR	0.9429	0.9388	0.0007	0.5920
17x17A01	HI-STAR	0.9161	0.9122	0.0006	0.6141
17x17B06	HI-STAR	0.9371	0.9331	0.0006	0.6705
17x17C02	HI-TRAC	0.9436	0.9396	0.0006	0.6773
17x17C02	HI-STAR	0.9437	0.9399	0.0006	0.6780

↳ 15x15I | HI-STAR | 0.9402 | 0.9359 | 0.0008 | 0.7318 |

HOLTEC INTERNATIONAL COPYRIGHTED MATERIAL

HI-STORM FSAR
 REPORT HI-2002444

Appendix 6.C-15

Rev. 7
 LAR 1014-8

7.0 Confinement Evaluation

- 7-1 Draft NUREG-1536, Revision 1C, "Standard Review Plan for Spent Fuel Dry Storage Systems at a General License Facility," and Draft Interim Staff Guidance – 25, "Pressure Test and Helium Leakage Test of the Confinement Boundary for Spent Fuel Storage Canister" have been issued for public comment and for which public comments have been resolved. These documents provide clarification to ANSI N14.5, and require helium leakage rate tests of the entire confinement boundary including welds and base material. The proposed Certificate of Compliance (CoC) states that helium leakage tests are performed on the MPC confinement boundary welds (excluding the lid-to-shell weld per ISG-18). Provide justification for the acceptability of weld helium leakage testing only (which is contrary to 10 CFR 72.236 (j) and (l) as well as the ANSI N14.5 consensus standard), or modify the FSAR to test the entire confinement boundary welds and base material. Also, FSAR Chapters 2, 7 and 9 do not appear to be consistent with the confinement boundary weld testing stated in the proposed CoC and should be clarified.

For example, Section 9.III of the HI-STORM 100 FSAR Supplement states, "The main body of this chapter remains fully applicable for the HI-STORM 100 System using the MPC-68M model fuel basket (with existing MPC enclosure vessel) except as described below." The main body of Chapter 9 in the HI-STORM 100 FSAR Rev. 7 does not appropriately address ANSI N14.5 fabrication leakage rate tests of the entire confinement boundary welds and base material (excluding the lid-to-shell weld per ISG-18).

Section 9.1.3 of the FSAR Rev. 7 states, "Leakage testing of the MPC shop welds (shell seams and shell-to-baseplate shop welds) and the field welded MPC lid-to-shell weld and closure ring welds are not required." Also in Section 9.1.3 of the FSAR Rev. 7, the applicant does not address performing a fabrication leakage rate test on the MPC shell, baseplate, and lid.

This information is needed to determine compliance with 10 CFR 72.236(j) and (l).

Holtec response:

The reviewer is correct that Revision 7 of the FSAR Section 9.1.3 does not indicate the helium leakage test on the MPC shop welds (shell seams and shell to base plate shop welds). This version of the FSAR was published on August 9, 2008, prior to the non-cited violation issued by the NRC (EA-09-190 dated August 6, 2009) and Holtec's corrective action provided in Reply to EA-09-190 (Holtec letter 5014690 dated September 2, 2009).

In the reply to EA-09-190, Holtec indicated that the FSAR was updated to re-establish the shop fabrication helium leak test of the MPC shell seam and shell to base plate welds with acceptance criteria of 1×10^{-7} atm-cc/s [air] ("leaktight" in accordance with ANSI N14.5 criteria). This change is published in FSAR Revision 8 (January 18, 2010) and again in FSAR Revision 9. FSAR Revision 9 was provided to the NRC as the biennial FSAR update in accordance with 72.248(c)(6) via Holtec letter 5014701 dated May 3,

2010. This LAR does not seek to remove or revise the shop fabrication helium leak test requirement.

CoC Amendment #7 which became effective December 28, 2009 includes, in Condition #3, the requirement for helium leak testing of the MPC shell seam and shell to baseplate confinement welds. Condition #3 of Holtec's proposed CoC to this LAR is identical to Condition #3 of CoC Amendment #7, i.e. this LAR does not seek to remove or revise the requirement.

In light of the recently published ISG-25 we understand that the NRC interprets ANSI N14.5 to require helium leak testing of not only the shop confinement welds but also the base metals of the confinement boundary.

Holtec International has been studying the safety imperative of performing helium leak testing of the MPC confinement boundary (base metal and welds) both theoretically and through physical tests of the MPCs in the shop and at the loading sites. Our analytical evaluations conclude that helium leak tests do not add value with respect to ensuring additional confidence in the leak-tightness of the MPC Enclosure vessel. Actual helium leak tests on hundreds of manufactured canisters in our factory over a period of nearly 10 years inform us that the helium leak test fails to reveal a state of leakage in a canister fabricated using ASME Section III Class 1 criteria in even a single instance. Nevertheless, CoC Amendment # 7, the latest CoC Amendment as of this writing, already requires the helium leak testing of the MPC shop fabrication welds.

Holtec considers that helium leak testing the ASME Code compliant and UT inspected confinement boundary base metals of the MPC (especially the substantially thick MPC lid) is unnecessary and that helium leak testing the base metal of the lid is not supported by ISG-25 as follows.

From ISG-25, page 2, "...the applicant may specify that the cask user perform a field pressure test with visual examination of only accessible portions of the canister. In this case, the applicant should identify an alternative test (i.e. ANSI N14.5 helium leakage test) to demonstrate fabrication integrity of the welds that are inaccessible during field pressure test."

Since an ASME code pressure test at the manufacturing facility is not performed (NRC approved ASME Code alternative), the user of the canister must perform a field pressure test with visual examination of the accessible portions of the canister (lid and lid-to-shell weld). Therefore, per ISG-25, an alternative test (i.e. ANSI N14.5 helium leakage test) to demonstrate fabrication integrity of these accessible portions of the canister is not required.

In summary, Holtec's position is that helium leak testing the confinement boundary base metals of an ASME Section III Class 1 fabricated 100% UT inspected MPC enclosure vessel, is unmerited. Furthermore, this new requirement is inconsistent with current and proven industry practice as well as previous Holtec license amendments. In any case, if the NRC staff believes helium leakage testing is a meaningful and necessary requirement

for the Holtec MPC design (including the thick MPC lid) then we request that the NRC staff update the CoC as appropriate and Holtec's QA program will ensure the FSAR is updated accordingly. Because any change to the CoC will only be reflected in CoC Amendment #8, this change will only apply to those MPCs loaded to Amendment #8 and not prior amendments.

- 7-2 Clarify step 8.1.5.9.f of the FSAR Rev. 7 to perform a helium leak test on the vent and drain port cover plates.

Section 8.III.0 of the FSAR Supplement states that the procedure steps outlined in Chapter 8 for loading, unloading, and recovery remain applicable. Step 8.1.5.8.f of the FSAR Rev. 7 states that a helium leak test will be performed on the vent and drain port cover plate welds. Step 8.1.5.9 of the FSAR Rev. 7 states, "Perform a leakage test of the MPC vent and drain port cover plates as follows:" While step 8.1.5.9.f of the FSAR Rev. 7 also states that a helium leak test will be performed on the vent and drain port cover plate welds.

This information is needed to determine compliance with 10 CFR 72.236(j) and (l).

Holtec response:

It was clarified in a telecom with the Staff that the intent of this question is to address helium leak testing of the cover plate base metal in addition to the helium leak testing of the cover plate welds. The surveillance in CoC Amendment #7 (SR 3.1.1.3), which we have retained in the proposed CoC to this LAR, states the user must verify that the helium leak rate through the MPC vent and drain port confinement welds meets the leaktight criteria of ANSI N14.5-1997.

The MPC vent and drain port cover plates are confinement boundary components that are welded to the MPC lid; therefore, the portion of response to RAI 7-1 concerning helium leak testing of MPC confinement boundary base metal is also applicable to this RAI. See response to RAI 7-1.

In summary, if the NRC staff believes helium leakage testing of the MPC vent and drain port cover plate base metal is a meaningful and necessary requirement for the Holtec MPC design then we request that the NRC staff update the CoC as appropriate and Holtec's QA program will ensure the FSAR is updated accordingly. Because any change to the CoC will only be reflected in CoC Amendment #8, this change will only apply to those MPCs loaded to Amendment #8 and not prior amendments.

- 7-3 Modify Chapter 7 of the HI-STORM 100 FSAR to address the damaged fuel assemblies that have been requested to be loaded in the MPC-68M basket. According to Table 2.1-1 Section VI of the proposed CoC provided by the applicant, damaged fuel will be loaded in the MPC-68M basket. Loading damaged fuel in the MPC-68M basket should additionally be addressed in Section 7.1.5 of the FSAR. The FSAR needs to be updated to reflect this upon approval of this amendment.

This information is needed to determine compliance with 10 CFR 72.24(c)(3).

Holtec response:

For consistency with the content/formatting style for MPC-68M information in the FSAR, Supplement 7.III, Subsection 7.III.1.5, is updated to address loading of damaged fuel assemblies and fuel debris in the MPC-68M instead of FSAR Subsection 7.1.5.

13.0 Materials Evaluation

13-1 FSAR Supplement Chapter 2. Clarify whether or not the fuel debris mentioned in FSAR supplement section 2.III.1 contains any materials not previously reviewed and accepted for storage applications. Previously reviewed and accepted fuel debris or non-fuel hardware materials include: boron carbide, borosilicate glass, silver-indium-cadmium alloy, and thorium oxide.

Should different materials from the above list be included in the fuel debris mentioned in FSAR supplement section 2.III.1, provide an assessment of potential chemical/galvanic reactions, as per FSAR Chapter 8.

This information is required to determine compliance with 10 CFR 72.120(d).

Holtec response:

As stated in the telecom documenting a clarifying phone call held on July 7, 2010 between Staff and Holtec this RAI question is retracted. It was indicated on the call that the reviewer was not intending to ask this question about fuel debris. No changes are requested by Holtec to the currently approved definition of fuel debris as part of this LAR. Additionally, Holtec is not requesting approval to load non-fuel hardware in the MPC-68M since BWR fuel does not contain these devices.

13-2 FSAR Supplement Chapter 4. Provide material property data and discussion which supports fuel basket operation above 350°C (662°F). The Metamic HT Sourcebook material property data is limited to a maximum temperature of 350° C (662°F). FSAR supplement tables 4.III.2, 4.III.5, and 4.III.7 all list normal operation or short-term/accident operating temperatures above 350° C (662° F).

This information is required to determine compliance with 10 CFR 72.124(b).

Holtec response:

Table 4.III.2 only provides the limits for the material temperatures, not results. Table 4.III.3 reports the maximum temperatures for normal conditions of storage, and as noted Table 4.III.5 reports the maximum temperatures for short-term operations (vacuum drying), and Table 4.III.7 reports the maximum temperatures for accident conditions (100% blocked inlets). The Metamic-HT coupons were tested at 450°C and 500°C using the same test procedures that were used to obtain the thermo-physical properties presented in the Metamic-HT Sourcebook. The 500°C test temperature comfortably bounds the maximum accident basket temperature reached in the 100% blocked inlet ducts accident. As the value of emissivity is already reported in the Sourcebook at 500°C, additional testing for the value of this property is not necessary. The additional tests therefore address the remaining thermal properties, namely conductivity and heat capacity, and structural properties as described in Appendix 1.III.B.

Table 4.III.5 reports the temperatures during vacuum drying of the MPC-68M and Table 4.III.7 reports a HI-STORM 100 blocked duct accident containing an MPC-68M. The maximum basket temperature under both of the above scenarios is below 500 °C and bounded by the above data.

13-3 FSAR Supplement Chapter 3. Justify structural performance based on material properties under high temperatures.

Table 4.III.2 in the FSAR supplement sets temperature limits for Metamic HT at 752° F (normal storage) or 1000° F (off-normal/design accident temperature of FSAR supplement table 4.III.2). It is unclear, without supporting data or calculations, how buckling or excessive plastic deformation of the basket, or other components such as anchor blocks, is precluded at such temperatures. These temperatures are higher than those previously considered in the HI-STORM FSAR, and contrary to information on the same supplement (e.g., FSAR supplement section 3.III.4.4.3.2 states that 325° C bounds the metal temperatures anywhere in the fuel basket under normal conditions. However, FSAR supplement table 4.III.2 states the normal storage temperature limit to be 752° F (400° C). Therefore, all cases for Normal, Off-Normal, Short-term Operations and Accident Conditions need to be reevaluated considering the effects on the materials of these temperatures.

This information is required to determine compliance with 10 CFR 72.236(l).

Holtec response:

The statement in section 3.III.4.4.3.2 and the temperature limits specified in Table 4.III.2 are compatible. The purpose of Table 4.III.2 is to provide the allowable temperature limits of Metamic-HT and Aluminum Alloy 2219 for various operating conditions considering the thermo-physical properties of the materials, as well as the applicable fuel cladding temperature limits. The temperature limits provided in Table 4.III.2 are only applicable to the thermal analysis, and they have no direct bearing on the structural calculations. That is because the structural calculations are carried out using input temperatures that bound the actual calculated temperatures in Table 4.III.3, rather than the maximum allowable temperature limits for the materials. Hence, the statement in section 3.III.4.4.3.2 is accurate. Although the limit of the material is 752°F, the maximum temperature of the Metamic-HT fuel basket during long term normal storage is 585°F (307°C) as indicated in Table 4.III.3. Using the properties of Metamic-HT at 325°C to perform the structural calculations for normal conditions is appropriate as it bounds the maximum basket temperature for normal long term storage.

Finally, the short-term operation, off-normal, and accident condition temperature limit for Metamic-HT in Table 4.III.2 has been reduced to 932°F to be consistent with the measured physical property data in the Metamic-HT Sourcebook (see response to RAI 13-2). The maximum calculated Metamic-HT metal temperature is bounded by 932°F under all short term operations, off-normal, and accident scenarios.

Table 2.1-3 (page 4 of 5)
BWR FUEL ASSEMBLY CHARACTERISTICS (Note 1)

Fuel Assembly Array/Class	10x10A	10x10B	10x10C	10x10D	10x10E	10x10F	10x10G
Clad Material	ZR	ZR	ZR	SS	SS	ZR	ZR
Design Initial U (kg/assy.) (Note 3)	≤ 188	≤ 188	≤ 179	≤ 125	≤ 125	≤ 192	≤ 188
Maximum PLANAR-AVERAGE INITIAL ENRICHMENT-(MPC-68, 68F, and 68FF) (wt.% ²³⁵ U) (Note 14)	≤ 4.2	≤ 4.2	≤ 4.2	≤ 4.0	≤ 4.0	Note 17	Note 17
Maximum PLANAR-AVERAGE INITIAL ENRICHMENT (MPC-68M) (wt.% ²³⁵ U) (Note 16)	≤ 4.8	≤ 4.8	≤ 4.8	Note 18	Note 18	≤ 4.7	≤ 4.6 (Note 15)
Initial Maximum Rod Enrichment (wt.% ²³⁵ U)	≤ 5.0	≤ 5.0	≤ 5.0	≤ 5.0	≤ 5.0	≤ 5.0	≤ 5.0
No. of Fuel Rod Locations	92/78 (Note 8)	91/83 (Note 9)	96	100	96	92/78 (Note 8)	96/84
Fuel Rod Clad O.D. (in.)	≥ 0.4040	≥ 0.3957	≥ 0.3780	≥ 0.3960	≥ 0.3940	≥ 0.4035	≥ 0.387
Fuel Rod Clad I.D. (in.)	≤ 0.3520	≤ 0.3480	≤ 0.3294	≤ 0.3560	≤ 0.3500	≤ 0.3570	≤ 0.340
Fuel Pellet Dia. (in.)	≤ 0.3455	≤ 0.3420	≤ 0.3224	≤ 0.3500	≤ 0.3430	≤ 0.3500	≤ 0.334
Fuel Rod Pitch (in.)	≤ 0.510	≤ 0.510	≤ 0.488	≤ 0.565	≤ 0.557	≤ 0.510	≤ 0.512
Design Active Fuel Length (in.)	≤ 150	≤ 150	≤ 150	≤ 83	≤ 83	≤ 150	≤ 150
No. of Water Rods (Note 11)	2	1 (Note 6)	5 (Note 10)	0	4	2	5 (Note 10)
Water Rod Thickness (in.)	≥ 0.030	> 0.00	≥ 0.031	N/A	≥ 0.022	≥ 0.030	≥ 0.031
Channel Thickness (in.)	≤ 0.120	≤ 0.120	≤ 0.055	≤ 0.080	≤ 0.080	≤ 0.120	≤ 0.060

AFFIDAVIT PURSUANT TO 10 CFR 2.390

I, Tammy S. Morin, being duly sworn, depose and state as follows:

- (1) I have reviewed the information described in paragraph (2) which is sought to be withheld, and am authorized to apply for its withholding.
- (2) The information sought to be withheld are Attachments 2 , 3 and 4 to Holtec Letter 5014712 which contain Holtec Proprietary information.
- (3) In making this application for withholding of proprietary information of which it is the owner, Holtec International relies upon the exemption from disclosure set forth in the Freedom of Information Act ("FOIA"), 5 USC Sec. 552(b)(4) and the Trade Secrets Act, 18 USC Sec. 1905, and NRC regulations 10CFR Part 9.17(a)(4), 2.390(a)(4), and 2.390(b)(1) for "trade secrets and commercial or financial information obtained from a person and privileged or confidential" (Exemption 4). The material for which exemption from disclosure is here sought is all "confidential commercial information", and some portions also qualify under the narrower definition of "trade secret", within the meanings assigned to those terms for purposes of FOIA Exemption 4 in, respectively, Critical Mass Energy Project v. Nuclear Regulatory Commission, 975F2d871 (DC Cir. 1992), and Public Citizen Health Research Group v. FDA, 704F2d1280 (DC Cir. 1983).

AFFIDAVIT PURSUANT TO 10 CFR 2.390

- (4) Some examples of categories of information which fit into the definition of proprietary information are:
- a. Information that discloses a process, method, or apparatus, including supporting data and analyses, where prevention of its use by Holtec's competitors without license from Holtec International constitutes a competitive economic advantage over other companies;
 - b. Information which, if used by a competitor, would reduce his expenditure of resources or improve his competitive position in the design, manufacture, shipment, installation, assurance of quality, or licensing of a similar product.
 - c. Information which reveals cost or price information, production, capacities, budget levels, or commercial strategies of Holtec International, its customers, or its suppliers;
 - d. Information which reveals aspects of past, present, or future Holtec International customer-funded development plans and programs of potential commercial value to Holtec International;
 - e. Information which discloses patentable subject matter for which it may be desirable to obtain patent protection.

The information sought to be withheld is considered to be proprietary for the reasons set forth in paragraphs 4.a and 4.b above.

- (5) The information sought to be withheld is being submitted to the NRC in confidence. The information (including that compiled from many sources) is of a sort customarily held in confidence by Holtec International, and is in fact so held. The information sought to be withheld has, to the best of my knowledge and belief, consistently been held in confidence by Holtec International. No public disclosure has been made, and it is not available in public sources. All

AFFIDAVIT PURSUANT TO 10 CFR 2.390

disclosures to third parties, including any required transmittals to the NRC, have been made, or must be made, pursuant to regulatory provisions or proprietary agreements which provide for maintenance of the information in confidence. Its initial designation as proprietary information, and the subsequent steps taken to prevent its unauthorized disclosure, are as set forth in paragraphs (6) and (7) following.

- (6) Initial approval of proprietary treatment of a document is made by the manager of the originating component, the person most likely to be acquainted with the value and sensitivity of the information in relation to industry knowledge. Access to such documents within Holtec International is limited on a "need to know" basis.
- (7) The procedure for approval of external release of such a document typically requires review by the staff manager, project manager, principal scientist or other equivalent authority, by the manager of the cognizant marketing function (or his designee), and by the Legal Operation, for technical content, competitive effect, and determination of the accuracy of the proprietary designation. Disclosures outside Holtec International are limited to regulatory bodies, customers, and potential customers, and their agents, suppliers, and licensees, and others with a legitimate need for the information, and then only in accordance with appropriate regulatory provisions or proprietary agreements.
- (8) The information classified as proprietary was developed and compiled by Holtec International at a significant cost to Holtec International. This information is classified as proprietary because it contains detailed descriptions of analytical approaches and methodologies not available elsewhere. This information would provide other parties, including competitors, with information from Holtec International's technical database and the results of evaluations performed by Holtec International. A substantial effort has been expended by Holtec International to develop this information. Release of this information would improve a competitor's position because it would enable Holtec's competitor to copy our technology and offer it for sale in competition with our company, causing us financial injury.

AFFIDAVIT PURSUANT TO 10 CFR 2.390

- (9) Public disclosure of the information sought to be withheld is likely to cause substantial harm to Holtec International's competitive position and foreclose or reduce the availability of profit-making opportunities. The information is part of Holtec International's comprehensive spent fuel storage technology base, and its commercial value extends beyond the original development cost. The value of the technology base goes beyond the extensive physical database and analytical methodology, and includes development of the expertise to determine and apply the appropriate evaluation process.

The research, development, engineering, and analytical costs comprise a substantial investment of time and money by Holtec International.

The precise value of the expertise to devise an evaluation process and apply the correct analytical methodology is difficult to quantify, but it clearly is substantial.

Holtec International's competitive advantage will be lost if its competitors are able to use the results of the Holtec International experience to normalize or verify their own process or if they are able to claim an equivalent understanding by demonstrating that they can arrive at the same or similar conclusions.

The value of this information to Holtec International would be lost if the information were disclosed to the public. Making such information available to competitors without their having been required to undertake a similar expenditure of resources would unfairly provide competitors with a windfall, and deprive Holtec International of the opportunity to exercise its competitive advantage to seek an adequate return on its large investment in developing these very valuable analytical tools.

APPENDIX 1.III.B: METAMIC-HT¹ PROPERTIES SUPPORTING MPC-68M SHORT-TERM OPERATIONS AND ACCIDENT EVALUATIONS

The temperature range at which the mechanical and thermo physical properties of Metamic-HT have been provided in Appendix 1.III.A is exceeded under certain short-term operations and accident conditions. To facilitate the evaluation of Metamic-HT integrity, Minimum Guaranteed Values (MGV) of Metamic-HT properties are defined in the same manner as described in Appendix 1.III.A and adopted in this Appendix. Metamic-HT properties germane to structural and thermal evaluation are as follows:

- ❖ *Ultimate Tensile Strength*
- ❖ *Yield Strength*
- ❖ *Area Reduction*
- ❖ *Young's Modulus*
- ❖ *Thermal Conductivity*
- ❖ *Emissivity*
- ❖ *Specific Heat*

Reasonably bounding MGVs of above properties are defined in Table 1.III.B.1 up to 500°C, which comfortably bounds all temperatures.

1.III.B.1 High Temperature Tensile Testing

To characterize the mechanical properties of Metamic-HT for this higher temperature range the Ultimate, Yield, Area Reduction and Young's Modulus of Metamic-HT coupons were tested under bounding test temperatures. The testing was conducted at the Westmoreland testing lab in Youngstown, PA. The test specimens were prepared and tested in accordance with the ASTM standards adopted in the Metamic-HT sourcebook for qualification testing. A total of fifteen coupons were tested at 450°C and 500°C in the as-extruded condition and test results archived in the Metamic-HT Sourcebook [1.III.A.3]. Thermal aging and irradiation effects were not included in the testing as prior testing archived in the Metamic-HT sourcebook have discerned no significant difference due to these effects.

To characterize lower bound strength of Metamic-HT the Minimum Measured Values (MMV) of the above properties were obtained, archived in the Metamic-HT sourcebook and MGV compliance evaluated. In all cases the Metamic-HT properties meet or exceed Minimum Guaranteed Values prescribed in Table 1.III.B.1. The high temperature strength values of Metamic-HT support the following:

- ❖ *Metamic-HT retains well over 50% of the operating temperature strength properties at a reasonably bounding 450°C accident temperature.*

¹ *This appendix is abstracted from the Metamic-HT Sourcebook [1.III.A.3].*

- ❖ *Under extremely high 500°C temperature reasonable values of strength properties are retained.*
- ❖ *The test data provides reasonable assurance of Metamic-HT integrity under thermally challenging events.*

1.III.B.2 High Temperature Thermo-physical Properties

To characterize the thermal properties of Metamic-HT for this higher temperature range the conductivity, emissivity and heat capacity of Metamic-HT coupons were tested under bounding test temperatures. With the exception of emissivity property wherein prior testing adequately covered the high temperature range up to 500°C additional tests were conducted to measure the conductivity and specific heat properties. A total of two specimens were tested for each of the conductivity and specific heat properties in accordance with the ASTM standards adopted in the Metamic-HT Sourcebook [1.III.A.3]. As thermo-physical properties are principally a function of composition the properties were tested in the as-manufactured condition from the extrusion plant. The coupons were tested at 450°C and 500°C and test results archived in the Metamic-HT Sourcebook. The results are evaluated in the following.

Conductivity Measurements

To characterize the lower bound conductivity of Metamic-HT the Minimum Measured Value (MMV) were obtained and MGV compliance confirmed. To discern data trends the MMV conductivity values in the operating temperature range and high temperature range are tabulated below.

<i>Temperature (°C)</i>	<i>205</i>	<i>370</i>	<i>450</i>	<i>500</i>
<i>Conductivity (W/m-°K)</i>	<i>188</i>	<i>187</i>	<i>193</i>	<i>193</i>

The above data supports the observation that Metamic-HT thermal conductivity is essentially constant for the temperature range spanning all operating and accident temperatures. Therefore a single valued lower bound conductivity defined in the MGV tables provides a conservative characterization of Metamic-HT conductivity for evaluation under normal, off-normal and accident conditions.

Emissivity Measurements

Emissivity measurements in the high temperature range at an upper bound 500°C temperature are covered by prior testing reported in the Metamic-HT Sourcebook. The measured emissivity data supports the Table 1.III.B.1 MGV requirement that high temperature Metamic-HT emissivity meets or exceeds $\epsilon = 0.8$.

Specific Heat Measurements

HOLTEC INTERNATIONAL COPYRIGHTED MATERIAL

In accordance with definition of heat capacity as a reference property in Table 1.III.B.1 the mean value of the measurements were obtained and added to Metamic-HT Sourcebook. To discern data trends the mean heat capacity values in the operating temperature range and high temperature range are tabulated below.

Temperature (°C)	350°C	450°C	500°C
Heat Capacity (J/kg-°K)	1024.2	1129.2	1098.2

The above data supports the observation that the heat capacity of Metamic-HT is a weak function of temperature. To provide a reasonable characterization of heat capacity in the range of 350°C to 500°C a linear function fitting the end points of the range is obtained and added to Table 1.III.B.1.

Table 1.III.B.1:
Reference & Minimum Guaranteed Values (MGVs) of Metamic-HT Mechanical and Thermal Characteristics Supporting Accident Evaluations

	Property	Temperature, °C	Design Value	Type
1.	Yield strength, σ_y (ksi)	450/500	8.5/6	MGV
2.	Tensile strength, σ_u (ksi)	450/500	9/6.5	MGV
3.	Young's Modulus, E (ksi)	450/500	4000/3500	MGV
4.	Area Reduction, A (%)	450/500	9.5/4	MGV
5.	Thermal conductivity, k (W/m °K)	450/500	180/180	MGV
6.	Emissivity (dimensionless), e	350 ≤ T ≤ 500	See Note 1	MGV
7.	Specific Heat, C_p (J/g-°C) (Note 2)	350 ≤ T ≤ 500	Note 3	Reference

Note 1: Emissivity Equation (Hard Anodized Metamic-HT)

$$e = 0.2 + 0.6 \sin[\pi(T-100)/1304] \quad (100^\circ\text{F} \leq T \leq 752^\circ\text{F})$$

$$e = 0.8 \quad (T > 752^\circ\text{F})$$

Note 2: These properties are reference values (not MGVs). Property variations in the small do not have significant effect on the safety evaluations in which these properties are used. Reference properties are characterized by the mean of the measured data.

Note 3: Heat Capacity Function

$$C_p = 1024.2 + 0.493(T-350)$$

SUPPLEMENT 3.III

STRUCTURAL EVALUATION OF THE MPC-68M

3.III.0 OVERVIEW

In this supplement, the structural adequacy of the MPC-68M is evaluated pursuant to the guidelines of NUREG-1536.

The organization of technical information in this supplement mirrors the format and content of Chapter 3 except that it only contains material directly pertinent to the MPC-68M.

The MPC-68M consists of a stainless steel (Alloy X) Enclosure Vessel, which is identical to that of the MPC-68, a BWR fuel basket made from Metamic-HT, and aluminum basket shims. Section 1.III.2 contains a complete description of the MPC-68M components.

The applicable codes, standards, and practices governing the structural analysis of the MPC-68M as well as the design criteria, are presented in Supplement 2.III. Throughout this supplement, the term "*safety factor*" is defined as the *ratio of the allowable stress (load) or displacement for the applicable load combination to the maximum computed stress (load) or displacement*. Where applicable, bounding safety factors are computed using values that bound the calculated results.

3.III.1 STRUCTURAL DESIGN

3.III.1.1 Discussion

A general discussion of the structural features of the MPC is provided in Subsection 3.1.1, and in general it applies to the MPC-68M with one notable exception. The MPC-68M fuel basket is qualified using a deflection-based acceptance criterion (see Subsection 2.III.0.1) as opposed to a stress-based criterion. The drawings of the MPC-68M fuel basket and MPC Enclosure Vessel are provided in Section 1.5.

3.III.1.2 Design Criteria

Same as in Subsection 3.1.2, including all of its paragraphs, except as modified in Subsection 2.III.0.1 for the MPC-68M fuel basket.

3.III.2 WEIGHTS AND CENTERS OF GRAVITY

Since the weight density of Metamic-HT is significantly less than that of Alloy X, the MPC-68M weighs less than the MPCs listed in Table 3.2.1. The bounding weights for the MPC-68M are provided in Table 3.III.1.

The center of gravity (CG) height of the empty MPC-68M, and various other configurations involving the MPC-68M, is provided in Table 3.III.2.

3.III.3 MECHANICAL PROPERTIES OF MATERIALS

The strength properties of Metamic-HT have been characterized through a comprehensive test program, and Minimum Guaranteed Values suitable for structural design are provided in Appendix 1.III.A and also archived in [1.III.A.3]. The fuel basket shims are made of an aluminum alloy (ASTM B221 2219-T851). Representative mechanical properties for the fuel basket shims are tabulated in Table 3.III.3. The mechanical properties for all other materials of construction are the same as in Section 3.3 (including all subsections and tables).

3.III.4 GENERAL STANDARDS FOR CASKS

3.III.4.1 Chemical and Galvanic Reactions

The materials used in the HI-STORM 100 System are examined in Subsection 3.4.1 to establish that they do not participate in any chemical or galvanic reactions when exposed to the various environments during all normal operating conditions and off-normal and accident events. The only new materials that are introduced in the MPC-68M are Metamic-HT (for the fuel basket) and aluminum (for the basket shims). The environmental compatibility of these materials is examined below.

The MPC-68M is principally constructed of stainless steel shell, aluminum basket shims, and Metamic-HT. Borated aluminum and stainless steel have been used in close proximity in wet storage for over 30 years. Many spent fuel pools at nuclear plants contain fuel racks, which are fabricated from Metamic (classic) and stainless steel materials. Not one case of chemical or galvanic degradation has been found in such fuel racks. This experience provides a sound basis to conclude that chemical and galvanic corrosion of these materials will be negligible. For further protection, both Metamic-HT and aluminum basket shims are installed in the anodized state in the MPC.

Furthermore, galvanic corrosion is not an applicable corrosion mechanism during long-term storage since the interior of the MPC during normal operation is both inerted with helium and essentially devoid of any moisture while the MPC shell surfaces are expected to be practically free from condensation and gross environmental contaminants. The cleanliness requirements and inspections during fabrication and fuel loading operations also ensure that the MPC has minimal surface debris and impurities.

Tests on Metamic-HT

Extensive tests [1.III.A.3] have been conducted to establish material properties of Metamic-HT including its corrosion-resistance characteristics. The Metamic-HT specimens were used for corrosion testing in demineralized water and in 2000 ppm boric acid solution. The tests

concluded that the Metamic-HT panels will sustain no discernible degradation due to corrosion when subjected to the severe thermal and aqueous environment that exists around a fuel basket during fuel loading or unloading conditions.

Aluminum Alloy

Aluminum alloy used in the fuel basket shims are hard anodized to achieve the desired emissivity specified in Supplement 3.III. The anodizing is an electrolytic passivation process used to increase the thickness of the natural oxide layer on the surface of metal parts. Anodizing increases corrosion resistance and wear resistance of the material surface. There is no mechanistic process for the basket shims with hard anodized surface to react with borated water or demineralized water during fuel loading operation. Under the long-term storage condition, the basket shims are exposed to dry and inert helium with no potential for reaction.

Finally, to ensure safe fuel loading operation, the operating procedure described in Chapter 8 provides for the monitoring of hydrogen gas in the area around the MPC lid prior to and during welding or cutting activities. Although the aluminum surfaces (Metamic-HT fuel basket and aluminum basket shims) are anodized, there is still a potential for generation of hydrogen in minute amounts when immersed in spent fuel pool water for an extended period. Accordingly, as a defense-in-depth measure, the lid welding procedure requires purging the space below the MPC lid prior to and during welding or cutting operation to eliminate any potential for formation of any combustible mixture of hydrogen and oxygen. Following the completion of the MPC lid welding and hydrostatic testing, the MPC-68M is drained and dried. After the completion of the drying operation, there is no credible mechanism for any combustible gases to be generated within the MPC-68M.

3.III.4.2 Positive Closure

Same as in Subsection 3.4.2.

3.III.4.3 Lifting Devices

The structural analyses of the lifting devices in Subsection 3.4.3 (including all paragraphs) are bounding for the MPC-68M for the following reasons:

- i. the MPC-68M does not require any changes to the HI-STORM overpacks or the HI-TRAC transfer casks for loading operations or long-term storage;
- ii. the MPC-68M utilizes the same MPC Enclosure Vessel design as all MPCs;
- iii. the fully loaded weight of the MPC-68M (Table 3.III.1) is less than bounding MPC weight analyzed in Chapter 3 (Table 3.2.1).

3.III.4.4 Heat

The thermal evaluation of the MPC-68M is reported in Supplement 4.III.

3.III.4.4.1 Summary of Pressures and Temperatures

The design pressures and design temperatures listed in Tables 2.2.1 and 2.2.3, respectively, are applicable to the MPC-68M. Temperature limits of MPC-68M fuel basket and basket shim materials are specified in Table 4.III.2.

3.III.4.4.2 Differential Thermal Expansion

The material presented in Supplement 4.III demonstrates that a physical interference between discrete components of the MPC-68M (e.g., fuel basket and enclosure vessel) will not develop due to differential thermal expansion during any operating condition.

3.III.4.4.3 Stress Calculations

The majority of the stress calculations reported in Paragraph 3.4.4.3 are unaffected by or bound the addition of the MPC-68M to the HI-STORM 100 System for the following reasons:

- i. the MPC-68M does not require any changes to the HI-STORM overpacks or the HI-TRAC transfer casks for loading operations or long-term storage;
- ii. the MPC-68M utilizes the same MPC Enclosure Vessel design as all MPCs;
- iii. the fully loaded weight of the MPC-68M (Table 3.III.1) is less than the bounding MPC weight analyzed in Chapter 3 (Table 3.2.1);

Therefore, the stress calculations reported in Paragraph 3.4.4.3 are not repeated here unless material, geometry, or load changes warrant new analysis or discussion. In other words, unless a new analysis is presented in this subsection, the results in Paragraph 3.4.4.3 for the HI-STORM 100 System are also valid for the MPC-68M either inside the HI-STORM overpack or the HI-TRAC transfer cask.

3.III.4.4.3.1 Analysis of Load Cases F.3.b and F.3.c (Table 3.1.3)

During a non-mechanistic tip-over event, the fuel assemblies exert a lateral force on the fuel basket panels as the overpack impacts the ground and decelerates. The lateral force causes the fuel basket panels to deflect potentially affecting the spacing between stored fuel assemblies. To maintain the fuel in a subcritical configuration, a deflection limit for the fuel basket panels is set in Subsection 2.III.0.1, which is supported by the criticality safety analysis in Supplement 6.III. Here a finite element analysis is performed using ANSYS to demonstrate that the maximum lateral deflection in the fuel basket panels under a bounding deceleration of 70g is less than the

limit specified in Section 2.III.0.1. *The 70g input deceleration is bounding because it exceeds the design basis deceleration limit of 45g for the non-mechanistic tip over of the HI-STORM storage overpack (see Subsection 3.III.4.10), as well as the design basis lateral deceleration limit of 60g for the HI-STAR transport cask [1.1.3] for future considerations.* The analysis methodology presented in this subsection is identical to the methodology used in [2.III.6.2] to qualify the F-37 fuel basket.

As shown in Figure 3.III.1, a representative slice of the MPC-68M fuel basket, consisting of a smaller end section and a full section, is modeled in detail including the contained fuel assemblies and supporting basket shims. The fuel basket panels are modeled with SOLSH190 solid shell elements. The basket shims and each fuel assembly are modeled with SOLID45 solid elements. Standard contact pairs using CONTA173/TARGE170 elements are defined at the interfaces of fuel assembly/basket panel, shim/basket panel, and between stacked basket panels including all the intersecting slot locations. The fuel basket material model is implemented with true stress-true strain multi-linear isotropic hardening plasticity model. An elastic material model is used for the basket shims since no plastic deformation is expected. To accommodate large plastic deformation in the fuel basket panels, sufficiently small element sizes (< 0.40 in) are used and 9 integration points through the thickness are specified. A sensitivity study was performed in [2.III.6.2] to confirm that the panel stresses and displacements obtained using solid shell elements are converged and comparable to those obtained using 5 solid elements through the thickness of the panel.

The 70g deceleration is applied to the model with the basket in the so-called 0° orientation (see Figure 3.III.5). This orientation is chosen for analysis because it maximizes the lateral load on a single basket panel, which in turn maximizes the lateral deflection of the panel. In the 0° orientation, the amplified weight of each stored fuel assembly (during the 70g impact event) bears entirely on one basket panel. Conversely, in the 45° orientation, the amplified weight of each stored fuel assembly is equally supported by two basket panels. The difference in loading between these two basket orientations is pictorially shown in Figure 3.III.5, where "m" denotes the fuel assembly mass, "a" denotes the maximum lateral deceleration, and "d" denotes the enveloping size of the fuel assembly. For comparison purposes, the pressure loads on the basket panels are defined as "p" and "q", respectively, for the 0° and 45° orientations. From the figure, the pressure load p that develops in the 0° orientation is 41% greater than the pressure load q that develops in the 45° orientation. Hence, the lateral deflection of a basket panel is much greater for the 0° orientation (which is why it is chosen for detailed analysis). It is also noted that the 90° corners where the basket panels intersect do not provide any additional moment resistance because of the slotted joint construction (see Figure 1.III.1); therefore, the 45° orientation (or any other orientation between 0° and 45°) does not give rise to any prying loads at the cell corners. Finally, to ensure that the analysis for the 0° orientation is conservative and bounds all other basket orientations, the analysis is performed based on a lateral impact deceleration of 70g even though, according to the results presented in Section 3.III.4.10, the maximum impact deceleration due to the non-mechanistic tip over event (measured at the top of the overpack lid) is less than 45g.

The stress and strain distributions in the fuel basket panels at 70g are shown in Figures 3.III.2 and 3.III.3, respectively. These figures show that the state of stress in the fuel basket panels is primarily elastic. The fuel basket displacements are plotted in Figure 3.III.4. Table 3.III.4 compares the maximum lateral displacement in a fuel basket panel (relative to its end supports) with the deflection limit specified in Subsection 2.III.0.1.

Per the licensing drawing, the nominal width of fuel basket panels in the vertical direction may be increased or decreased provided that the length of the panel slots is increased or decreased proportionally. This means that the fixed-height fuel basket may be assembled using more (or fewer) panels than the number depicted on the licensing drawing. The results of the ANSYS static analysis for the fuel basket presented herein are valid for any panel width since (a) the lateral load on the fuel basket per unit (vertical) length remains the same and (b) the length of the slots measured as a percentage of the panel width remains the same.

Finally, to evaluate the potential for crack propagation and growth for the MPC-68M fuel basket under the non-mechanistic tipover event, a crack propagation analysis is carried out for the MPC-68M fuel basket using the same methodology utilized in Attachment D of [1.III.A.3] to evaluate the HI-STAR 180 F-37 fuel basket in support of the HI-STAR 180 Transport Package [2.III.6.2].

The crack propagation analysis is informed by the results from the ANSYS finite element analysis of the MPC-68M fuel basket under a bounding load of 70-g, which is described above. In particular, the stress distribution in the Metamic-HT basket panels, as determined by ANSYS, is shown in Figure 3.III.2. The maximum stress occurs at one of the basket notches, which are conservatively modeled as sharp (90 degree) corners in the finite element model. This peak stress is used as input to the following crack propagation analysis.

Per [1.III.A.3] the critical stress intensity factor of Metamic-HT panels is estimated to be

$$K_{IC} = 30\text{ksi}\sqrt{\text{in}}$$

based on Charpy V-notch absorbed energy (CVE) correlations for steels. The estimated value is consistent with the range for aluminum alloys, which is 20 to 50 MPa $\sqrt{\text{m}}$ or 18.2 to 45 ksi $\sqrt{\text{in}}$ per Table 3 of [3.III.4]. Next the minimum crack size, a_{min} for crack propagation to occur is calculated below using the formula for a through-thickness edge crack given in [3.1.5]. Although the formula is derived for a straight-edge specimen, the use of the peak stress, σ_{max} at a notch in the fuel basket panel (instead of the average stress in the panel as required by the formula) essentially compensates for the geometric difference between the basket panel and the specimen. Moreover, the maximum size of a pre-existing crack (1/16") in the fuel basket panel is less than 1/6th of the basket panel thickness (0.40"). Thus, the assumption of a through-thickness edge crack is very conservative. The result is

$$a_{min} = \frac{\left(\frac{K_{IC}}{1.12\sigma_{max}} \right)^2}{\pi} = \frac{\left[\frac{30\text{ksi}\sqrt{\text{in}}}{1.12(18.025\text{ksi})} \right]^2}{\pi} = 0.703\text{in}$$

and the safety factor against crack propagation (based on a 1/16" minimum detectable flaw size) is

$$SF = \frac{a_{min}}{a_{det}} = \frac{0.703\text{in}}{0.0625\text{in}} = 11.2$$

The calculated minimum crack size is more than 11 times greater than the maximum possible pre-existing crack size in the fuel basket (based on 100% surface inspection of each panel). The large safety factor ensures that crack propagation in the MPC-68M fuel basket will not occur due to the non-mechanistic tipover event.

3.III.4.4.3.2 Elastic Stability and Yielding of the MPC-68M Fuel Basket under Compression Loads (Load Case F3 in Table 3.1.3)

Under certain conditions, the fuel basket plates may be under direct compressive load. Although the finite element simulations can predict the onset of an instability and post-instability behavior, the computation in this subsection uses (the more conservative) classical instability formulations to demonstrate that an elastic instability of the basket plates is not credible.

A solution for the stability of the fuel basket plate is obtained using the classical formula for buckling of a wide bar [3.III.1]. Material properties are selected corresponding to a metal temperature of 325°C, which bounds the computed metal temperatures anywhere in the fuel basket (see Table 4.III.3). The critical buckling stress for a pin-ended bar is:

$$\sigma_{cr} = (\pi)^2 \frac{E}{12(1-\nu^2)} \left(\frac{h}{a} \right)^2$$

where h is the plate thickness, a is the unsupported plate length, E is the Young's Modulus of Metamic-HT at 325°C, ν is Poisson's Ratio (use 0.3 for this calculation)

From the drawings in Section 1.5, h = 0.40 in, a = 6.05 in, and E = 8,050 ksi (Table 1.III.A.1). Then, the classical critical buckling stress is computed as 31.8 ksi, which exceeds the yield strength of the material. This demonstrates that basket plate instability by elastic buckling is not possible.

3.III.4.5 Cold

Same as in Subsection 3.4.5.

3.III.4.6 HI-STORM 100 Kinematic Stability under Flood Condition (Load Case A in Table 3.1.1)

The stability evaluation of the HI-STORM 100 overpack under flood conditions in Subsection 3.4.6 bounds the scenario of a loaded MPC-68M inside a HI-STORM overpack. The previous analysis is bounding because it uses as input the empty weight of the HI-STORM overpack (i.e., no MPC inside) combined with the maximum CG height from Table 3.2.3.

3.III.4.7 Seismic Event and Explosion

Since there are no physical changes to the HI-STORM overpacks and the MPC-68M reduces the CG height of the loaded HI-STORM overpacks, relative to those analyzed in Chapter 3, the seismic event and explosion analyses presented in Subsection 3.4.7 (including all paragraphs) bound the scenario of a loaded MPC-68M inside a HI-STORM overpack.

3.III.4.8 Tornado Wind and Missile Impact (Load Case B in Table 3.1.1 and Load Case 04 in Table 3.1.5)

The results for the post-impact response of the HI-STORM 100 overpack in Subsection 3.4.8 for the combination of tornado missile plus either steady tornado wind or instantaneous tornado pressure drop bound the results for a loaded MPC-68M inside a HI-STORM overpack. The results are bounding because they are calculated assuming a lower bound weight for the loaded HI-STORM and an upper bound CG height (as compared to a loaded MPC-68M inside a HI-STORM).

In addition, since the MPC-68M does not require any physical changes to the HI-STORM overpacks or the HI-TRAC transfer casks for MPC loading, the missile penetration analyses presented in Subsection 3.4.8 remain valid.

3.III.4.9 HI-TRAC Drop Events

The HI-TRAC drop analyses presented in Subsection 3.4.9 (including all paragraphs) are valid for a loaded MPC-68M inside a HI-TRAC for the following reasons:

- i. the MPC-68M does not require any changes to the HI-TRAC transfer casks for MPC loading;
- ii. the MPC and its contents are modeled as a solid body (i.e., no explicit modeling of MPC fuel basket);
- iii. the difference in weight between a fully loaded MPC-68M and the MPC analyzed in Subsection 3.4.9 is less than 5% of the total drop weight.

3.III.4.10 HI-STORM 100 Non-Mechanistic Tip-over and Vertical Drop Event
(Load Cases 02.a and 02.c in Table 3.1.5)

Pursuant to the provision in NUREG-1536, a non-mechanistic tip-over of a loaded MPC-68M inside a HI-STORM overpack on to the ISFSI pad is considered in this supplement. Calculations are also performed to determine the maximum vertical carry height limit such that the deceleration sustained by a vertical free fall of a HI-STORM overpack carrying a loaded MPC-68M onto the ISFSI pad is less than design basis deceleration limit specified in Table 3.1.2.

The tip-over analysis performed in Appendix 3.A is based on the HI-STORM 100 geometry and a bounding weight. Since the MPC-68M has a slightly higher center of gravity and weighs less than the MPC modeled in Appendix 3.A, it is not a foregone conclusion that the maximum rigid body deceleration level is, in fact, reduced if a HI-STORM 100, with a loaded MPC-68M inside, suffers a non-mechanistic tip-over onto the identical target. In what follows, we present a summary of the analysis undertaken to demonstrate conclusively that the result for maximum deceleration level is less than design basis deceleration limit specified in Table 3.1.2 when the MPC-68M is stored inside the HI-STORM 100 overpack. The analysis employs the methodology previously established in Subsection 3.4.10 for analyzing the HI-STORM 100S overpack.

Appendix 3.A presents a result for the angular velocity of the cylindrical body representing a HI-STORM 100 just prior to impact with the defined target. The result is expressed in Subsection 3.A.6 in terms of the cask geometry, and the ratio of the mass divided by the mass moment of inertia about the corner point that serves as the rotation origin. Since the mass moment of inertia is also linearly related to the mass, the angular velocity at the instant just prior to target contact is independent of the cask mass. Subsequent to target impact, we investigate post-impact response by considering the cask as a cylinder rotating into a target that provides a resistance force that varies linearly with distance from the rotation point. We measure "time" as starting at the instant of impact, and develop a one-degree-of freedom equation for the post-impact response (for the rotation angle into the target) as:

$$\ddot{\theta} + \omega^2\theta = 0$$

where

$$\omega^2 = \frac{kL^3}{3I_A}$$

The initial conditions at time zero are: the initial angle is zero and the initial angular velocity is equal to the rigid body angular velocity acquired by the tip-over from the center-of-gravity over corner position. In the above relation, L is the length of the overpack, I is the mass moment of inertia defined in Appendix 3.A, and k is a "spring constant" associated with the target

resistance. If we solve for the maximum angular acceleration subsequent to time zero, we obtain the result in terms of the initial angular velocity as:

$$\ddot{\theta}_{\max} = \omega \dot{\theta}_0$$

If we form the maximum linear acceleration at the top of the overpack lid, we can finally relate the decelerations of the HI-STORM 100 configuration analyzed in Appendix 3.A and the HI-STORM 100/MPC-68M configuration solely in terms of their geometry properties and their mass ratio. The value of “k”, the target spring rate is the same for both overpacks so it does not appear in the relationship between the two decelerations. After substituting the appropriate geometry and calculated masses, we determine that the ratio of maximum rigid body decelerations at the top surface of the lids is:

$$A_{\text{HI-STORM 100-68M}}/A_{\text{HI-STORM 100}} = 1.01$$

The fact that the calculated ratio is only marginally above 1.0 indicates that the MPC-68M has a minor effect on the non-mechanistic tip-over analysis performed in Appendix 3.A. The maximum rigid body deceleration for the HI-STORM 100/MPC-68M configuration is determined by scaling the calculated result from Appendix 3.A as follows:

$$A_{\text{HI-STORM 100-68M}} = 1.01 \times A_{\text{HI-STORM 100}} = 1.01 \times 42.98g = 43.42g$$

This demonstrates that when the MPC-68M is stored inside the HI-STORM 100 overpack the result for maximum deceleration level is less than the design basis deceleration limit specified in Table 3.1.2. Based on the comparative evaluations in Subsection 3.4.10, the HI-STORM 100 overpack is the limiting overpack for the non-mechanistic tip-over event. Therefore, when the MPC-68M is inside the HI-STORM 100S or the HI-STORM 100S Version B overpack, the maximum rigid body deceleration at the top surface of the lid is less than the deceleration above.

Next we demonstrate that the deceleration sustained by a vertical free fall of a HI-STORM overpack carrying a loaded MPC-68M onto the ISFSI pad is less than the design basis deceleration limit specified in Table 3.1.2. According to Appendix 3.A, analysis of a single mass impacting a spring with a given initial velocity shows that the maximum deceleration “ a_M ” of the mass is related to the dropped weight “ w ” and the drop height “ h ” as follows:

$$a_M \sim \frac{\sqrt{h}}{\sqrt{w}}$$

In other words for a fixed drop height, as the dropped weight decreases, the maximum deceleration of the mass increases. Since the MPC-68M weighs less than the MPC analyzed in Appendix 3.A, the maximum deceleration calculated in Appendix 3.A is not bounding. From the above relationship, the maximum deceleration for the HI-STORM 100/MPC-68M configuration is determined as:

$$a_{100-68M} = \sqrt{\frac{w_{100}}{w_{100-68M}}} a_{100}$$

where $w_{100-68M}$ is the weight of a HI-STORM 100 carrying a loaded MPC-68M, w_{100} is the weight of a loaded HI-STORM 100 overpack as analyzed in Appendix 3.A, and a_{100} is the maximum deceleration of the HI-STORM 100 calculated in Appendix 3.A for an 11" vertical drop. The above equation yields the following result:

$$a_{100-68M} = 44.39g$$

Although the result is higher than the maximum deceleration calculated in Appendix 3.A, it is still less than the design basis vertical deceleration limit specified in Table 3.1.2. Therefore, the previously established lift height limit of 11 inches for a loaded HI-STORM overpack is also applicable to HI-STORM overpacks carrying the MPC-68M.

Finally, Subsection 3.4.10 provides the results of a simple elastic strength of materials calculation, which demonstrates that the cylindrical storage overpack will not permanently deform to the extent that the MPC cannot be removed by normal means after a tip-over event. Those results are valid for the MPC-68M since:

- i. there are no changes to the HI-STORM overpack stemming from the MPC-68M;
- ii. the external dimensions of the MPC-68M are the same as all other MPC types;
- iii. the results are calculated using upper bound impact decelerations.

3.III.4.11 Storage Overpack and HI-TRAC Transfer Cask Service Life

Same as in Subsection 3.4.11 (including all paragraphs).

3.III.4.12 MPC Service Life

Same as in Subsection 3.4.12 and with the following supplementary information provided herein.

3.III.4.12.1 Metamic-HT Considerations

Metamic-HT has been extensively tested as indicated in Appendix A of Supplement 1.III. Testing has included extensive tests for creep, irradiation and corrosion to ensure long-term fuel basket performance under normal conditions of storage. The Metamic-HT is also not susceptible to structural fatigue and brittle fracture under long term conditions of storage. Corrosion is discussed further in Subsection 3.III.4.1. Creep and boron depletion are further discussed below.

i) Fuel Basket Creep

The Metamic sourcebook contains data on the testing to determine the creep characteristics of the Metamic-HT under both unirradiated and irradiated conditions. A creep equation to estimate a bounding estimate of total creep as a function of stress and temperature is also provided. The creep equation developed from this test provides a conservative prediction of accumulated creep strain by direct comparison to measured creep in unirradiated and irradiated coupons.

The creep equation for Metamic-HT that bounds *all* measured data (tests run for 20,000 hours) is of the classical exponential form in stress and temperature (see Appendix A of Supplement 1.III), which is written symbolically as $\epsilon = f(\sigma, T)$.

Creep in the MPC-68M fuel basket will not be a reactivity modifier because the basket is arrayed in the vertical orientation. The lateral loading of the fuel basket walls is insignificant and hence no mechanistic means for the basket panels to undergo lateral deformation from creep exists, even if the panel material were susceptible to creep.

The creep effect would tend to shorten the fuel basket under the self-weight of the basket. An illustrative calculation of the cumulative reduction of the basket length is presented below to demonstrate the insignificant role of creep in the MPC-68M fuel basket.

The in-plane compressive stress, σ , at height x in the basket panel is given by

$$\sigma = \rho(H-x) \quad (3.III.1)$$

where:

ρ = weight density of Metamic-HT

H = height of the fuel basket

Using the above stress equation, the total creep shrinkage, δ , is given by

$$\delta = \int_0^H f(\sigma, T) dx \quad (3.III.2)$$

where:

T = panel's metal temperature (conservatively assumed to be 350°C for a period of 60 years)

H = height of the basket (conservatively assumed to be 200 inches)

Using the creep equation (provided in Appendix A of Supplement 1.III) and performing the above integration numerically yields $\delta = 0.095$ inch. In other words, the computed shrinkage of the basket is less than 0.048% of its original length. Therefore, it is concluded that for the vertical storage configuration the creep effects of the MPC-68M fuel basket are insignificant due to absence of any meaningful loads on the panels. Therefore, creep in the Metamic-HT fuel basket is not a matter of safety concern.

ii) Fuel Basket Boron Depletion

The similarities between Metamic-HT and Metamic (classic) neutron absorbers and their exposure to the same long-term conditions of storage in the HI-STORM 100 system provide a logical basis to expect negligible neutron absorber boron depletion in Metamic-HT. However, to assure criticality safety during worst case design basis conditions over the 40-year design life, the analysis discussed in Subsection 6.III demonstrates that the boron depletion in the Metamic-HT is negligible over a 50-year duration. Thus, sufficient levels of boron are present in the fuel basket to maintain criticality safety over the 40-year design life of the MPC.

3.III.4.12.2 Basket Shim Considerations:

i) Basket Shim Creep

Like the fuel basket, the basket shims are not subject to any significant loading during storage. The ability of the basket shims (made of a creep resistant aluminum alloy) has been evaluated and qualified in Docket No. 71-9325 [2.III.6.2] for transport applications where the stress level (in horizontal configuration) is significant. Therefore, in light of the minuscule stress levels from self-weight in long-term storage, creep is ruled out as a viable concern for the basket shims.

ii) Basket Shim Corrosion

Basket shim corrosion is discussed in Subsection 3.III.4.1.

3.III.4.13 Design and Service Life

Same as in Subsection 3.4.13.

3.III.5 FUEL RODS

Same as in Section 3.5.

3.III.6 SUPPLEMENTAL DATA

3.III.6.1 Additional Codes and Standards Referenced in HI-STORM 100 System
Design and Fabrication

Same as in Subsection 3.6.1.

3.III.6.2 Computer Programs

ANSYS 11.0, which is a public domain finite element code, has been utilized to perform structural analyses documented in this supplement.

3.III.6.3 Appendices Included in Supplement 3.III

None.

3.III.6.4 Calculation Packages

A calculation package containing the structural calculations supporting Supplement 3.III has been prepared, reviewed, and archived according to Holtec International's quality assurance program (see Chapter 13).

3.III.7 COMPLIANCE WITH NUREG-1536

The material in this supplement for the MPC-68M provides the same information as previously provided for the other MPC types in Chapter 3. Therefore, to the extent applicable, the information provided is in compliance with NUREG-1536.

3.III.8 REFERENCES

- [3.III.1] Buckling of Bars, Plates, and Shells, D.O. Brush and B.O. Almroth, McGraw-Hill, 1975, p.22.
- [3.III.2] Properties of Aluminum Alloys, Tensile, Creep, and Fatigue Data at High and Low Temperatures, ASM International, November 2006.
- [3.III.3] ASME Boiler & Pressure Vessel Code, Section II, Parts A and D, American Society of Mechanical Engineers, 2007.
- [3.III.4] *“Mechanical Testing and Evaluation”, ASM Handbook, Volume 8, 2000.*

**TABLE 3.III.1
WEIGHT DATA FOR MPC-68M**

Item	Bounding Weight (lb)
MPC-68M <ul style="list-style-type: none"><li data-bbox="264 478 479 510">• Without SNF<li data-bbox="264 520 822 552">• Fully loaded with SNF and Fuel Spacers	30,000 90,000

**TABLE 3.III.2
CENTERS OF GRAVITY OF HI-STORM SYSTEM CONFIGURATIONS
INVOLVING MPC-68M**

Component	Height of CG Above Datum (in)
MPC-68M (empty)	114.9
HI-STORM 100 Overpack w/ fully loaded MPC-68M	118.4
HI-STORM 100S(232) Overpack w/ fully loaded MPC-68M	113.3
HI-STORM 100S(243) Overpack w/ fully loaded MPC-68M	117.7
HI-STORM 100S Version B(218) Overpack w/ fully loaded MPC-68M	108.5
HI-STORM 100S Version B(229) Overpack w/ fully loaded MPC-68M	112.8
HI-TRAC 125 Transfer Cask w/ Top Lid, Pool Lid, and fully loaded MPC-68M (water jacket filled)	97.4
HI-TRAC 100 Transfer Cask w/ Top Lid, Pool Lid, and fully loaded MPC-68M (water jacket filled)	96.5
HI-TRAC 125D Transfer Cask w/ Top Lid, Pool Lid, and fully loaded MPC-68M (water jacket filled)	96.9
HI-TRAC 100D Transfer Cask w/ Top Lid, Pool Lid, and fully loaded MPC-68M (water jacket filled)	94.3

Notes:

1. The datum used for calculations involving the HI-STORM is the bottom of the overpack baseplate. The datum used for calculations involving the HI-TRAC is the bottom of the pool lid.
2. The datum used for calculations involving only the MPC is the bottom of the MPC baseplate.
3. The CG height of the HI-STORM overpack is calculated based on standard density concrete (i.e., 166 pcf dry) in the radial cavity. At higher densities, the CG height is slightly lower, which makes the HI-STORM overpack less prone to tipping.

HOLTEC INTERNATIONAL COPYRIGHTED MATERIAL

**TABLE 3.III.3
FUEL BASKET SHIMS – NOMINAL MECHANICAL PROPERTIES**

Aluminum Alloy (B221 2219-T8511)					
Temp. °C (°F)	S _y	S _u	E	α	% Elongation
25 (75)	340 (49)	450 (65)	7.2 (10.5)	–	11
150 (300)	285 (41)	345 (50)	6.8 (9.5)	23.9 (13.3)	14
204 (400)	220 (32)	260 (38)	6.3 (9.1)	24.5 (13.6)	18
230 (450)	200 (29)	235 (34)	6.1 (8.8)	24.8 (13.8)	19
260 (500)	180 (26)	205 (30)	5.9 (8.5)	25.0 (13.9)	19
290 (550)	115 (17)	130 (19)	5.5 (8.0)	25.4 (14.1)	23

Definitions:

S_y = Yield Stress, MPa (ksi)

α = Mean Coefficient of thermal expansion, cm/cm-°C x 10⁻⁶ (in/in-°F x 10⁻⁶)

S_u = Ultimate Stress, MPa (ksi)

E = Young's Modulus, MPa x 10⁴ (psi x 10⁶)

Notes:

1. Source for S_y, S_u, E and % Elongation values is "Properties of Aluminum Alloys", page 82 [3.III.2] (properties listed in the table above are not affected by time at temperature).
2. Source for α is Table TE-2 of [3.III.3] (values listed in TE-2 are also considered representative of Aluminum Alloy (2219-T8511) (UNS No. A92219)).

TABLE 3.III.4
MAXIMUM DISPLACEMENT IN MPC-68M FUEL BASKET

Maximum Lateral Displacement in Fuel Basket Panel, θ (dimensionless) (Note 1)	Maximum Allowable Value of θ (from Table 2.III.4)	Safety Factor
9.6×10^{-4}	0.005	5.21

Notes:

1. See Subsection 2.III.0.1 for definition of θ .

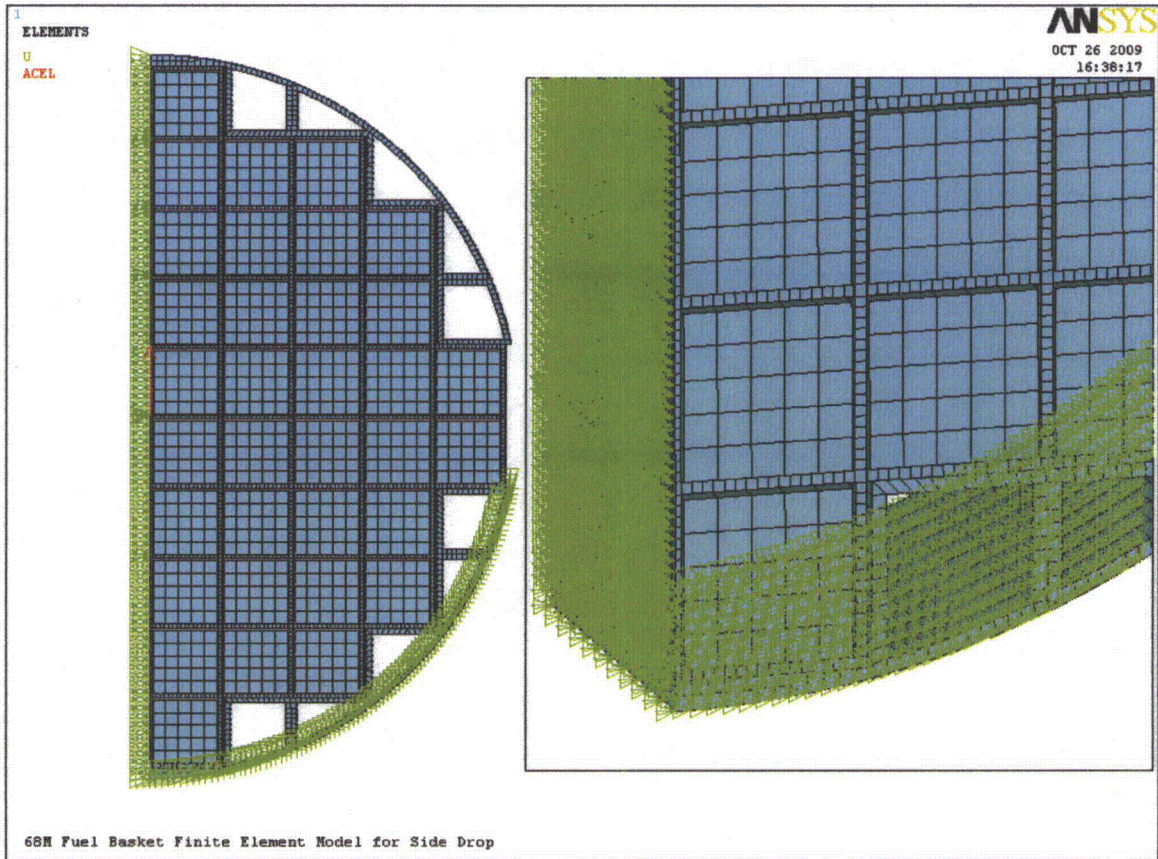


FIGURE 3.III.1: FINITE ELEMENT MODEL OF MPC-68M FUEL BASKET

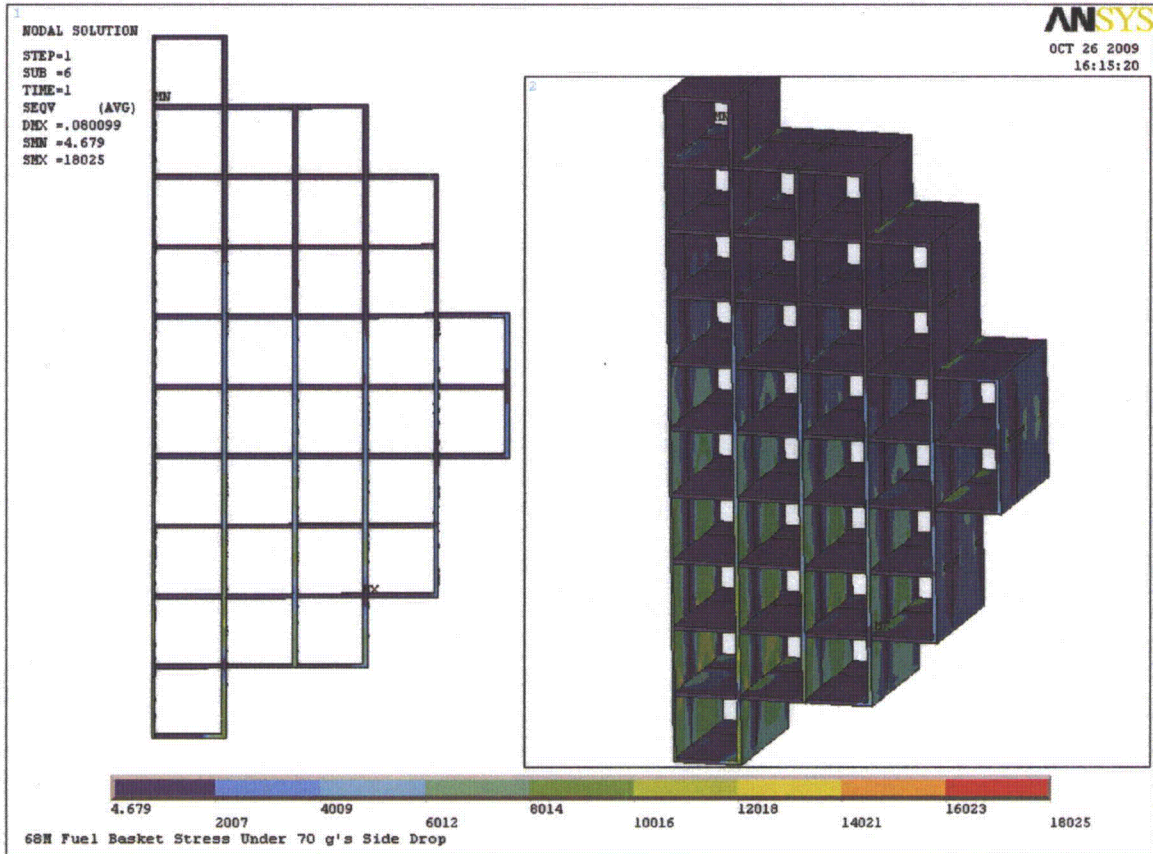


FIGURE 3.III.2: VON MISES STRESS DISTRIBUTION IN MPC-68M FUEL BASKET UNDER 70g LOAD

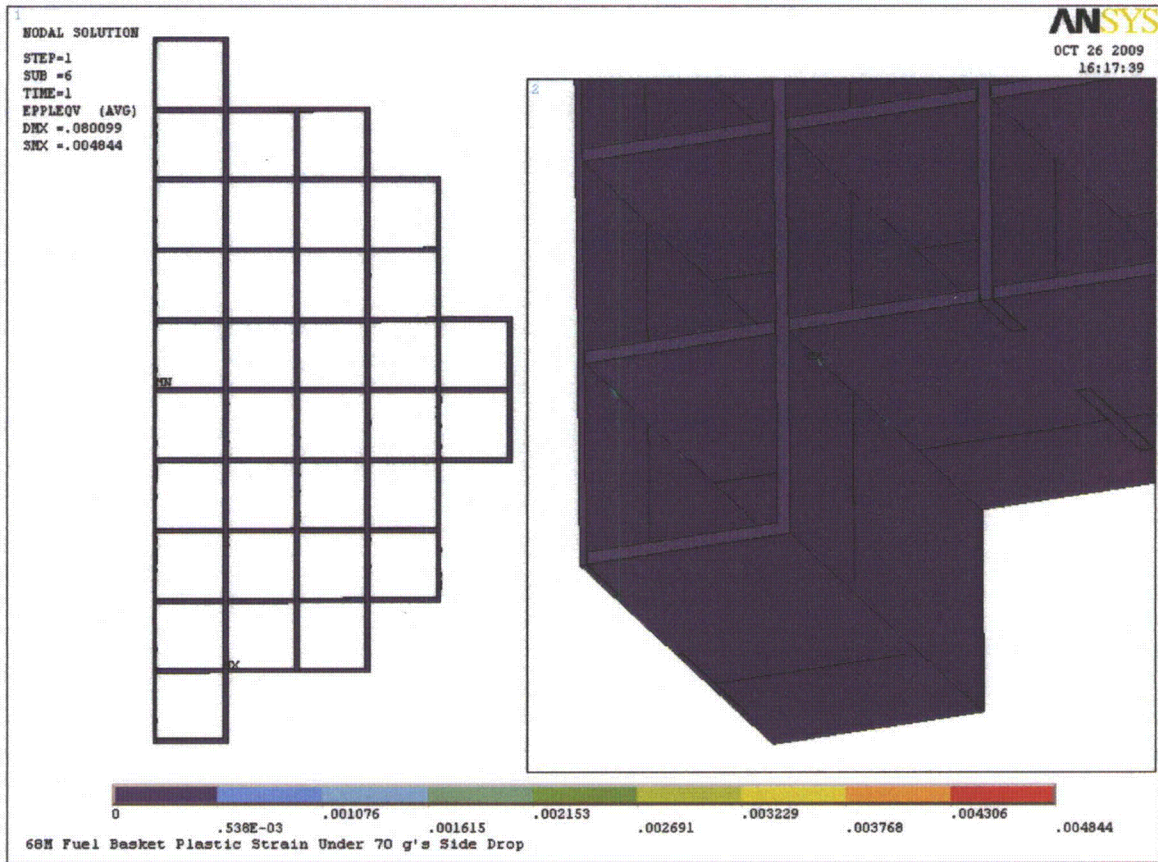


FIGURE 3.III.3: PLASTIC STRAIN DISTRIBUTION IN MPC-68M FUEL BASKET UNDER 70g LOAD

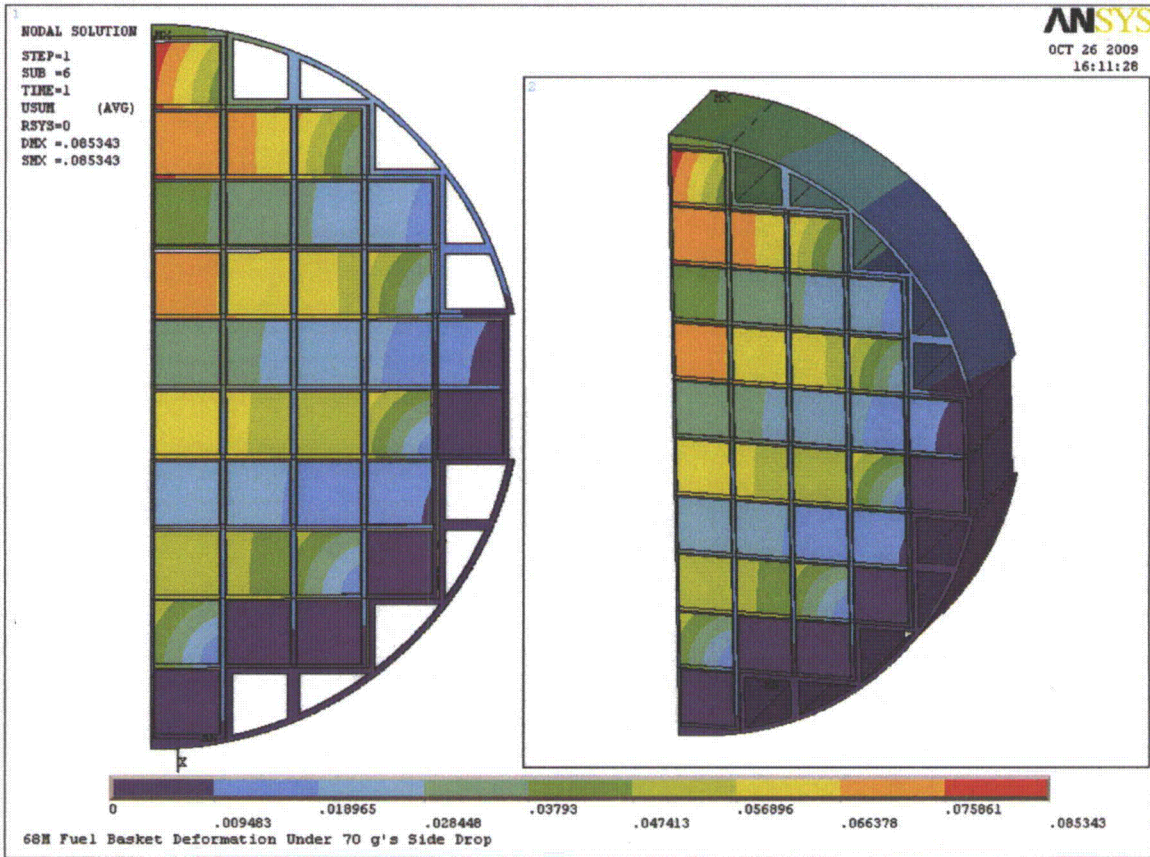
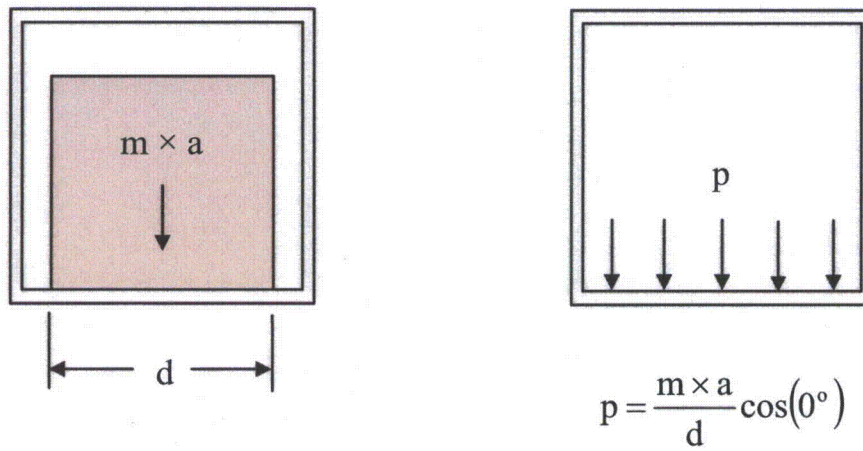
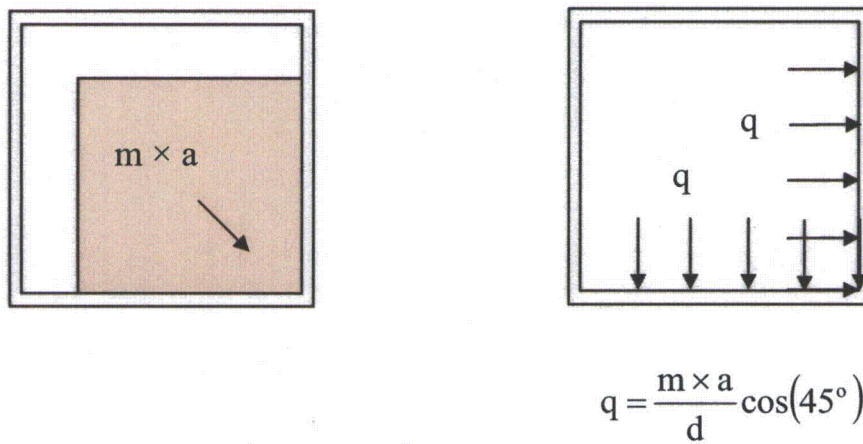


FIGURE 3.III.4: DISPLACEMENT CONTOURS IN MPC-68M FUEL BASKET UNDER 70g LOAD



(a) 0° Orientation



(b) 45° Orientation

FIGURE 3.III.5: FUEL LOADING FOR 0° AND 45° BASKET ORIENTATIONS

SUPPLEMENT 4.III¹**THERMAL EVALUATION OF THE MPC-68M****4.III.0 OVERVIEW**

The MPC-68M is a 68 cell BWR canister engineered with a high B¹⁰ containing Metamic-HT basket for enhanced criticality control. The MPC-68M is evaluated for storage in the aboveground family of HI-STORM overpacks. For a bounding evaluation an MPC-68M emplaced in the most flow resistive HI-STORM 100S Version B overpack² is analyzed under normal, off-normal and accident conditions. The evaluations described herein parallel those of the aboveground HI-STORM cask contained in the main body of Chapter 4 of this FSAR. To ensure readability, the section in the main body of the chapter to which each section in this supplement corresponds is clearly identified. All tables in this supplement are labeled sequentially.

4.III.1 INTRODUCTION

The information presented in this supplement is intended to serve as a complement to the information provided in the main body of Chapter 4. Except for the fuel basket and basket support materials, the information in Chapter 4 that remains applicable to the MPC-68M analysis is not repeated herein. Specifically the following information in the main body of Chapter 4 is not repeated:

1. The thermal properties of materials in Section 4.2 applicable to the MPC-68M.
2. The specifications for components in Section 4.3 applicable to the MPC-68M.
3. The descriptions of the thermal modeling of the MPC and its internals, including fuel assemblies, in Section 4.4 which are applicable in their entirety to the MPC-68M.
4. The descriptions of the short-term loading operations, carried out using the HI-TRAC transfer cask, in Section 4.5 applicable to the MPC-68M.

As confirmed by appropriate supporting analyses, the heat rejection capacity of the MPC-68M³ is equal to or better than its counterparts (strictly speaking, much better because of the highly conducting Metamic-HT fuel basket). This renders its resistance to accident events such as fire with greater margins of safety.

¹ For ease of supplement review the sections are numbered in parallel with the main Chapter 4.

² This approach is identical to the HI-STORM thermal analysis in Section 4.4.

³ Heat rejection capacity is defined as the amount of heat the storage system containing an MPC loaded with CSF stored in uniform storage will reject with the ambient environment at the normal temperature and the peak fuel cladding temperature at 400°C.

4.III.2 THERMAL PROPERTIES OF MATERIALS¹

The material properties compiled in Section 4.2 of the FSAR provide the required information, except for the material properties of Metamic-HT fuel basket and aluminum basket shims. The Metamic-HT and shims thermo-physical properties data is provided in Table 4.III.1.

4.III.3 SPECIFICATIONS FOR COMPONENTS²

All applicable material temperature limits in Section 4.3 of the FSAR continue to apply to the MPC-68M. Temperature limits of MPC-68M fuel basket and basket shim materials is specified in Table 4.III.2.

4.III.4 THERMAL EVALUATION FOR NORMAL CONDITIONS OF STORAGE³

4.III.4.1 Thermal Model

The MPC-68M thermal design is same as that of the currently licensed MPC-68. It features a 68 cells capacity fuel basket for storing BWR fuel. The basket is engineered with a bottom plenum by providing flow holes, a top open plenum by providing an engineered clearance and a peripheral downcomer to facilitate heat dissipation by thermosiphon action. The MPC-68M is helium pressurized to same backfill specifications defined in Chapter 4, Table 4.4.12. The principal differences are in the basket material of construction (Metamic-HT), the installation of aluminum basket shims in the basket peripheral spaces and replacement of the cell walls sandwich construction by monolithic (i.e. gaps free) basket panels. The design characteristics of the basket are as follows:

- i. The fuel basket is assembled from a rectilinear gridwork of thick plates having precision machined slots for facilitating snug-fit assembly and ensuring uninterrupted lateral dissipation of heat.
- ii. Aluminum basket shims conforming to the shapes of the fuel basket and MPC shell are installed in the peripheral spaces between the outside walls of the fuel basket and the inside walls of the Enclosure Vessel. The axial holes in the basket shims serve as the passageway for the downward flow of the helium gas under the thermosiphon action, which is intrinsic to the thermal design of all MPCs in the HI-STORM 100 system.
- iii. The fuel basket consists of adjacent square openings (cells) separated by one monolithic wall of the Metamic-HT neutron absorber.

¹ This section supplements Section 4.2.

² This section supplements Section 4.3.

³ This section supplements Section 4.4.

In this supplement the MPC-68M placed in an above ground HI-STORM 100 System is evaluated under normal, off-normal and accident conditions and during short-term operations. The thermal evaluations use *the same aboveground MPC 3-D thermal modeling methodology* and the *same 3-Zone porous media model* used in the thermal analysis of the aboveground overpack (HI-STORM 100S¹) to represent the flow resistance of bounding BWR (GE-10x10) fuel assemblies (See Chapter 4, Subsection 4.4.1.2).

The key attributes of MPC-68M thermal model are as follows:

1. The MPC-68M is modeled as a geometrically accurate 3D array of square shaped cells inside a cylindrical shell with bottom and top closures. The fuel basket bottom flow holes with understated flow area and top plenum are explicitly modeled.
2. The helium flow within the MPC is modeled as laminar. This is the same modeling approach used in the HI-STORM 100 cask analyses.
3. The hydraulic resistance of the fuel assemblies stored within the MPC is represented in the 3D model by 3-Zone porous media flow resistances. This is the same as used in the HI-STORM 100 modeling (See Chapter 4, Subsection 4.4.1.2).

Consistent with the HI-STORM 100 cask analyses a geometrically accurate 3D model of the HI-STORM 100 overpack is constructed for thermal analysis. The inlet and outlet vents and internal flow passages are explicitly modeled. The airflow through the cooling passages of the HI-STORM 100 overpack is modeled as turbulent, using the $k-\omega$ model with transitional option as recommended in the Holtec-proprietary benchmarking report [4.1.6]. This is the same modeling approach used in the HI-STORM 100 cask analyses. The underside of the HI-STORM 100 concrete pad is assumed to be supported on a subgrade at 77°F. This is the same boundary condition applied to the bottom of the ISFSI pad for the HI-STORM 100 modeling in Section 4.4.

4.III.4.2 Thermal Analysis

The MPC-68M has been designed to permit storage under the array of uniform and regionalized heat loads defined in Chapter 2 as a function of the regionalization parameter X. As shown in Chapter 4 the highest cladding temperatures are reached under regionalized storage at $X = 0.5$. This scenario is co-incident with the maximum permissible MPC heat load and therefore temperatures of other sub-systems (such as fuel basket, MPC shell and overpack) also reach their highest values. This scenario is adopted for demonstration of compliance with the temperature and pressure limits set forth in this Supplement and Chapter 2. The limiting scenario is analyzed and maximum temperatures and pressures under normal storage tabulated in Tables 4.III.3 and 4.III.4. The results are below the Chapter 2 and Supplement 4.III normal temperature and

¹ The aboveground HI-STORM System includes a classical overpack design (HI-STORM 100) and a shortened version (HI-STORM 100S). The limiting design (HI-STORM 100S) is used in the aboveground thermal analysis.

pressure limits. In accordance with NUREG-1536 MPC-68M pressures are computed assuming 1% (normal), 10% (off-normal) and 100% (accident) rod ruptures with 100% rods fill gases and fission gases release in accordance with NUREG-1536 release fractions. The pressures are computed and tabulated in Table 4III.4. The 100% rods rupture pressure is below the accident design pressure (Table 2.2.1).

4.III.4.3 Engineered Clearances to Eliminate Thermal Interferences

To minimize thermal stresses in load bearing members, the MPC-68M is engineered with adequate gaps to permit free thermal expansion of the fuel basket and MPC in axial and radial directions. In this subsection, differential thermal expansions are evaluated to ensure the adequacy of engineered gaps. The following gaps are evaluated:

- a. Fuel Basket-to-MPC Radial Gap
- b. Fuel Basket-to-MPC Axial Gap
- c. MPC-to-Overpack Radial Gap
- d. MPC-to-Overpack Axial Gap

The FLUENT thermal model articulated above provides the temperature field in the HI-STORM overpack and MPC-68M from which the changes in the above gaps are directly computed. The initial minimum gaps and their corresponding value under normal storage conditions is tabulated in Table 4.III.8. The calculations show significant margins against restraint to free-end expansion are available in the design.

4.III.4.4 Evaluation of Fuel Debris Storage

Fuel debris is permitted for storage in up to eight peripheral cells under the uniform loading heat load limits specified in Section 2.4 of the Technical Specifications. Although fuel debris is not required to meet cladding temperature limits, its effect on fuel stored in the interior cells must be assessed. Fuel debris in the canister is thermally conservatively evaluated assuming a bounding debris configuration and design heat load in all storage cells. The following assumptions are adopted to maximize the computed cladding temperatures:

1. *The fuel debris is assumed to be completely pulverized and compacted into a square prismatic bar enclosed by the damaged fuel canister (DFC) with open helium space above it. In this manner the height of the prismatic bar emitting heat is minimized resulting in the maximization of lineal thermal loading (kw/ft) of the DFC and coincident local heating of the fuel basket and neighboring storage cells.*
2. *Fuel debris assumed to be completely composed of UO₂. As UO₂ has a lower conductivity relative to cladding, heat dissipation is understated.*
3. *The fuel debris is assumed to block through flow of helium inside the DFC.*
4. *All 16 peripheral storage locations (not just the 8 permitted by CoC) are assumed to contain fuel debris emitting maximum heat permitted by Technical Specifications*

(CoC Appendix B, Section 2.4, Table 2.4-1) and all interior cells are emitting design heat under the uniform loading storage scenario.

5. *The MPC operating pressure is understated to minimize internal convection heat transfer*

The results of the analysis are tabulated in Table 4.III.11. The results support the following conclusions:

- *Cladding temperature is substantially below the ISG-11, Rev. 3 limit.*
- *MPC basket is below the design limit (Table 4.III.2) by large margin.*
- *MPC shell and Overpack metal temperatures are below design limits (Table 2.2.3).*
- *Overpack body and lid concrete are well below design limits (Table 4.3.1).*

4.III.5 THERMAL EVALUATION OF SHORT TERM OPERATIONS

4.III.5.1 HI-TRAC Thermal Model

The HI-TRAC thermal model presented in Section 4.5 is adopted for the evaluation of MPC-68M under short term operations.

4.III.5.2 Maximum Time Limit During Wet Transfer Operations

As the MPC thermal inertia credited in the time-to-boil calculations is bounded by the MPC-68M thermal inertia the evaluation of wet transfer operations in Section 4.5 remains applicable to the MPC-68M.

4.III.5.3 MPC Temperature During Moisture Removal Operations

4.III.5.3.1 Vacuum Drying

Prior to helium backfill the MPC-68M must be drained of water and demineralized. At the start of draining operation, both the HI-TRAC annulus and the MPC are full of water. The presence of water in the MPC ensures that the fuel cladding temperatures are lower than design basis limits by large margins. As the heat generating region is uncovered during the draining operation, the fuel and basket mass will undergo a monotonic heat up from the initially cold conditions when the heated surfaces were submerged under water. To limit fuel temperatures demineralization of the MPC-68M by the vacuum drying method is permitted provided the HI-TRAC annulus remains water filled during vacuum drying operations. To support vacuum drying operations two limiting scenarios are defined below:

Scenario A: The MPC-68M is loaded with Moderate Burnup Fuel assemblies generating heat at the maximum permissible rate defined in Chapter 2 under the bounding regionalized storage scenario $X = 0.5$.

Scenario B: The MPC-68M is loaded with one or more High Burnup Fuel assemblies and the MPC-68M decay heat is less than a conservatively defined threshold heat load $Q_T = 29 \text{ kW}^1$.

To evaluate the above scenarios the vacuum drying analysis methodology presented in Section 4.5 is adopted and an MPC-68M specific thermal model constructed. The principal features of the thermal model are as follows:

- i. A bounding steady-state analysis is performed under the heat loads defined in the scenarios above.
- ii. The water in the HI-TRAC annulus is conservatively assumed to be boiling under the hydrostatic head of water at the annulus bottom (232°F).
- iii. The bottom surface of the MPC is insulated.

The thermal model articulated above is used to compute the maximum cladding temperature under the vacuum drying scenarios defined above. The results tabulated in Table 4.III.5 are in compliance with the ISG-11 temperature limits of Moderate Burnup Fuel (Scenario A) and High Burnup Fuel (Scenario B).

4.III.5.3.2 Forced Helium Dehydration

Evaluation of Forced Helium Dehydration in Section 4.5 is applicable to MPC-68M.

4.III.5.4 Cask Cooldown and Reflood During Fuel Unloading Operations

Evaluation of cask cooldown and reflood operation in Section 4.5 is applicable to MPC-68M.

4.III.5.5 HI-TRAC Onsite Transfer Operation

A 3D FLUENT thermal model of an MPC-68M emplaced in a HI-TRAC transfer cask is constructed to evaluate the thermal state of fuel under onsite transport in the vertical orientation². A bounding analysis is performed under the following conditions:

- (i) Steady state maximum temperatures have reached.
- (ii) The MPC-68M is loaded with fuel generating heat at the maximum permissible level under the limiting regionalized storage scenario X = 0.5.
- (iii) The HI-TRAC annulus is air filled.

The scenario defined above represents upper bound temperatures reached in the HI-TRAC without the aid of any auxiliary cooling such as the Supplemental Cooling System (SCS) defined

¹ Threshold heat load is defined as the product of maximum loaded assembly heat load q_{\max} and the number of fuel storage cells ($n=68$). Under this stipulation q_{\max} must not exceed 0.426 kW.

² In accordance with Section 4.5 onsite transfer in the horizontal orientation is not permitted.

in Section 4.5. The maximum cladding temperatures computed using the thermal model articulated above are tabulated in Table 4.III.6. As the cladding temperatures are below the limiting High Burnup Fuel temperature limits mandated by ISG-11 [4.1.4] SCS cooling is not necessary for ensuring cladding safety under onsite transfer operations involving the MPC-68M. Accordingly SCS cooling is not mandated in the MPC-68M Technical Specifications.

4.III.6 THERMAL EVALUATION OF OFF-NORMAL AND ACCIDENT CONDITIONS¹

4.III.6.1 Off-Normal Conditions

(a) Elevated Ambient Air Temperature

The principal effect of elevated ambient temperature is a rise of the HI-STORM 100 temperatures from the baseline normal storage temperatures by the difference between elevated ambient and normal ambient temperatures. As the normal storage temperatures under MPC-68M storage in the HI-STORM 100 overpack are bounded by the HI-STORM 100 System temperatures reported in Section 4.4, the temperatures under this event are likewise bounded by the off-normal ambient evaluation in Section 4.6.

(b) Partial Blockage of Air Inlets

The principal effect of partial inlets blockage is a rise in the HI-STORM 100 annulus temperature from the baseline normal storage temperatures and to leading order a similar rise in the MPC temperatures. As the normal storage temperatures under MPC-68M storage in the HI-STORM 100 overpack are bounded by the HI-STORM 100 System temperatures reported in Section 4.4, the temperatures under this event are likewise bounded by the partial ducts blockage evaluation in Section 4.6.

(c) Off-Normal Pressure

This event is defined as a combination of (a) maximum helium backfill pressure (Table 4.4.12), (b) 10% fuel rods rupture, and (c) limiting fuel storage configuration. The principal objective of the analysis is to demonstrate that the MPC off-normal design pressure (Table 2.2.1) is not exceeded. The MPC-68M off-normal pressure is reported in Table 4.III.4. The result² is below the off-normal design pressure (Table 2.2.1).

¹ This section supplements Section 4.6.

² Pressures relative to 1 atm absolute pressure (i.e. gauge pressures) are reported throughout this section.

4.III.6.2 Accident Conditions

(a) Fire

Although the probability of a fire accident affecting a HI-STORM 100 System during storage operations is low due to the lack of combustible materials at an ISFSI, a conservative fire event has been assumed and analyzed. The only credible concern is a fire from an on-site transport vehicle fuel tank. Under a postulated fuel tank fire, the outer layers of HI-TRAC or HI-STORM overpacks are heated for the duration of fire by the incident thermal radiation and forced convection heat fluxes. The amount of fuel in the on-site transporter is limited to a volume of 50 gallons.

(i) HI-STORM Fire¹

The fuel tank fire is conservatively assumed to surround the HI-STORM Overpack. Accordingly, all exposed overpack surfaces are heated by radiation and convection heat transfer from the fire. Based on NUREG-1536 and 10 CFR 71 guidelines [4.III.2], the following fire parameters are assumed:

- 1. The average emissivity coefficient must be at least 0.9. During the entire duration of the fire, the painted outer surfaces of the overpack are assumed to remain intact, with an emissivity of 0.85. It is conservative to assume that the flame emissivity is 1.0, the limiting maximum value corresponding to a perfect blackbody emitter. With a flame emissivity conservatively assumed to be 1.0 and a painted surface emissivity of 0.85, the effective emissivity coefficient is 0.85. Because the minimum required value of 0.9 is greater than the actual value of 0.85, use of an average emissivity coefficient of 0.9 is conservative.*
- 2. The average flame temperature must be at least 1475 °F (800 °C). Open pool fires typically involve the entrainment of large amounts of air, resulting in lower average flame temperatures. Additionally, the same temperature is applied to all exposed cask surfaces, which is very conservative considering the size of the HI-STORM cask. It is therefore conservative to use the 1475 °F (800 °C) temperature.*
- 3. The fuel source must extend horizontally at least 1 m (40 in), but may not extend more than 3 m (10 ft), beyond the external surface of the cask. Use of the minimum ring width of 1 meter yields a deeper pool for a fixed quantity of combustible fuel, thereby conservatively maximizing the fire duration.*
- 4. The convection coefficient must be that value which may be demonstrated to exist if the cask were exposed to the fire specified. Based upon results of large pool fire thermal*

¹ The HI-STORM fire accident methodology is same as the generic methodology in Section 4.6 of the HI-STORM 100 FSAR.

measurements [4.III.3], a conservative forced convection heat transfer coefficient of 4.5 Btu/(hr × ft² × °F) is applied to exposed overpack surfaces during the short-duration fire.

Based on the 50 gallon fuel volume, the overpack outer diameter and the 1 m fuel ring width [4.III.2], the fuel ring surrounding the overpack covers 147.6 ft² and has a depth of 0.54 in. From this depth and fuel consumption rate of 0.15 in/min, the fire duration is calculated to be 3.62 minutes. The fuel consumption rate of 0.15 in/min is a lowerbound value from a Sandia National Laboratories report [4.III.3]. Use of a lowerbound fuel consumption rate conservatively maximizes the duration of the fire.

To evaluate the impact of fire heating of the HI-STORM overpack, a thermal model of the overpack cylinder was constructed and evaluated in Section 4.6 of the HI-STORM FSAR with overstated inputs. As justified below this overpack fire analysis remains conservative. It is recognized that the ventilation air in contact with the inner surface of the HI-STORM Overpack under design-basis decay heat varies between 80 °F at the bottom and 275 °F at the top of the overpack. It is further recognized that the inlet and outlet ducts occupy a miniscule fraction of area of the cylindrical surface of the massive HI-STORM Overpack. Due to the short duration of the fire event and the relative isolation of the ventilation passages from the outside environment, the ventilation air is expected to experience little intrusion of the fire combustion products. However, as a conservative measure the air in the HI-STORM Overpack ventilation passages was held constant at a substantially elevated temperature (300 °F) during the entire duration of the fire event.

During the fire the overpack external shell temperatures are substantially elevated (~550°F) and an outer layer of concrete approximately 1 inch thick reaches temperatures in excess of short term temperature limit. This condition is addressed specifically in NUREG-1536 (4.0,V,5.b), which states that:

“The NRC accepts that concrete temperatures may exceed the temperature criteria of ACI 349 for accidents if the temperatures result from a fire.”

These results demonstrate that the fire accident event analyzed in a most conservative manner is determined to have a minor affect on the HI-STORM Overpack. Localized regions of concrete are exposed to temperatures in excess of accident temperature limit. The bulk concrete temperature away from the localized regions remains below the accident limit. The temperatures of steel structures are within allowable limits.

Having evaluated the effects of the fire on the overpack, we now evaluate the effects on the MPC-68M and contained fuel assemblies. Guidance for the evaluation of the MPC and its internals during a fire event is provided by NUREG-1536 (4.0,V,5.b), which states:

“For a fire of very short duration (i.e., less than 10 percent of the thermal time constant of the cask body), the NRC finds it acceptable to calculate the fuel temperature increase by assuming that the cask inner wall is adiabatic. The fuel

temperature increase should then be determined by dividing the decay energy released during the fire by the thermal capacity of the basket-fuel assembly combination.”

The time constant of the cask body (i.e., the overpack) can be determined using the formula:

$$\tau = \frac{c_p \times \rho \times L_c^2}{k}$$

where:

c_p = Overpack Specific Heat Capacity (Btu/lb-°F)

ρ = Overpack Density (lb/ft³)

L_c = Overpack Characteristic Length (ft)

k = Overpack Thermal Conductivity (Btu/ft-hr-°F)

The concrete contributes the majority of the overpack mass and volume, so we will use the specific heat capacity (0.156 Btu/lb-°F), density (140 lb/ft³) and thermal conductivity (1.05 Btu/ft-hr-°F) of concrete for the time constant calculation. The characteristic length of a hollow cylinder is its wall thickness. The characteristic length for the HI-STORM Overpack is therefore 29.5 in, or approximately 2.46 ft. Substituting into the equation, the overpack time constant is determined as:

$$\tau = \frac{0.156 \times 140 \times 2.46^2}{1.05} = 126 \text{ hrs}$$

One-tenth of this time constant is approximately 12.6 hours (756 minutes), substantially longer than the fire duration of 3.62 minutes, so the MPC is evaluated by considering the MPC canister as an adiabatic boundary. The fuel temperature rise is computed next.

Table 4.III.10 lists lower-bound thermal inertia values for the MPC-68M and the contained fuel assemblies. Applying design heat load (36.9 kW (1.26x10⁵ Btu/hr)) and adiabatic heating for the 3.62 minutes fire, the fuel temperature rise computes as:

$$\Delta T_{\text{fuel}} = \frac{\text{Decay heat} \times \text{Time duration}}{(\text{MPC} + \text{Basket \& Shims} + \text{Fuel}) \text{ heat capacities}} = \frac{1.26 \times 10^5 \text{ Btu/hr} \times (3.62 / 60) \text{ hr}}{(2400 + 2339 + 2780) \text{ Btu/}^\circ\text{F}} = 1.0^\circ\text{F}$$

This is a very small increase in fuel temperature. Consequently, the impact on the MPC internal helium pressure will be quite small. Based on a conservative analysis of the HI-STORM 100 System response to a hypothetical fire event, it is concluded that the fire event does not adversely affect the temperature of the MPC or contained fuel. We conclude that the ability of the HI-STORM 100 System to cool the spent nuclear fuel within design temperature limits during and after fire is not compromised.

(ii) HI-TRAC Fire¹

To demonstrate the fuel cladding and MPC pressure boundary integrity under an exposure to a hypothetical short duration fire event during on-site handling operations, a fire accident analysis of the loaded 100-ton HI-TRAC is performed. This analysis, because of the lower mass of the 100-ton HI-TRAC, bounds the effects for the 125-ton HI-TRAC. In this analysis, the contents of the HI-TRAC are conservatively postulated to undergo a transient heat-up as a lumped mass from the decay heat input and heat input from the short duration fire. The rate of temperature rise of the HI-TRAC depends on the thermal inertia of the cask, the cask initial conditions, the spent nuclear fuel decay heat generation, and the fire heat flux. Using conservatively bounding inputs – lowerbound thermal inertia, steady state maximum cask temperatures (Table 4.III.6) and design heat load (36.9 kW) - a bounding cask temperature rise of 5.178 °F per minute is computed from the combined radiant and forced convection fire and decay heat inputs to the cask. During the handling of the HI-TRAC transfer cask, the transporter is limited to a maximum of 50 gallons. The duration of the 50-gallon fire using the methodology articulated above for HI-STORM fire is 4.775 minutes. Therefore, the temperature rise computed as the product of the rate of temperature rise and the fire duration is 24.7 °F, and the co-incident fuel cladding temperature $(664.7^{\circ}\text{F})^2$ is below the 1058 °F accident limit.

The elevated temperatures as a result of the fire accident will cause the pressure in the water jacket to increase and cause the overpressure relief valves to vent steam to the atmosphere. Based on the fire heat input to the water jacket, less than 11% of the water in the water jacket can be boiled off. However, it is conservatively assumed, for dose calculations, that all the water in the water jacket is lost. In the 125-ton HI-TRAC, which uses Holtite in the lids for neutron shielding, the elevated fire temperatures would cause the Holtite to exceed its design accident temperature limits. It is conservatively assumed, for dose calculations, that all the Holtite in the 125-ton HI-TRAC is lost.

Due to the increased temperatures the MPC experiences as a result of the fire accident in the HI-TRAC transfer cask, the MPC internal pressure increases. The pressure rise is computed using the Ideal Gas Law and upperbound helium backfill pressure defined in Chapter 4, Table 4.4.12 and results tabulated in Table 4.III.9. The computed MPC accident pressure is substantially below the accident design pressure (Table 2.2.1).

(b) Flood

The flood accident is defined in Chapter 2 as a deep submergence event. The worst flood from a thermal perspective is a “smart flood” that just rises to the top of the inlets to prevent airflow without the benefit of MPC cooling by water. This effect is bounded by the 100% inlets ducts blockage accident evaluated herein in Section 4.III.6.2(d).

¹ The HI-TRAC fire accident methodology is same as the generic methodology in Section 4.6 of the HI-STORM 100 FSAR.

² Computed by adding the fire temperature rise to initial fuel temperature (Table 4.III.6).

(c) Burial Under Debris

The burial under debris evaluation in Section 4.6 is bounding because of the following:

- (i) The MPC thermal inertia is neglected.
- (ii) The initial storage temperatures under MPC-68M storage are less than the HI-STORM 100 System temperatures.

(d) 100% Blockage of Air Ducts

This accident is defined in Section 4.6 as 100% blockage of the air inlet ducts for 32 hours. This event is evaluated by blocking the air inlets in the FLUENT thermal model and computing the 32-hour temperature rise of the MPC and stored fuel. The results of this analysis are tabulated in Table 4.III.7. The results show that fuel cladding and component temperatures remain below their respective accident limits specified in Chapter 2 and Supplement 4.III. The increase in temperature results in a concomitant rise of the MPC pressure. The maximum accident pressure tabulated in Table 4.III.7 is below the design limit specified in Chapter 2.

(e) Extreme Environmental Temperature

The principal effect of elevated ambient temperature is a rise of the HI-STORM 100 temperatures from the baseline normal storage temperatures by the difference between elevated ambient and normal ambient temperatures. As the normal storage temperatures under MPC-68M storage in the HI-STORM 100 overpack are bounded by the HI-STORM 100 System temperatures reported in Section 4.4, the temperatures under this event are likewise bounded by the extreme ambient evaluation in Section 4.6.

(f) 100% Rods Rupture Accident

In accordance with NUREG-1536 a 100% rods rupture accident is evaluated assuming 100% of the rods fill gases and fission gases release in accordance with NUREG-1536 release fractions. The MPC-68M pressure under this postulated accident is computed and tabulated in Table 4.III.4. The pressure is below the accident design pressure (Table 2.2.1).

(g) Jacket Water Loss

The principal effect of jacket water loss accident is a temperature increment in the stored fuel and MPC from the baseline conditions under in a HI-TRAC. As the MPC-68M temperatures in the HI-TRAC are bounded by MPC-68 temperatures the jacket water loss temperatures are likewise bounded by the HI-TRAC jacket water loss evaluation in Section 4.6.

4.III.7 REGULATORY COMPLIANCE

As required by ISG-11, the fuel cladding temperature at the beginning of dry cask storage is maintained below the anticipated damage-threshold temperatures for normal conditions for the licensed life of the HI-STORM System.

As required by NUREG-1536 (4.0,IV,3), the maximum internal pressure of the cask remains within its design pressure for normal, off-normal, and accident conditions. Design pressures are specified in Table 2.2.1.

As required by NUREG-1536 (4.0,IV,4), all cask materials and fuel cladding are maintained within their temperature limits under normal, off-normal and accident conditions to enable them to perform their intended safety functions. Material temperature limits are specified in Tables 2.2.3 and 4.III.2.

As required by NUREG-1536 (4.0,IV,5), the cask system ensures a very low probability of cladding breach during long-term storage. For long-term normal conditions, the maximum CSF cladding temperature is below the ISG-11 limit of 400°C (752°F).

As required by NUREG-1536 (4.0,IV,7), the cask system is passively cooled. All heat rejection mechanisms described in this supplement, including conduction, natural convection, and thermal radiation, are passive.

As required by NUREG-1536 (4.0,IV,8), the thermal performance of the cask is within the normal storage design criteria specified in Chapters 2 and 4. All thermal results are within the limits under normal conditions of storage.

4.III.8 REFERENCES

- [4.III.1] Aluminum Alloy 2219 Material Data Sheet, ASM Aerospace Specification Metals, Inc., Pompano Beach, FL.
- [4.III.2] *United States Code of Federal Regulations, Title 10, Part 71.*
- [4.III.3] Gregory, J.J. et. al., "Thermal Measurements in a Series of Large Pool Fires", SAND85-1096, Sandia National Laboratories, (August 1987).
- [4.III.4] Jakob, M. and Hawkins, G.A., "Elements of Heat Transfer," John Wiley & Sons, New York, (1957).

Table 4.III.1: Thermal Properties of Fuel Basket and Basket Shim Materials

Property	Minimum Value	Reference
Metamic-HT (fuel basket)		
Conductivity	104 Btu/ft-hr-°F	Appendix 1.III.A
Emissivity	Note 1	Appendix 1.III.A
Density	168.7 lb/ft ³	Appendix 1.III.A
Heat Capacity	0.21 Btu/lb-°F	Appendix 1.III.A
Aluminum Alloy 2219 (basket shims)		
Conductivity	69.3 Btu/ft-hr-°F	[4.III.1]
Emissivity	Note 1	Appendix 1.III.A
Density	177.3 lb/ft ³	[4.III.1]
Heat Capacity	0.207 Btu/lb-°F	[4.III.1]
Note 1: Fuel basket and basket shims are hard anodized to yield high emissivities. Lowerbound surface emissivity of hard anodized surfaces is defined in Appendix 1.III.A.		

Table 4.III.2: Temperature Limits of Fuel Basket and Basket Shim Materials

Metamic-HT (Note 1)	
Normal storage	752°F
Short term operations, Off-Normal and Accident conditions	932°F
Aluminum Alloy 2219 Shims (Note 2)	
Normal storage	752°F
Short term operations, Off-normal and Accident conditions	932°F
Notes: <ol style="list-style-type: none"> 1. The B₄C component in Metamic-HT is a refractory material that is unaffected by <i>these</i> temperatures and the aluminum component is solid at temperatures in excess of 1000°F. 2. To preclude melting the temperature limits are set well below the melting temperature of Aluminum Alloys. 	

Table 4.III.3: Maximum Temperatures Under Normal Long-Term Storage

Component	Temperature (°F)
Fuel Cladding	598
Basket	585
Basket Shims	500
MPC Shell	443
Overpack Inner Shell	309
Overpack Body Concrete	234
Overpack Lid Concrete	228
Overpack Outer Shell	169
Area Averaged Air Outlet ¹	220

¹ Reported herein for the option of outlet ducts air temperature surveillance set forth in the Technical Specifications.

Table 4.III.4: Maximum Pressures Under Normal Long Term Storage

Condition	Pressure (psig)
Initial backfill* (at 70°F)	48.5
Normal: intact rods	95.5
1% rods rupture**	96
Off-Normal (10% rods rupture)	100.5
Accident (100% rods rupture)	145.8
* Conservatively assumed at the Tech. Spec. maximum value (see Table 4.4.12).	
** Per NUREG-1536, pressure analyses with ruptured fuel rods (including BPRA rods for PWR fuel) is performed with release of 100% of the ruptured fuel rod fill gas and 30% of the significant radioactive gaseous fission products.	

Table 4.III.5: Maximum MPC-68M Temperatures Under Vacuum Drying Scenarios

Component	Scenario A (°F)	Scenario B (°F)
Cladding	754	732
Fuel Basket	729	698
Basket Shims	522	482
MPC Shell	325	307
Notes:		
(1) The cladding temperatures are below the ISG 11 temperature limits of Moderate Burnup Fuel (Scenario A) and High Burnup Fuel (Scenario B).		
(2) The component temperatures are below the Chapter 2 and Supplement III temperature limits.		

Table 4.III.6: Maximum HI-TRAC Temperatures and Pressures
Under On-site Transfer Operations

Component	Temperature [°F]
Fuel Cladding	640 ¹
MPC Basket	626
Basket Periphery	567
MPC Outer Shell Surface	442
Aluminum Shims	528
HI-TRAC Inner Shell Inner Surface	331
Water Jacket Inner Surface	264
Enclosure Shell Outer Surface	261
Water Jacket Bulk Water	250
Top Lid Neutron Shield (Holtite) ²	296
Pressure (psig)	
Initial Backfill	48.5
Operating Pressure	101.6
With 1% rods rupture	102.1
With 10% rods rupture	106.9

¹ The calculated value is below the permissible limit for high-burnup fuel. Therefore auxiliary cooling of the HI-TRAC is not necessary to ensure cladding safety under onsite transfer operations involving the MPC-68M. Accordingly SCS cooling is not mandated in the MPC-68M Technical Specifications

² Local neutron shield section temperature.

Table 4.III.7: Maximum Temperatures and Pressures Under
32-Hour 100% Air Inlets Blockage Accident

Component	Temperature (°F)
Fuel Cladding	722
Fuel Basket	709
Basket Shims	626
MPC Shell	571
MPC Lid	543
Overpack Inner Shell	462
Body Concrete	304
Lid Concrete	295
Pressure (psig)	
MPC	111.6

Table 4.III.8: Differential Thermal Expansion

Gap Description	Cold Gap U mm (in)	Differential Expansion δ_i mm (in)	Is Free Expansion Criterion Satisfied (i.e., $U > \delta_i$)
Fuel Basket-to-MPC Radial Gap	3.175 (0.125)	2.55 (0.101)	Yes
Fuel Basket-to-MPC Axial Gap	63.5 (2.5)	9.69 (0.382)	Yes
MPC-to-Overpack Radial Gap	7.9375 (0.3125)	3.07 (0.121)	Yes
MPC-to-Overpack Minimum Axial Gap	182.5625 (7.1875)	13.16 (0.52)	Yes

HOLTEC INTERNATIONAL COPYRIGHTED MATERIAL

Table 4.III.9: MPC-68M Pressure Under HI-TRAC Fire Accident

<i>Initial Operating Pressure</i>	<i>101.6 psig</i>
<i>Fire Pressure Rise</i>	<i>2.9 psig</i>
<i>Fire Accident Pressure</i>	<i>104.5 psig</i>

Table 4.III.10: MPC-68M Thermal Inertia

<i>Fuel</i>	<i>2780 Btu/°F</i>
<i>Basket and Aluminum Shims</i>	<i>2339 Btu/°F</i>
<i>Pressure Boundary (lid, baseplate and shell)</i>	<i>2400 Btu/°F</i>

Table 4.III.11: HI-STORM Temperatures Under Fuel Debris Storage

<i>Component</i>	<i>Temperature</i>
<i>Cladding</i>	<i>583°F^{Note 1}</i>
<i>Basket</i>	<i>561°F</i>
<i>Aluminum Shims</i>	<i>451°F</i>
<i>MPC Shell</i>	<i>406°F</i>
<i>Overpack Inner Shell</i>	<i>268°F</i>
<i>Overpack Outer Shell</i>	<i>162°F</i>
<i>Overpack Body Concrete</i>	<i>194°F</i>
<i>Overpack Lid Concrete</i>	<i>210°F</i>
<i>Average Air Outlet</i>	<i>208°F</i>

Note 1: It is recognized that the assumption of all 16 DFC locations having fuel debris instead of permitted 8 cells has the effect of slightly understating the MPC heat load because of the lower per assembly heat permitted in DFC cells. However, because the effect is small (32.288 kW with all 16 cells versus 33.144 kW with permitted 8 cells) and the margins from limits are substantial, this has no adverse effect on the reported temperatures or conclusions. Moreover, the DFC is stored in the basket periphery cells. The effect of a slight change in the heat load in the periphery cells will have a second order effect on the peak cladding temperature which occurs in the inner cell locations.

SUPPLEMENT 5.III**EVALUATION OF THE MPC-68M BASKET, AND THE 10x10F AND 10x10G ASSEMBLY CLASSES****5.III.0 DISCUSSION**

The MPC-68M is a variation of the 68 cell BWR canister MPC-68 evaluated in the main part of this chapter, but with a basket design consisting of aluminum oxide and finely ground boron carbide dispersed in a metal matrix of pure aluminum. The boron carbide content is 10% (minimum) by weight. This results in a B-10 areal density that is slightly above that in the MPC-68. To show that the baskets are essentially identical from a shielding perspective, the relevant differences between the baskets are listed below, and then discussed in respect to its effect on the photon and neutron dose rates.

Differences between the MPC-68M compared to the MPC-68, in respect to the characteristics important for the dose calculations, are as follows:

- The MPC-68M has a slightly higher B-10 content
- The MPC-68M is lighter, since it consists of aluminum and boron carbide, but no steel
- In the enclosure shell, the MPC-68M is surrounded by aluminum basket shims

To evaluate the effect of these differences, studies in the main part of Chapter 5 regarding dose contributions from a regionalized loading scheme are utilized. These studies, described in Section 5.4, show that the inner region on an MPC-68 (32 assemblies = 47 % of the content) contributes about 27% of the neutron dose rate, but only about 2 % of the photon dose rate. This means that the self shielding of the fuel and basket for neutron radiation is low, while for photon radiation it is very high. The low neutron self shielding means that the neutron doses are not significantly affected by the reduced basket weight, since the majority of the neutron shielding function is provided by the overpack around the MPC. Also, for MPCs filled with water, there is a further reduction in neutron dose due to the increased absorption of thermal neutrons from the increased B-10 loading. The high self shielding for photons means that only the outer basket panels are effective for gamma shielding. For the MPC-68M, the shielding in this area is enhanced due to the presence of the basket shims, and therefore comparable to the absorption in the steel basket walls. In summary, the effect of the design differences between MPC-68 and MPC-68M on dose rates is small. Therefore, no specific dose calculations are performed for the MPC-68M, and all results and conclusions from the MPC-68 are directly applicable here.

Additionally, two BWR array classes designated 10x10F and 10x10G have been added as approved contents in the MPC-68M only. From a radiological perspective, the additional array classes are bounded by the design basis GE 7x7 source term calculations, since those design basis assemblies have higher initial uranium masses. In terms of grouping assemblies for the polynomial factors presented in Section 2.1.9, the new array classes are added to groups which represent assemblies of a higher mass. This is conservative since a heavier assembly results in a

higher decay heat, which reduces the allowable assembly burnup. In summary, no new analyses are necessary to qualify those additional array classes.

Therefore, the main body of this chapter remains fully applicable for the HI-STORM 100 System using an MPC-68M and the new assembly classes.

SUPPLEMENT 6.III¹: CRITICALITY EVALUATION OF THE MPC-68M**6.III.1 DISCUSSION AND RESULTS**

In conformance with the principles established in NUREG-1536 [6.III.1.1], 10CFR72.124 [6.III.1.2], and NUREG-0800 Section 9.1.2 [6.III.1.3], the results in this supplement demonstrate that the effective multiplication factor (k_{eff}) of the HI-STORM 100 System with the MPC-68M, including all biases and uncertainties evaluated with a 95% probability at the 95% confidence level, does not exceed 0.95 under all credible normal, off-normal, and accident conditions.

Criticality safety of the HI-STORM 100 System with the MPC-68M depends on the following principal design parameters:

- The inherent geometry of the fuel basket design of the MPC-68M;
- The incorporation of spatially distributed B-10 isotope in the Metamic-HT fuel basket structure. Based on the tests for the neutron absorber content in Metamic-HT (see Appendix 1.III.A and Supplement 9.III), and consistent with the approach taken for Metamic (see Section 9.1.5.3.2), 90% of the minimum B-10 (B_4C) content is credited in the analysis. With a specified minimum B_4C content of 10 wt%, the concentration credited in the analysis is therefore 9 wt%.

The off-normal and accident conditions defined in Section 2.2 are applicable to the HI-STORM System using the MPC-68M. These accidents are considered in Supplement 11.III and have no adverse effect on the design parameters important to criticality safety, except for the non-mechanistic tip-over event, which could result in limited plastic deformation of the basket. However, a bounding basket deformation is already included in the criticality models for normal conditions, and thus, from the criticality safety standpoint, the off-normal and accident conditions are identical to those for normal conditions.

Results of the design basis criticality safety calculations for a single internally flooded HI-TRAC transfer cask with full water reflection on all sides (limiting cases for the HI-STORM 100 System), loaded with intact fuel assemblies are listed in Table 6.III.1.1, conservatively evaluated for the worst combination of manufacturing tolerances (as identified in Section 6.III.3), and including the calculational bias, uncertainties, and calculational statistics. In addition, a result for a single internally dry (no moderator) HI-STORM storage cask with full water reflection on all external surfaces of the overpack, including the annulus region between the MPC and overpack, is listed in Table 6.III.1.2 to confirm the low reactivity of the HI-STORM 100 System with an MPC-68M in storage. The maximum k_{eff} for an MPC-68M loaded with up to 16 DFCs is listed in Table 6.III.1.3.

¹ Evaluations and results presented in this chapter are supported by documented calculation package(s) [6.III.1.4].

TABLE 6.III.1.1

BOUNDING MAXIMUM keff VALUES FOR EACH ASSEMBLY CLASS IN THE MPC-68M
(HI-TRAC 100)

Fuel Assembly Class	Maximum Allowable Planar-Average Enrichment (wt% U-235)	Maximum keff
7x7B	4.8	0.9243
8x8B	4.8	0.9294
8x8C	4.8	0.9302
8x8D	4.8	0.9307
8x8E	4.8	0.9211
8x8F	4.5	0.9245
9x9A	4.8	0.9341
9x9B	4.8	0.9330
9x9C	4.8	0.9254
9x9D	4.8	0.9254
9x9E/F	4.5	0.9254
9x9G	4.8	0.9211
10x10A	4.8	0.9360
10x10B	4.8	0.9353
10x10C	4.8	0.9321
10x10F	4.7	0.9356
10x10G	4.6	0.9393

Note: The results presented in the table above have an additional bias of 0.0021 applied to the 10x10 fuel assembly classes to conservatively account for any potential distributed enrichment effects. See Section 6.III.2.

TABLE 6.III.1.2

REPRESENTATIVE k_{eff} VALUES FOR MPC-68M IN THE HI-STORM 100 OVERPACK

Fuel Assembly Class	Maximum Allowable Planar-Average Enrichment (wt% ^{235}U)	Maximum k_{eff}
10x10A	4.8	0.3754

TABLE 6.III.1.3

BOUNDING MAXIMUM k_{eff} VALUES FOR THE MPC-68M WITH UP TO 16 DFCs

Fuel Assembly Class	Maximum Allowable Planar-Average Enrichment (wt% ^{235}U)	Maximum k_{eff}
All BWR Classes except 8x8F, 9x9E/F, 10x10F and 10x10G	4.8	0.9408
8x8F, 9x9E/F and 10x10G	4.0	0.9131
10x10F	4.7	0.9362

Note: The results presented in Tables 6.III.1.2 and 6.III.1.3 above have an additional bias of 0.0021 applied to the 10x10 fuel assembly classes to conservatively account for any potential distributed enrichment effects. See Section 6.III.2.

6.III.2 SPENT FUEL LOADING

The BWR fuel assembly classes/arrays which are authorized for the MPC-68 are qualified for the MPC-68M, except for the 6x6A, 6x6B, 6x6C, 7x7A, 8x8A, 10x10D and 10x10E. Additionally, the MPC-68M is qualified for two new assembly classes, 10x10F and 10x10G. Information on those classes is provided in Supplement 2.III, Table 2.III.3. Table 2.1.4 in Chapter 2 provides the acceptable fuel characteristics for all other fuel array/class authorized for storage in the MPC-68M, however fuel with planar-average initial enrichments up to 4.8 wt% ^{235}U are authorized in the MPC-68M.

BWR assemblies are specified in the Table 2.1.4 and Table 2.III.3 with a maximum planar-average enrichment. The analyses presented in this chapter use a uniform enrichment, equal to the maximum planar-average. Analyses presented in Appendix 6.B *for the MPC-68* show that this is a conservative approach, i.e. that a uniform enrichment bounds the planar-average enrichment in terms of the maximum k_{eff} . To confirm this for the higher enrichments analyzed here, additional calculations were performed *for the assembly class 10x10A in the MPC-68M*, and are presented in Table 6.III.2.1 in comparison with the results for the uniform enrichment. Since the maximum planar-average enrichment of 4.8 wt% ^{235}U is above the actual enrichments of those assemblies, actual (as-built) enrichment distributions are not available. Therefore, several bounding cases are analyzed. Note that since the maximum planar-average enrichment of 4.8 wt% ^{235}U is close to the maximum rod enrichment of 5.0 wt% ^{235}U , the potential enrichment variations within the cross section are somewhat limited. To maximize the differences in enrichment under these conditions, the analyzed cases assume that about 50% of the rods in the cross section are at an enrichment of 5.0 wt% ^{235}U , while the remainder of the rods are at an enrichment of about 4.6 wt%, resulting in an average of 4.8 wt%. Calculations are performed for cross sections where all full-length and part-length, or only all full-length rods are present. For each case, two conditions are analyzed that places the different enrichment in areas with different local fuel-to-water ratios. Specifically, one condition places the higher enriched rods in locations where they are more surrounded by other rods, whereas the other condition places them in locations where they are more surrounded by water, such as near the water-rods or the periphery of the assembly. The results in Table 6.III.2.1 *indicate that there may be a potential positive reactivity effect (+0.0021) due to distributed enrichments. Therefore, additional studies with distributed enrichments were performed and are presented in Table 6.III.2.2. These include all cases from Appendix B (for 8x8 and 9x9 assembly types), now evaluated in the MPC-68M, and additional cases for the 10x10G which has the highest reactivity of all assembly classes. The cases from Appendix B show no statistically significant increase, and in most cases a decrease in reactivity as a result of the distributed enrichment. However, the assembly class 10x10G also shows a slight increase for one of the cases (+0.0012). Note that the small positive reactivity effect for the two 10x10 assembly classes is likely due to the very conservative selection of enriched rod locations used in the study (in the study they were placed close to the periphery and water rods, locations that are unlikely for actual fuel assemblies but were selected for the study to cover unknown rod patterns). Nevertheless, for conservatism an additional bias of 0.0021 is applied to the results for all 10x10 fuel assembly classes in Section 6.III.1, including the cases with damaged fuel. Note that for the studies presented in the remainder of this supplement this bias is not included since those studies focus on reactivity differences rather than absolute values of k_{eff} .*

TABLE 6.III.2.1

REACTIVITY EFFECT OF DISTRIBUTED ENRICHMENTS in BWR Fuel in the MPC-68M

Fuel Assembly/ Parameter Variation	reactivity effect	Maximum k_{eff}	standard deviation
10x10A (Reference, full-length rods only)	Reference	0.9339	0.0004
distributed enrichment, Case 1	-0.0004	0.9335	0.0004
distributed enrichment, Case 2	+0.0021	0.9360	0.0004
distributed enrichment, Case 3	-0.0092	0.9247	0.0004
distributed enrichment, Case 4	-0.0118	0.9221	0.0004

TABLE 6.III.2.2

ADDITIONAL CALCULATIONS OF THE REACTIVITY EFFECT OF DISTRIBUTED ENRICHMENTS in BWR FUEL IN THE MPC-68M

Assembly Class	Enrichment	Maximum k_{eff}	Description	Delta-k_{eff}
8x8C	4.8	0.8273	Average Enrichment	-0.0044
8x8C	4.8	0.8229	Distributed Enrichment	
8x8C	4.8	0.8876	Average Enrichment	-0.0040
8x8C	4.8	0.8836	Distributed Enrichment	
8x8D	4.8	0.8550	Average Enrichment	+0.0004
8x8D	4.8	0.8554	Distributed Enrichment	
8x8D	4.8	0.8774	Average Enrichment	-0.0017
8x8D	4.8	0.8757	Distributed Enrichment	
8x8D	4.8	0.8855	Average Enrichment	-0.0026
8x8D	4.8	0.8829	Distributed Enrichment	
9x9B	4.8	0.9103	Average Enrichment	-0.0023
9x9B	4.8	0.9080	Distributed Enrichment	
9x9D	4.8	0.8467	Average Enrichment	-0.0095
9x9D	4.8	0.8372	Distributed Enrichment	
8x8C	4.8	0.9023	Average Enrichment	-0.0025
8x8C	4.8	0.8998	Distributed Enrichment	
8x8C	4.8	0.9165	Average Enrichment	-0.0003
8x8C	4.8	0.9162	Distributed Enrichment	
10x10G	4.6	0.9372	Average Enrichment	-0.0233
10x10G	4.6	0.9139	Distributed Enrichment	
10x10G	4.6	0.9372	Average Enrichment	-0.0285
10x10G	4.6	0.9087	Distributed Enrichment	
10x10G	4.6	0.9372	Average Enrichment	+0.0012
10x10G	4.6	0.9384	Distributed Enrichment	
10x10G	4.6	0.9372	Average Enrichment	-0.0014
10x10G	4.6	0.9358	Distributed Enrichment	

HOLTEC INTERNATIONAL COPYRIGHTED MATERIAL

6.III.3 MODEL SPECIFICATION

Calculational models for the MPC-68M are generally the same as those described in Section 6.3 except for the different basket as noted below.

Figures 6.III.3.1 and 6.III.3.2 show representative cross sections of the criticality models for the MPC-68M basket. Figure 6.III.3.1 shows a single cell of the basket, while Figure 6.III.3.2 shows the entire MPC-68M basket. All calculations are performed with eccentric fuel positioning, where the fuel is placed closest to the center of the basket in each basket cell. The wall thickness of the basket shims is modeled as 1 inch, while some of them are only ½ inch thick. This is conservative, since the model replaces water with aluminum, which reduces absorption and moderation outside of the basket.

To account for the potentially higher fuel density of higher enriched fuel, a conservative fuel stack density of 97.5% of the theoretical density (i.e. $10.96 \text{ g/cm}^3 * 97.5\% = 10.686 \text{ g/cm}^3$) is used in all analyses for the MPC-68M.

The basket geometry can vary due to manufacturing tolerances and due to potential deflections of basket walls as the result of accident conditions. The basket tolerances are defined on the drawings in Section 1.5. The structural acceptance criterion for the basket during accident conditions is that the permanent deflection of the basket panels is limited to a fraction of 0.005 (0.5%) of the panel width (see Chapter 3). The analyses in Supplement 3.III demonstrate that permanent deformations of the basket walls during accident conditions are far below this limit. Nevertheless, it is conservatively assumed that 2 adjacent cell walls in each cell are deflected to the maximum extent possible over their entire length and width, i.e. that the cell ID is reduced by 0.5% of the cell width, or 0.03" for MPC-68M cells. Maximum k_{eff} results (including the bias, uncertainties, or calculational statistics), along with the selected dimensions, for a number of dimensional combinations are shown in Table 6.III.3.1 for various fuel types. The cell ID is evaluated for minimum (tolerance only), minimum with deformation, nominal and an increased value. The wall thickness is evaluated for nominal and minimum values.

Based on the calculations, the conservative dimensional assumptions listed in Table 6.III.3.2 were determined for the basket designs. Note that, as expected, the bounding basket condition correspond to the minimum wall thickness and minimum cell-id. Because the reactivity effect (positive or negative) of the manufacturing tolerances is not assembly dependent (see Table 6.III.3.1), these dimensional assumptions were employed for all criticality analyses.

The basket is manufactured from individual slotted panels. The panels are expected to be in direct contact with each other (see Drawing in Section 1.5). However, to show that small gaps between panels would have essentially no effect on criticality, calculations are performed with a postulated 0.06" gap between panels, repeated in the axial direction every 10" in all panels. The results are summarized in Tables 6.III.3.3 and show statistically equivalent results for calculations with and without the gap. This indicates that the effect of small gaps between the METAMIC panels is negligible. Therefore, all other calculations are performed without any gaps between panels.

The MPC-68M uses the same principal neutron poison material as the MPC-68 (i.e. ^{10}B in the form of B_4C). The evaluation provided in Section 6.3.2, which concludes that ^{10}B depletion is negligible, is therefore directly applicable to the MPC-68M, and no additional evaluations are required in that respect.

Composition of the Metamic-HT is listed in Table 6.III.3.4.

TABLE 6.III.3.1

EVALUATION OF BASKET MANUFACTURING TOLERANCES FOR MPC-68M

Box I.D.	Box Wall Thickness	Maximum keff
10x10A, 4.8% Enrichment		
nominal (6.05")	nominal (0.40")	0.9263
nominal (6.05")	minimum (0.38")	0.9307
increased (6.07")	minimum (0.38")	0.9288
minimum (5.99")	minimum (0.38")	0.9334
minimum, including deformation (5.96")	minimum (0.38")	0.9339
7x7B, 4.8% Enrichment		
nominal (6.05")	nominal (0.40")	0.9154
nominal (6.05")	minimum (0.38")	0.9196
minimum, including deformation (5.96")	minimum (0.38")	0.9243
8x8D, 4.8% Enrichment		
nominal (6.05")	nominal (0.40")	0.9230
nominal (6.05")	minimum (0.38")	0.9265
minimum, including deformation (5.96")	minimum (0.38")	0.9307
9x9A, 4.8% Enrichment		
nominal (6.05")	nominal (0.40")	0.9263
nominal (6.05")	minimum (0.38")	0.9301
minimum, including deformation (5.96")	minimum (0.38")	0.9341
10x10G, 4.6% Enrichment		
nominal (6.05")	nominal (0.40")	0.9314
nominal (6.05")	minimum (0.38")	0.9349
minimum, including deformation (5.96")	minimum (0.38")	0.9372
10x10A, 4.8% Enrichment, Damaged Fuel		
nominal (6.05")	nominal (0.40")	0.9316
nominal (6.05")	minimum (0.38")	0.9348
minimum, including deformation (5.96")	minimum (0.38")	0.9387

Note: The results for the 10x10 fuel assembly classes do not include the bias for distributed enrichments discussed in Section 6.III.2.

TABLE 6.III.3.2

MPC-68M BASKET DIMENSIONAL ASSUMPTIONS

Box I.D.	Box Wall Thickness
minimum, including deformation (5.96")	minimum (0.38")

TABLE 6.III.3.3

REACTIVITY EFFECTS GAPS IN BASKET CELL PLATES

Gaps in Metamic-HT	MPC-68M (10x10A, 4.8% ENRICHMENT)	
	Max. k_{eff}	1 Sigma
None	0.9339	0.0004
0.06" every 10"	0.9346	0.0003

Note: The results do not include the bias for distributed enrichments discussed in Section 6.III.2.

TABLE 6.III.3.4

COMPOSITION OF THE METAMIC-HT

METAMIC HT, 9% B₄C, DENSITY 2.6 g/cm³	
Nuclide	Wgt. Fraction
13027	0.91
6000	0.01956
5010	0.01289
5011	0.05755

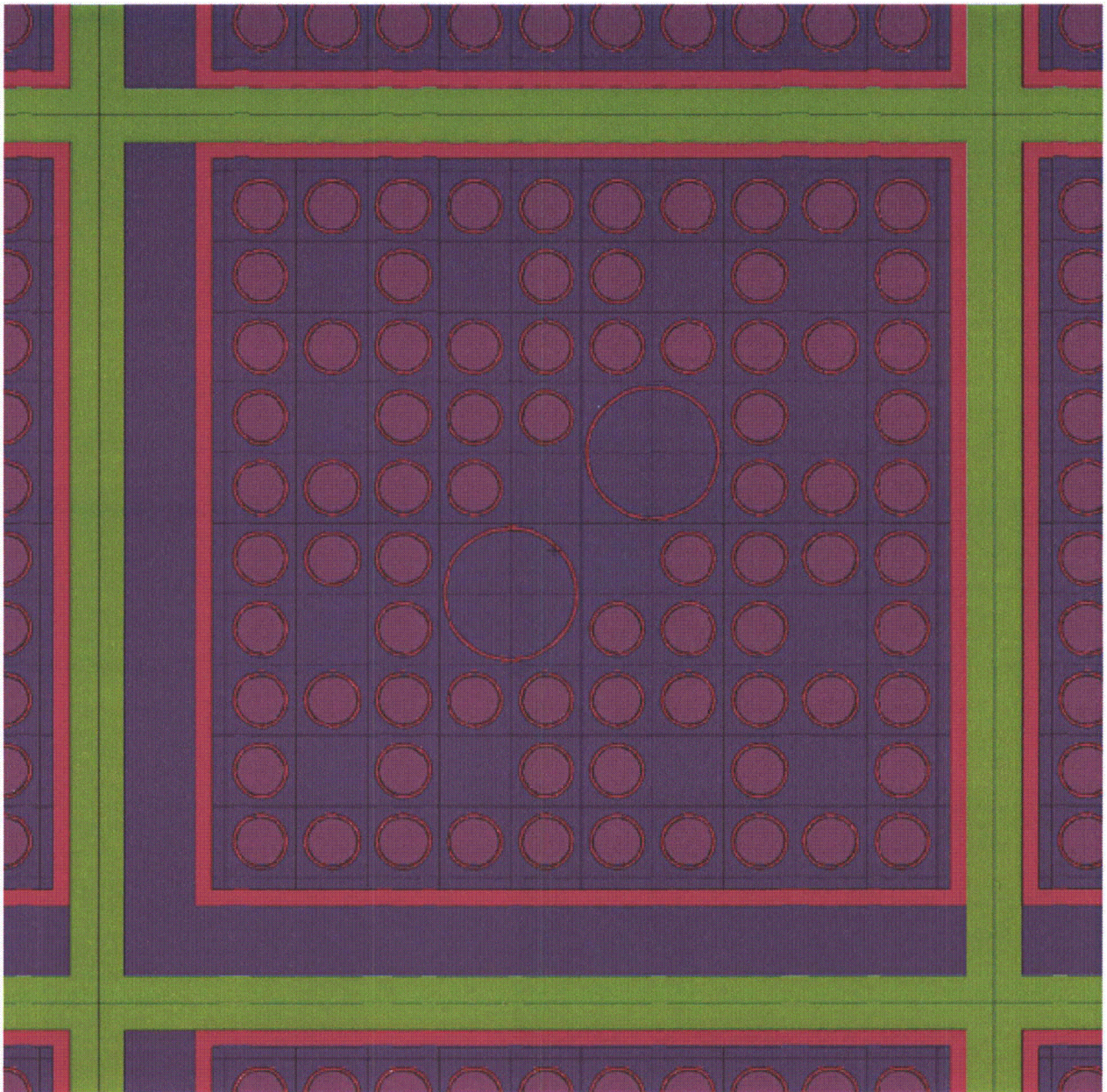


Figure generated directly from MCNP input file using the MCNP plot function. For Cell ID and Cell Wall Thickness see Table 6.III.3.2. For true dimensions see the drawing in Section 1.5. Note that the figure depicts an assembly with full and part length rods, showing the cross section where only full length rods are present.

Figure 6.III.3.1: Typical Cell of the Calculational Model (planar cross-section) with representative fuel in the MPC-68M

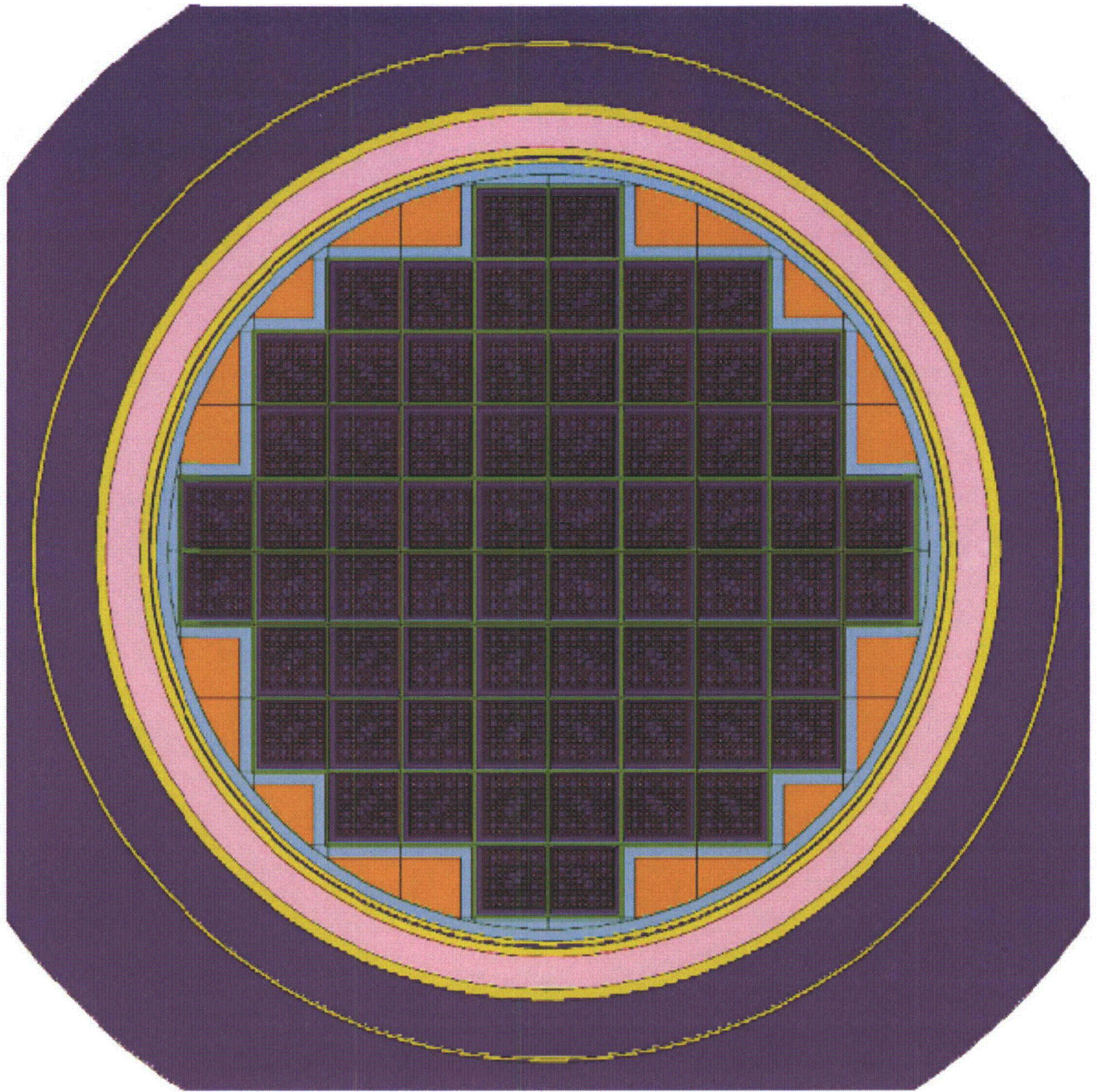


Figure generated directly from MCNP input file using the MCNP plot function. Radial dimensions of the HI-TRAC used in the analyses are unchanged from the analyses in the main part of this chapter. For true dimensions see the drawings in Section 1.5.

Figure 6.III.3.2: Calculational Model (planar cross-section) of the MPC-68M

6.III.4 CRITICALITY CALCULATIONS

The calculations in this supplement use the same computer codes and methodologies that are used in the main part of Chapter 6. Specifically, the conservative approach to model damaged fuel *and fuel debris*, using arrays of bare fuel rods, is the same (*see discussion in Subsection 6.III.4.1 below*).

The basket design of the MPC-68M is essentially identical to that of the MPC-68, in respect to the characteristics important to criticality safety. Specifically,

- The number and configuration of the cells for intact and damaged fuel/fuel debris are unchanged;
- The basket dimensions are essentially the same; and
- The same poison material (B₄C) is used, but a larger ¹⁰B content in the basket walls.

The content is also the same, except for the following

- Higher enrichments are qualified, consistent with the higher ¹⁰B content in the basket walls; and
- Two additional fuel assembly types are analyzed, that are variations of existing types with slightly different dimension.

To verify that the bounding fuel parameter variations analyzed in the MPC-68 are also applicable to the MPC-68M, additional studies are performed and discussed in Subsection 6.III.4.2 below.

Due to the strong similarity in the basket design, the conclusions of the various studies presented in the main part of this Chapter on the MPC-68 are directly applicable to the MPC-68M. *Nevertheless, to confirm this is also applicable to the MPC-68M*, numerous studies with various moderation conditions that conclude that the fully flooded basket is the bounding case are re-analyzed *and discussed in subsection 6.III.4.3*. All analyzes are therefore performed under the following condition:

- Basket, and DFCs as applicable, are fully flooded with pure water at the maximum density; and
- Pellet-to-clad gaps of intact assemblies are assumed flooded (*see also discussion in Subsection 6.III.4.2 below*)
- All assemblies and DFCs are located eccentrically in the basket, closest to the center of the basket.

Results for all design basis calculations are listed in Subsection 6.III.1. All maximum k_{eff} values are below the regulatory limit of 0.95.

6.III.4.1 Damaged Fuel and Fuel Debris

For damaged fuel and fuel debris in the MPC-68M the same conservative approach is used as in the main part of this chapter, see discussion in Section 6.4.4, specifically 6.4.4.2. Important aspects of this approach that ensure its conservatisms are as follows:

- *All damaged fuel and fuel debris must be in damaged fuel containers (DFCs), and located in specifically designated cells on the periphery of the basket as specified in Table 2.1.22.*
- *A conservative model is used that bounds both damaged fuel and fuel debris. In other words, damaged fuel is always conservatively modeled as fuel debris.*
- *The model consists of regular arrays of fuel rods without cladding. The rods pitch (array size) is varied to determine the optimum moderation condition.*
- *Intact and damaged fuel/fuel debris in the same basket have the same enrichment limit, which may be different from the enrichment limit for intact fuel only.*
- *The results for loading with intact fuel only in Table 6.III.1.1 utilize different enrichment limits for different assembly classes, to ensure that the maximum k_{eff} is always below 0.95. It is therefore not possible to establish a single bounding assembly class/enrichment combination to be used in all analyzes with damaged fuel/fuel debris. Therefore, and in order to optimize the enrichment for the loading of intact and damaged fuel/fuel debris for each assembly class, intact assemblies are grouped by enrichment limit, and the intact assembly with the highest maximum k_{eff} in each group is used for the calculations together with damaged fuel/fuel debris. These are:

 - *Intact assemblies of 4.5 and 4.6 wt%: Assembly class 10x10G. For the calculations with intact and damaged fuel, an enrichment of 4.0 wt% is used.*
 - *Intact assembly of 4.7 wt%: Assembly class 10x10F. For the calculations with intact and damaged fuel, an enrichment of 4.0 wt% is used.*
 - *Intact assembly of 4.8 wt%: Assembly class 10x10A. For the calculations with intact and damaged fuel, an enrichment of 4.8 wt% is used.**
- *Consistent with the results in the main part of this chapter for the MPC-68, array sizes of 10x10 and 11x11 show the optimum moderation condition. This is confirmed for intact assembly classes 10x10A and 10x10G by evaluating all arrays from 3x3 to 17x17 rods. For assembly class 10x10F it is only confirmed that it is bounded by the cases with the 10x10A class (see Table 6.III.4.1).*

6.III.4.2 Fuel Parameters and Parameter Variations

In the main part of the FSAR, extensive analyses of fuel dimensional variations have been performed. These calculations demonstrate that the maximum reactivity corresponds to:

- *maximum active fuel length,*
- *maximum fuel pellet diameter,*
- *maximum fuel rod pitch,*
- *minimum cladding outside diameter (OD),*
- *maximum cladding inside diameter (ID),*
- *minimum guide tube/water rod thickness, and*
- *maximum channel thickness (for BWR assemblies only)*

- *part length rods (if present) removed.*

The reason that those are bounding dimensions, i.e. that they result in maximum reactivity is directly based on, and can be directly derived from the three main characteristics affecting reactivity, namely 1) characteristics of the fission process; 2) the characteristics of the fuel assemblies and 3) the characteristics of the neutron absorber in the basket. These affect the reactivity as follows:

- *The neutrons generated by fission are fast neutrons while the neutrons that initiate the fission need to be thermal neutrons. A moderator (water) is therefore necessary for the nuclear chain reaction to continue.*
- *Fuel assemblies are predominantly characterized by the amount of fuel and the fuel-to-water (moderator) ratio. Increasing the amount of fuel, or the enrichment of the fuel, will increase the amount of fissile material, and therefore increase reactivity. Regarding the fuel-to-water ratio, it is important to note that commercial BWR assemblies are undermoderated, i.e. they do not contain enough water for a maximum possible reactivity.*
- *The neutron poison in the basket walls uses B-10, which is an absorber of thermal neutrons. This poison therefore also needs water (moderator) to be effective. This places a specific importance on the amount of water between the outer rows of the fuel assemblies and the basket cell walls. Note that this explains some of the differences in reactivity between the different assembly types in the same basket, even for the same enrichment, where assemblies with a smaller cross section, i.e. which have more water between the periphery of the assembly and the surrounding wall, generally have a lower reactivity.*

Based on these characteristics, the following conclusions can be made:

- *Since fuel assemblies are undermoderated, any changes in geometry inside the fuel assembly that increases the amount of water while maintaining the amount of fuel are expected to increase reactivity. This explains why reducing the cladding or guide tube/water rod thicknesses, or increasing the fuel rod pitch results in an increase in reactivity.*
- *Increasing the active length will increase the amount of fuel while maintaining the fuel-to-water ratio, and therefore increase reactivity.*
- *The channel of the BWR assembly is a structure located outside of the rod array. It therefore does not affect the water-to-fuel ratio within the assembly. However, it reduces the amount of water between the assembly and the neutron poison, therefore reducing the effective thermalization for the poison. Therefore, an increase of the channel wall thickness will increase reactivity.*
- *In respect to the effect of the fuel pellet diameter, several compensatory effects need to be considered. Increasing the diameter will tend to increase the reactivity due to the increase in the fuel amount. However, it will also change the fuel-to-water-ratio, and will therefore make the fuel more undermoderated, which in turn tends to reduce reactivity. The effect of this change in moderation may depend on the condition of the pellet-to-clad gap. Assuming an empty pellet-to clad gap, which would be consistent with undamaged fuel rods, the change in moderation is small, and the net effect is an increase in reactivity, since the effect of the increase in the fissionable material dominates. In this case, the maximum pellet*

diameter is more reactive. When the pellet-to-clad gap is conservatively flooded, as recommended by NUREG 1536, a reduction of the fuel pellet diameter will also result in an increase in the amount of water, i.e. have a double effect on the water-to-fuel ratio. In this case, it is possible that a slight reduction may result in no reduction or even an increase in reactivity. However, this is caused by a further amplification of the conservative assumption of the flooded pellet-to-clad gap, not by a positive increase in reactivity from the reduction in fuel (which would be counter-intuitive). Therefore, the maximum fuel pellet diameter is used for the fuel specification.

- *Several assembly types contain part length rods (9x9A, 10x10A, B and G):*
 - *For 9x9A and 10x10A and B it was shown in the main part of the chapter (Tables 6.2.29, 36 and 37, respectively) that the condition with the part lengths rods completely removed is bounding. This condition is therefore used in the design basis calculations, so a specification of the lengths of the part length rods is not required. Applicability to the MPC-68M is confirmed by showing that all assemblies are undermoderated, which means the increase of water from completely removing the part length rods increases reactivity. All calculations for the MPC-68M for assembly classes 9x9A and 10x10A and B are therefore performed with models where the part length rods are replaced by water.*
 - *For assembly class 10x10G, the part length rods are located near the periphery and the water rod of the assembly, i.e. not surrounded by other rods on all sides. For this fuel assembly class, calculations with various part length rod lengths were performed and show that using full length rods in place of part length rods is more conservative. These calculations are listed in Table 6.III.4.4 (Note that the 75% case and the 100% case in the tables are statistically equivalent, i.e. they do not indicate that a reduced length would result in a higher reactivity). The case with all rods full length is therefore conservatively used in Table 6.III.1.1. This again removes the need to specify a length for the part lengths rods.*

Since all assemblies have the same principal design, i.e. consist of bundles of clad fuel rods, most of them with embedded guide/instrument tubes or water rods or channels, the above conclusions apply to all of them, and the bounding dimensions are therefore also common to all fuel assemblies analyzed here. Nevertheless, to clearly demonstrate that the main assumption is true, i.e. that all assemblies are undermoderated, a study was performed for all assembly types where the pellet-to-clad gap is empty instead of being flooded (a conservative assumption for the design basis calculations) The results are listed in Table 6.III.4.2, in comparison with the results of the reference cases with the flooded gap. In all cases, the reactivity is reduced compared to the reference case. This verifies that all assembly types considered here are in fact undermoderated, and therefore validates the main assumption stated above. All assembly types are therefore behaving in a similar fashion, and the bounding dimensions are therefore applicable to all assembly types.

The discussion provided above regarding the principal characteristics of fuel poison is also important for the various studies presented in this section, and supports the fact that those studies only need to be performed for a single BWR assembly type, and that the results of those studies are

then generally applicable to all assembly types. The studies and the relationship to the discussion above are listed below.

Basket Manufacturing Tolerance: The two aspects of the basket tolerance that are evaluated are the cell wall thickness and the cell ID. The reduced cell wall thickness results in a reduced amount of poison (since the material composition of the wall is fixed), and therefore in an increase in reactivity. The reduced cell ID reduces amount of water between the fuel the poison, and therefore the effectiveness of the poison material. Both effects are simply a function of the geometry, and are independent of the fuel type. However, calculations are performed for various fuel types and this study is presented in Table 6.III.3.1.

Panel Gaps: Similar to the basket manufacturing tolerance for the cell wall thickness, this tolerance has a small effect on the overall poison amount of the basket, which would affect the reactivity of the system independent of the fuel type. This study is presented in Table 6.III.4.5.

Eccentric positioning: When a fuel assembly is located in the center of a basket cell, it is surrounded by equal amounts of water on all sides, and hence the thermalization of the neutrons that occur between the assembly and the poison in the cell wall, and hence the effectiveness of the poison, is also equal on all sides. For an eccentric positioning, the effectiveness of the poison is now reduced on those sides where the assembly is located close to the cell walls, and increased on the opposite sides. This creates a compensatory situation for a single cell, where the net effect is not immediately clear. However, for the entire basket, and for the condition where all assemblies are located closest to the center of the basket, the four assemblies at the center of the basket are now located close to each other, separated by poison plates with a reduced effectiveness since they are not surrounded by water on any side. This now becomes the dominating condition in terms of reactivity increase. This effect is also applicable to all assembly types, since those assemblies are all located close to the center of the basket, i.e. the eccentric position with all assemblies moved towards the center will be bounding regardless of the assembly type. An additional study is presented in Table 6.III.4.6 to confirm this effect for the MPC-68M.

In addition, additional fuel assembly characteristics important to criticality control are the location of guide tubes, water rods, part length rods, and rods with differing dimensions (classes 9x9E/F only). These are identified in the assembly cross sections provided in Figure 6.III.4.1.

Various additional studies were performed to address conditions for specific assembly classes:

- Fuel assembly class 8x8B and 8x8D are specified with various fuel rod numbers and water rod locations (see Figure 6.III.4.1). Calculations are performed to show that the results listed in Table 6.III.1 are bounding. These calculations are listed in Table 6.III.4.3.*
- Fuel assembly class 9x9E/F has two rod diameters, and two water rod patterns (see Figure 6.III.4.1). A study is performed and documented in Table 6.III.4.3 that shows that the result listed in Table 6.III.1 is bounding.*

6.III.4.3 Moderation Conditions

Additional studies were performed to verify that the fully flooded condition is bounding for the MPC-68M, as it is for the MPC-68 basket analyzed in the main part of this chapter:

- *Internal and External Moderation: The studies presented in Table 6.III.4.2 show that all assemblies essentially behave identical in respect to water moderation, specifically, that all assemblies are undermoderated. The principal effect of changes to the internal and external moderation would therefore be independent of the fuel type. Calculations for the MPC-68M design with external moderators of various densities are shown in Table 6.III.4.7, all performed for the HI-TRAC and the MPC fully flooded. The results show that the maximum k_{eff} is essentially independent from the external water density. Nevertheless, all further evaluations are performed with full external water density. In a definitive study, Cano, et al. [6.4.2] have demonstrated that the phenomenon of a peak in reactivity at low moderator densities (sometimes called "optimum" moderation) does not occur in the presence of strong neutron absorbing material or in the absence of large water spaces between fuel assemblies in storage. All calculations are therefore performed with full water density inside the MPCs.*
- *Partial Flooding: The partial flooding of the basket, either in horizontal or vertical direction, reduces the amount of fuel that partakes effectively in the thermal fission process, while essentially maintaining the fuel-to-water ratio in the volume that is still flooded. This will therefore result in a reduction of the reactivity of the system (similar to that of the reduction of the active length), and due to the similarity of the fuel assemblies is not dependent on the specific fuel type. The reactivity changes during the flooding process were evaluated in both the vertical and horizontal positions for all MPC designs. For these calculations, the cask is partially filled (at various levels) with full density (1.0 g/cm^3) water and the remainder of the cask is filled with steam consisting of ordinary water at a low partial density (0.002 g/cm^3 or less), as suggested in NUREG-1536. Results of these calculations are shown in Table 6.III.4.8. In all cases, the reactivity increases monotonically as the water level rises, confirming that the most reactive condition is fully flooded. Note that the studies for partial flooding are performed with the design basis model for the assembly class 10x10A that has the partial length rods removed for added conservatism, while the calculations in the main part of the chapter for the MPC-68 were performed for an assembly class that did not include partial length rods. This shows that the conclusion from partial flooding, i.e. that the fully flooded condition is bounding, applies equally to assemblies with and without partial lengths rods.*
- *Pellet-to-clad Gap Flooding: As demonstrated by the studies shown in Table 6.III.4.2, all assemblies are undermoderated. Flooding the pellet-to-clad gap will therefore improve the moderation and therefore increase reactivity for all assembly types.*
- *Preferential Flooding: The only preferential flooding situation that may be credible is the flooding of the bottom section of the DFCs while the rest of the MPC internal cavity is already drained. In this condition, the undamaged assemblies have a negligible effect on the system reactivity since they are not flooded with water. The dominating effect is from the damaged fuel model in the DFCs. However, the damaged fuel model is conservatively based on an optimum moderated array of bare fuel rods in water, and therefore representative of*

all fuel types and therefore the fully flooded condition is bounding of the preferential flooding condition.

TABLE 6.III.4.1

MAXIMUM k_{eff} VALUES IN THE MPC-68M WITH INTACT (UNDAMAGED)
AND DAMAGED FUEL/FUEL DEBRIS

Bare Rod Array inside the DFC	Maximum k_{eff}		
	Assembly Classes 8x8F, 9x9E/F and 10x10G (4.0 wt%)	Assembly Class 10x10F (4.7 wt%)	All other assembly classes (4.8 wt%)
3x3	0.8985	n/c [†]	0.9267
6x6	0.9032	n/c	0.9295
8x8	0.9070	n/c	0.9344
9x9	0.9087	n/c	0.9371
10x10	0.9110	n/c	0.9387
11x11	0.9105	0.9341	0.9381
12x12	0.9099	n/c	0.9373
13x13	0.9084	n/c	0.9353
14x14	0.9075	n/c	0.9352
16x16	0.9064	n/c	0.9335
17x17	0.9042	n/c	0.9328

Note: The results do not include the bias for distributed enrichments discussed in Section 6.III.2.

[†] n/c = not calculated

HOLTEC INTERNATIONAL COPYRIGHTED MATERIAL

HI-STORM 100 FSAR
REPORT HI-2002444

6.III-22

Proposed Rev. 8

Table 6.III.4.2

*MAXIMUM k_{eff} VALUES IN THE MPC-68M FOR VARIOUS FUEL
TYPES WITH VOIDED PELLETT TO CLAD GAP*

<i>Assembly Classes</i>	<i>Enrichment</i>	<i>Maximum k_{eff} (Voided Gap)</i>	<i>Reference k_{eff} (Flooded Gap)</i>	<i>Delta k_{eff}</i>
<i>7X7B</i>	4.8	0.9185	0.9243	-0.0058
<i>8x8B</i>	4.8	0.9210	0.9294	-0.0084
<i>8x8C</i>	4.8	0.9243	0.9302	-0.0059
<i>8x8D</i>	4.8	0.9245	0.9307	-0.0062
<i>8x8E</i>	4.8	0.9152	0.9211	-0.0059
<i>8x8F</i>	4.5	0.9191	0.9245	-0.0054
<i>9x9A</i>	4.8	0.9290	0.9341	-0.0051
<i>9x9B</i>	4.8	0.9202	0.9330	-0.0128
<i>9x9C</i>	4.8	0.9203	0.9254	-0.0051
<i>9x9D</i>	4.8	0.9210	0.9254	-0.0044
<i>9x9E</i>	4.5	0.9157	0.9254	-0.0097
<i>9x9G</i>	4.8	0.9160	0.9211	-0.0051
<i>10x10A</i>	4.8	0.9311	0.9339	-0.0028
<i>10x10B</i>	4.8	0.9242	0.9332	-0.0090
<i>10x10C</i>	4.8	0.9253	0.9300	-0.0047
<i>10x10F</i>	4.7	0.9301	0.9335	-0.0034
<i>10x10G</i>	4.6	0.9335	0.9372	-0.0037

Note: The results for the 10x10 fuel assembly classes do not include the bias for distributed enrichments discussed in Section 6.III.2.

Table 6.III.4.3

MAXIMUM k_{eff} VALUES IN THE MPC-68M FOR VARIOUS FUEL ROD NUMBERS, OTHER STUDIES

<i>Assembly Class 8x8B (4.8% Enrichment), variable fuel rod number</i>				
<i>Assembly Class</i>	<i>Maximum k_{eff}</i>	<i>Description</i>	<i>Reference</i>	
<i>8x8B</i>	<i>0.9256</i>	<i>Variable Rod Numbers</i>	<i>0.9294</i>	<i>-0.0038</i>
<i>Assembly Class 8x8D (4.8% Enrichment), variable fuel rod number and water rod number</i>				
<i>8x8D</i>	<i>0.9271</i>	<i>Variable Rod Numbers - 2L/2S</i>	<i>0.9307</i>	<i>-0.0036</i>
<i>8x8D</i>	<i>0.9256</i>	<i>Variable Rod Numbers - 4L</i>	<i>0.9307</i>	<i>-0.0051</i>
<i>8x8D</i>	<i>0.9275</i>	<i>Variable Rod Numbers - 4S</i>	<i>0.9307</i>	<i>-0.0032</i>
<i>8x8D</i>	<i>0.9259</i>	<i>Variable Rod Numbers - GE-9</i>	<i>0.9307</i>	<i>-0.0048</i>
<i>8x8D</i>	<i>0.9277</i>	<i>Variable Rod Numbers - 3L</i>	<i>0.9307</i>	<i>-0.0030</i>
<i>Assembly Class 9x9E/F (4.5% enrichment) With Alternate (Closer) Location of the Water Rods</i>				
<i>9x9E/F</i>	<i>0.9231</i>	<i>Closer Water Rods</i>	<i>0.9271</i>	<i>-0.0040</i>

Table 6.III.4.4

*MAXIMUM k_{eff} VALUES IN THE MPC-68M
FOR VARIOUS PART LENGTH ROD LENGTHS (10x10G, 4.6% Enrichment)*

<i>Maximum k_{eff}</i>	Description
0.9117	Full Length Rods Only
0.9217	Part Length Rods 25% length
0.9312	Part Length Rods 50% length
0.9374	Part Length Rods 75% length
0.9372	All Rods

Note: The results do not include the bias for distributed enrichments discussed in Section 6.III.2.

Table 6.III.4.5

*MAXIMUM k_{eff} VALUES IN THE MPC-68M
FOR METAMIC POISON GAP TOLERANCE CALCULATION
(10x10A, 4.8% Enrichment)*

<i>Description</i>	<i>Maximum k_{eff}</i>
<i>Reference</i>	0.9339
<i>Tolerance</i>	0.9334

Note: The results do not include the bias for distributed enrichments discussed in Section 6.III.2.

Table 6.III.4.6

*MAXIMUM k_{eff} VALUES IN THE MPC-68M
FOR ECCENTRIC FUEL ASSEMBLY POSITION
(10x10A, 4.8% Enrichment)*

<i>Position</i>	<i>Maximum k_{eff}</i>	<i>Delta-k</i>
<i>In</i>	0.9339	0.0074
<i>Center</i>	0.9265	reference
<i>Out</i>	0.9095	-0.0170

Note: The results do not include the bias for distributed enrichments discussed in Section 6.III.2.

Table 6.III.4.7

*MAXIMUM k_{eff} VALUES IN THE MPC-68M
FOR EXTERNAL FLOODING*

<i>Internal Water Density (%)</i>	<i>External Water Density (%)</i>	<i>7x7B (4.8%)</i>	<i>8x8F (4.5%)</i>	<i>9x9C (4.8%)</i>	<i>10x10A (4.8%)</i>	<i>10x10G (4.6%)</i>
100	100	0.9243	0.9245	0.9254	0.9348	0.9372
100	70	0.9238	0.9250	0.9259	0.9353	0.9388
100	50	0.9235	0.9239	0.9249	0.9336	0.9380
100	20	0.9234	0.9245	0.9259	0.9342	0.9383
100	10	0.9234	0.9245	0.9257	0.9351	0.9390
100	05	0.9238	0.9247	0.9258	0.9346	0.9387
100	01	0.9230	0.9256	0.9261	0.9341	0.9377

Note: The results do not include the bias for distributed enrichments discussed in Section 6.III.2.

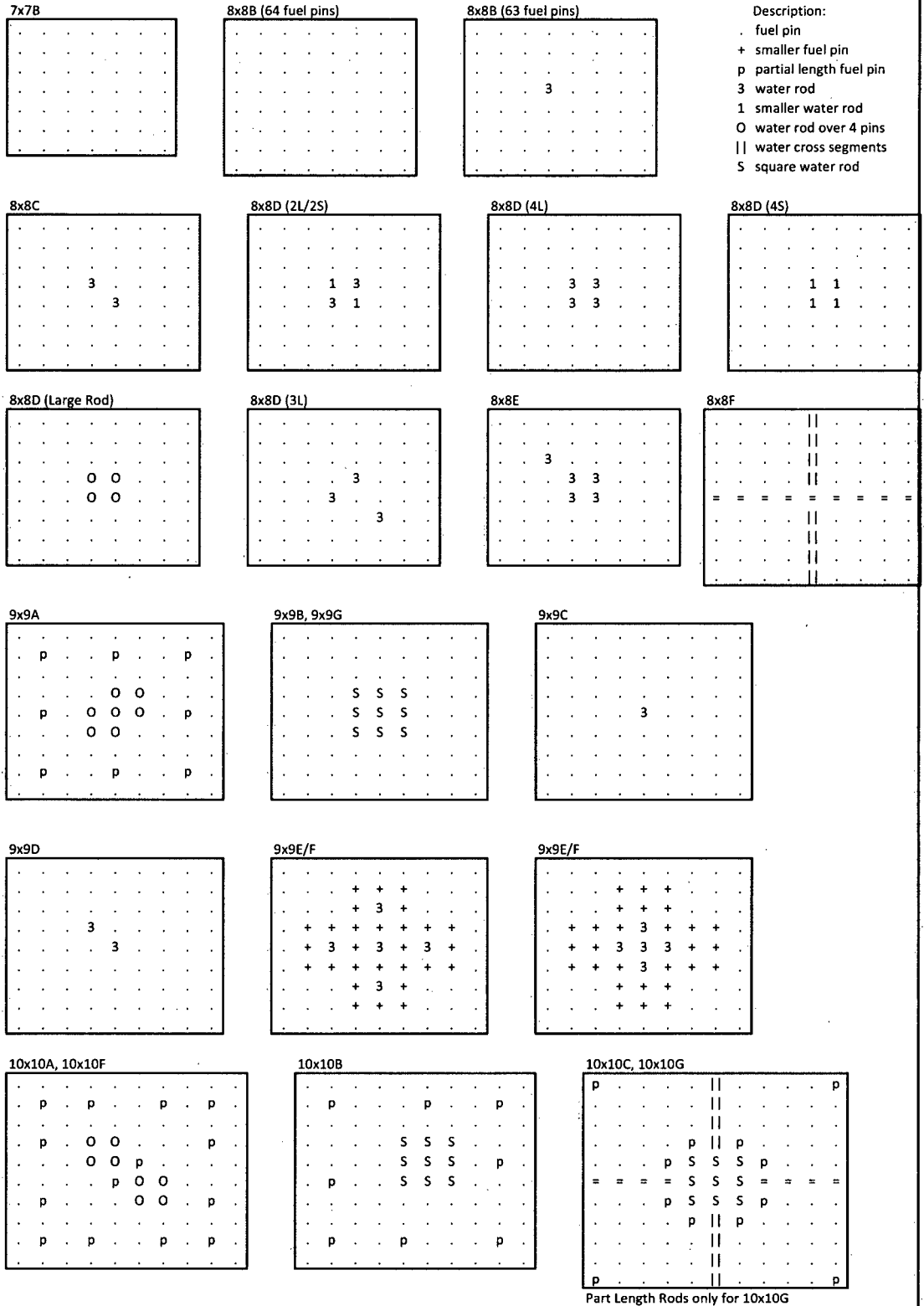
Table 6.III.4.8

*MAXIMUM k_{eff} VALUES IN THE MPC-68M
FOR PARTIAL FLOODING*

<i>10x10A (4.8%)</i>		
<i>Flooded Condition (% Full)</i>	<i>Maximum k_{eff}, Horizontal Orientation</i>	<i>Maximum k_{eff}, Vertical Orientation</i>
<i>25</i>	<i>0.7897</i>	<i>0.9122</i>
<i>50</i>	<i>0.9044</i>	<i>0.9290</i>
<i>75</i>	<i>0.9297</i>	<i>0.9326</i>
<i>100</i>	<i>0.9337</i>	<i>0.9337</i>

Note: The results do not include the bias for distributed enrichments discussed in Section 6.III.2.

Figure 6.III.4.1 Assembly Cross Sections



6.III.5 CRITICALITY BENCHMARK EXPERIMENTS

Same as in Section 6.5

6.III.6 REGULATORY COMPLIANCE

Same as in Section 6.6

6.III.7 REFERENCES

- [6.III.1.1] NUREG-1536, Standard Review Plan for Dry Cask Storage Systems, USNRC, Washington, D.C., January 1997.
- [6.III.1.2] 10CFR72.124, "Criteria For Nuclear Criticality Safety."
- [6.III.1.3] USNRC Standard Review Plan, NUREG-0800, Section 9.1.2, Spent Fuel Storage, Rev. 2 - July 1981.
- [6.III.1.4] "HI-STAR 100 AND HI-STORM 100 ADDITIONAL CRITICALITY CALCULATIONS", Holtec Report HI-2012771 Rev.15 (proprietary)

SUPPLEMENT 7.III**CONFINEMENT OF MPC-68M**

7.III.0 The main body of this chapter remains fully applicable for the HI-STORM 100 System using an MPC-68M *except as indicated below* since the MPC-68M fuel basket is used with the MPC enclosure vessel which is the confinement boundary of the system.

7.III.1.5 Damaged Fuel Container

The MPC-68M is designed to allow for the storage of specified damaged fuel assemblies and fuel debris in a specially designed damaged fuel container (DFC). Section 2.III.1 specifies the fuel assembly characteristics for damaged fuel and fuel debris acceptable for loading in the MPC-68M.